MODELING AND SIMULATION OF REACTIVE DIVIDED WALL DISTILLATION COLUMN

A Dissertation

Submitted in partial fulfillment of the requirements

for the award of the degree

of
MASTER OF TECHNOLOGY
in
CHEMICAL ENGINEERING
(With specialization in Computer Aided Process Plant Design)

By

SHASHANK SRIVASTAVA

DEPERTMENT OF CHEMICAL ENGINEERING
INDIAN INSTITUTE OF TECHNOLOGY ROORKEE,
ROORKEE-247667 (INDIA)
JUNE 2013

DECLARATION

I hereby declare that the work being presented in this dissertation entitled "Modeling and Simulation of Reactive Divided Wall Distillation Column" in partial fulfillment of the requirements for the award of the degree of Master of Technology in Chemical Engineering with specialization in Computer Aided Process Plant Design and submitted in the Department of Chemical Engineering of the Indian Institute of Technology, Roorkee, Roorkee is an authentic record of my own work carried out by me during the period from May 2012 to June 2013 under the supervision of Prof. I.M. Mishra, Department Of Chemical Engineering, Indian Institute of Technology, Roorkee, Roorkee, India.

The matter presented in this Dissertation has not been submitted by me for the award of any other degree of this or any other institute.

Place: Roorkee (Shashank Srivastava)

Date: 14 June, 2013 Enrolment. No. 11514021

CERTIFICATE

This is to certify that the above statement made by the candidate is correct to the best of my knowledge and belief.

(Dr. I.M. Mishra)
Professor, Department of Chemical Engineering
Indian Institute of Technology, Roorkee
Roorkee-247667, Uttarakhand

Date: June 14, 2013

ACKNOWLEDGEMENT

I wish to express my sincere gratitude and appreciation to Prof. I. M. Mishra, Department of Chemical Engineering, Indian Institute of Technology, Roorkee, Roorkee for providing me an opportunity to work under his guidance. His superb guidance with enriched knowledge, regular encouragement and invaluable suggestions at every stage of the present work has proved to be extremely beneficial to me. I consider myself fortunate to have had the opportunity to work under his able guidance and enrich myself from his depth of knowledge.

I also wish to acknowledge the help and assistance provided to me Dr. Vikas Sangal, Asstt. Professor, Department of Chemical Engineering, Thapar University, Patiala during the course of my work, particularly for use of RSM for optimization of iterations and parametric optimization of DWC.

I also wish to place on record the assistance provided by the Head, Prof. V. K. Agarwal and Prof. Vineet Kumar during the course of my dissertation.

Shashank Srivastava
Enrollment No.:- 11514021
M.Tech. (Chemical Engg.)
(Computer Aided Process Plant Design)

CONTENTS

LIST OF FIGURES

LIST OF TABLES

ABSTRACT

Distillation is an operation which is best governed by the concept of vapor-liquid equilibrium. For simulation purposes the minor change in pressure does not affect the equilibrium significantly. So the change in pressure (plate by plate) is usually neglected and it is assumed to be constant or having constant pressure drop. Pressure difference is more or less act as a deciding factor for total molar vapor or liquid flow across the trays, especially in the case of divided wall distillation column (DWC) or reactive DWC. In the present work the analysis is done for reactive DWC, for the feasible operation the process parameters vapor split ratio, liquid split ratio and reflux rate are adjusted in such a way that the difference in pressure drops at both sides of the wall is zero. Several simulations are performed using two thermally coupled RADFRAC columns of Aspen Plus followed by optimization using Box behnken design operated under multiple response surface methodology. The results show that the pressure drop difference is the key factor for the product purity and energy efficiency of the column; it plays a major role for the control and operation of reactive DWC through optimized liquid split and vapor split.

CHAPTER-1

INTRODUCTION

The chemical process industries have the challenging and formidable task to devise and develop green and effective technologies for the production of various chemicals and products optimally with minimal input in terms of raw materials, energy, water, etc. and with minimum discharges of wastes and other bye products in equipment requiring minimum volume. Process intensification is one of the desired answers to these problems. Process intensification aims to decrease the physical size of the equipment while giving high production and a decrease in total annual cost.

Distillation is the backbone of the separation methods used in chemical process industries (CPI). Distillation separates the feed mixture of two or more components into streams which are rich in some individual components based on the differences in the boiling points of various components. The process of distillation creates a vapour phase and a liquid phase with different compositions of various components. The composition difference is obtained because of the difference in vapour pressure or volatility of individual components in the feed mixture. Several methods and design sequences have been proposed for the separation of binary, ternary or multi-component mixtures, and they are categorized according to the purity of the products or the energy requirements.

Dividing wall distillation column (DWC) is a step forward towards economical distillation; it is beneficial in several aspects such as reduction in physical size of the plant employed for particular process, reduction in energy requirement for a given separation, and an increase in the purity of the products. This provides the separation of ternary mixture from the single shell column consisting of a dividing wall in the column with the use of a single reboiler and a single condenser. The theory of dividing wall has its origin from fully thermally coupled distillation column or petlyuk column. A petlyuk column compises two columns connected by two streams of liquid flow and two streams of vapour flow. However, the DWC operation takes place in a single shell, whereas the Petlyuk column operation takes place in two different columns. Hence the DWC is more effective and efficient in terms of area and total cost than that of a Petlyuk column. In case of separation of ternary mixture, at least two column sequence is essential, such as direct and indirect sequence of conventional distillation sequences as shown in Figure1.1. An energetically favorable alternative configuration is shown in Figure 1.2. In this so-called Petlyuk configuration, the vapour and liquid streams leaving the first column are directly connected with the second column. The first column performs a sharp split between A (light key component) and C (heavy key component), whereas the middle key component B get distributed in a natural way between the top and bottom products. Additional separation towards high-purity components takes place in the second column. The improvement of the thermal efficiency, due primarily to unnecessary mixing effects, leads to significant energy savings of about 30% as compared to the direct or indirect sequences. Since only one reboiler and one condenser are used in a DWC, the capital cost of the system is also reduced considerably. A more efficient way to reduce the capital cost is by integrating the two columns into a single shell, and adding up a wall inside the column as shown in Figure 1.3 given below. Thus the column is divided in two parts, which are called as a prefractionator and the main column. The overall thermodynamic efficiency of a Petlyuk column and its thermodynamic equivalent DWC is significantly larger than that of the conventional configuration. This configuration allows prevention of the formation of entropy of mixing caused by composition differences between the feed stream and the feed stage, as well as the minimization of re-mixing effect of middle boiling components during the separation of mixtures with more than two components. This is effectively a direct loss of separation work.

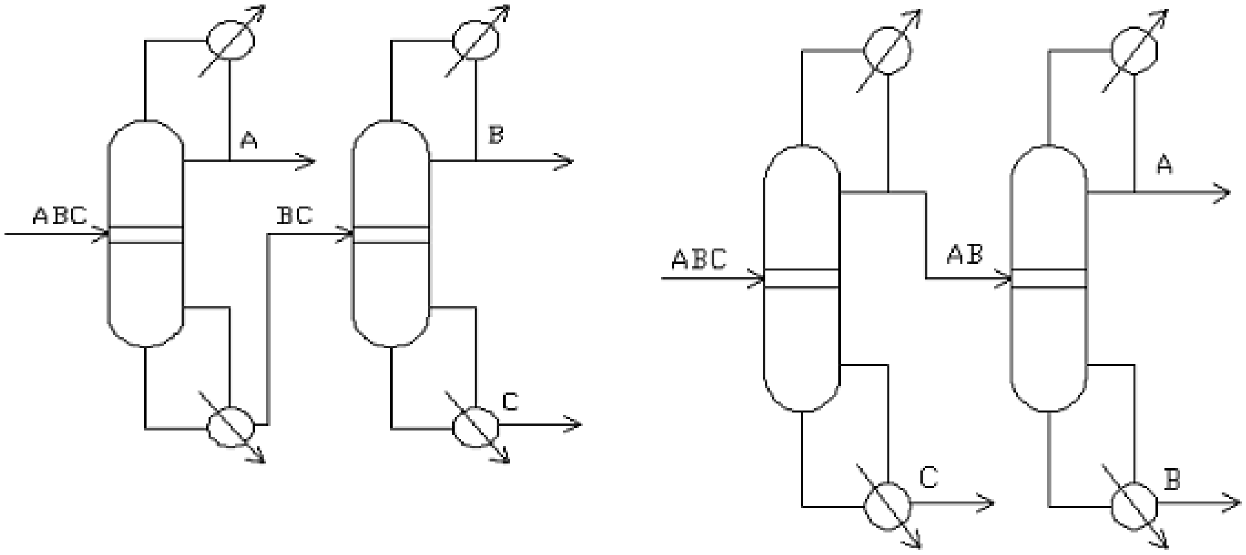

Figure 1.1: Direct Sequence Indirect Sequence

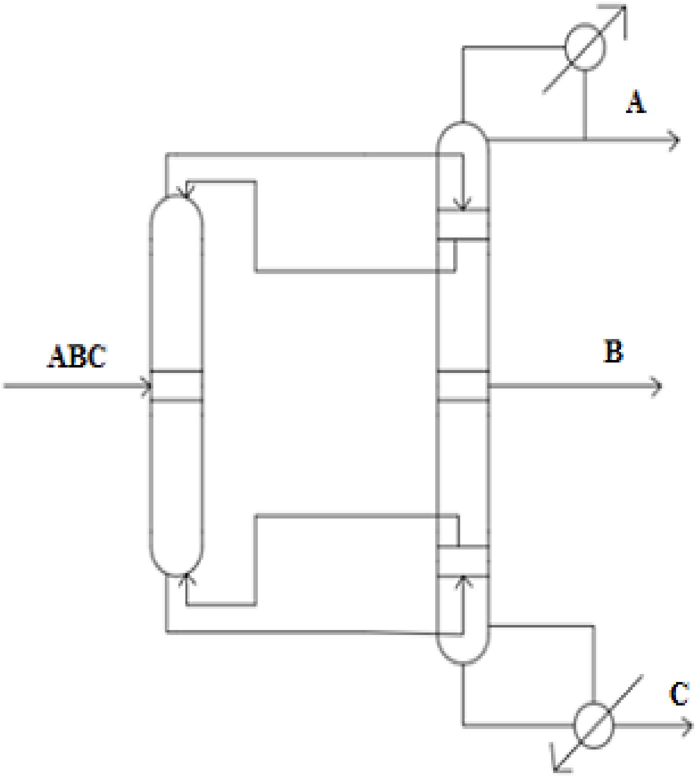

Figure 1.2: Petlyuk Column

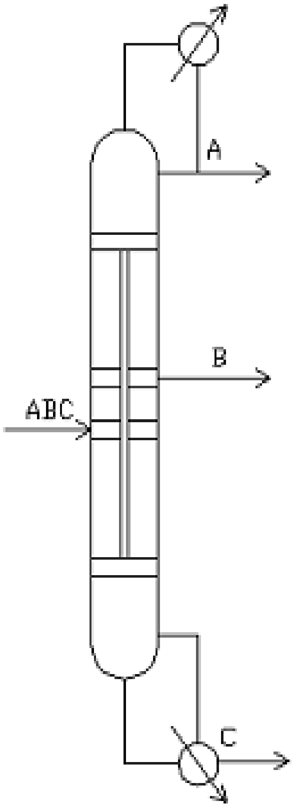

Figure 1.3: Divided Wall Distillation Column

Reactive distillation (RD) involves chemical reaction, phase separation and enriched product streams leaving the column at different heights of the column; all the processes occurring simultaneously. This process provides an increase in the product formation, shifting of equilibrium towards the product side and hence increasing the equilibrium conversion. Because both reaction and separation occur in a single vessel operating at some pressure, the temperatures required for reaction and separation are not independent. Therefore, RD is limited to systems in which the temperatures conducive to reaction are compatible with temperatures conducive for vapor–liquid separation. Pressure of the conventional distillation design is usually set by a minimum temperature in the reflux drum (so that cooling water can be used) or a maximum temperature in the reboiler (to prevent fouling or thermal decomposition). Maintaining the optimum pressure in a RD column is more complex because of the interplay between reaction and phase separation. Most vapor liquid equilibrium (VLE) relationships show an increase in volatility with decreasing temperature. The reaction rates generally decrease with decreasing temperature. If the reaction is exothermic, the chemical equilibrium constant increases with decreasing temperature. So for the low reaction rates, a large amount of catalyst or liquid tray hold- up is required in order to operate at low operating pressure or temperature which facilitates the phase separation. In conventional distillation design, tray holdup has insignificant effect on steady-state composition. In RD, tray holdup (or amount of catalyst) has a large effect on chemical conversion, column composition profiles and product composition. Therefore, a RD column has, in addition to the normal design parameters of number of trays, reflux ratio, feed tray location and pressure, other design parameter of tray holdup.

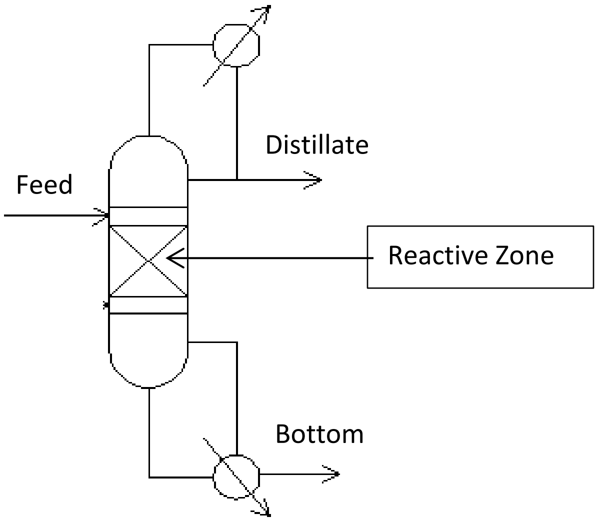

Figure 1.4: RD system

Reactive DWC is an example of high degree of process intensification, as it provides high purity of components of the liquid mixture in a single shell. This can be grouped in two processes such as RD and DWC. Within one apparatus, more than two products can be obtained and the capital cost can be reduced drastically. Furthermore, the well-known reduction in energy demand for DWCs in comparison to a sequence of conventional distillation columns, can lead to reduced operating costs. However, the simulation, design and operation of such complex columns is complicated. The reactive DWC has high degree of process integration; however, this configuration must be thoroughly examined to ascertain whether it can lead to additional synergistic effects. The DWC configuration allows three high-purity product streams in a single column. The reactive DWC is used for three main situations, such as reactive systems with more than two products obtained as pure fractions; reactive system with two products and one non-reacting component such as the inert component to be obtained as the pure fraction, and the reactive system with the reactant in excess where the separation results in appropriate purity of products and the reactant obtained from the same column.

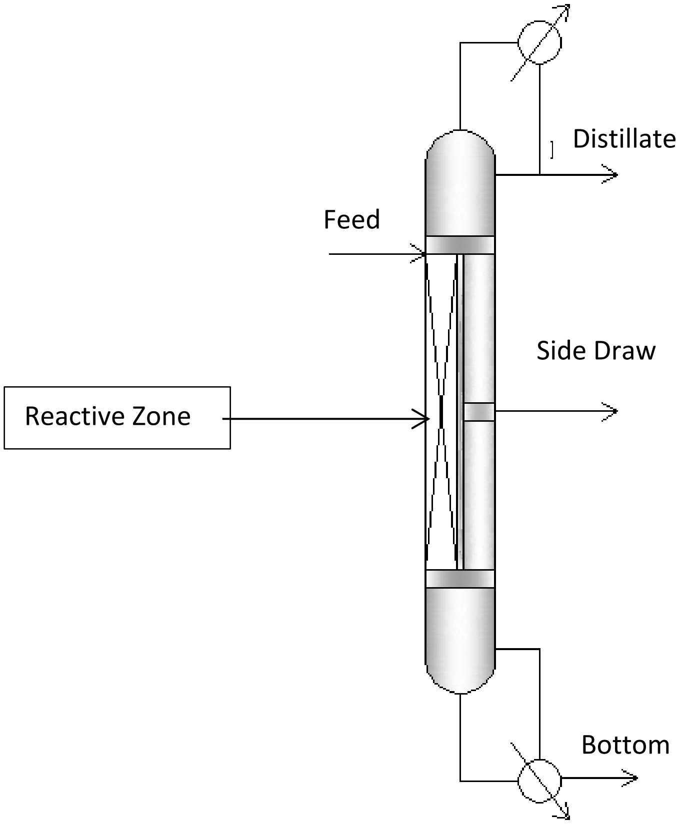

Figure 1.5: Reactive DWC

RD is employed in several unit processes such as acetylation, aldol condensation, alkylation, nitration dehydration, esterification, hydrolysis, isomerization, oligomerization, transesterification, etc. Reactive DWC can also be applied to all such processes.

The process intensification has played an important role in the field of separation technology during the past decade. Due to complications in the control of DWC, it has not been implemented in industries on a large scale. However, several citations on control strategies of DWC have been presented in the literature explaining the advantages and disadvantages of different controllers used in the DWC.

CHAPTER- 2

LITERATURE REVIEW

2.1 Divided Wall Distillation Column

The concept of placing the partition wall inside the column was first given by Monroe in 1933. According to him, the partition wall was placed at the bottom part of the column. Wright (1949) in his patented design gave energy efficient design for the separation of ternary feed mixture in a distillation column by placing a partition wall in the middle part of the column. The design consisted of ordinary distillation column shell with a single feed inlet approximately at the middle of the top and bottom of the column, side product outlet, top product outlet, bottom product outlet and the division of the column by a vertical wall at the middle part of the column passing through a set of trays. The feed inlet and the side stream outlet are at the same vertical height on the above discussed column and the dividing wall extends approximately equidistant above and below the feed inlet and the side stream outlet of the column. The Wright proposed design is as shown in Figure 2.1.

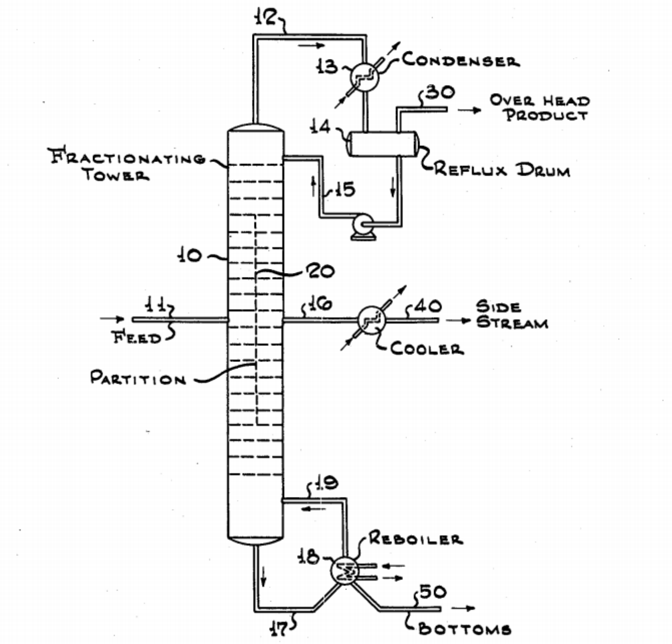

Figure 2.1: Schematic diagram as patented by Wright (1949)

(Reference: US patent number US2,471,134)

Later on Petlyuk et al. (1965**)** gave the two column implementation for the separation of a ternary mixture. The motto of their design was to prevent the thermodynamic losses from mixing of different streams at feed tray location. The schematic representation of their design is shown in Figure 2.2. The configuration given by these researchers is popularly called the Petlyuk configuration or Petlyuk design. This configuration consists of a pre-fractionating column or a prefractionator with liquid and vapour streams leaving the column and refluxed back to the column, with one condenser and one reboiler. This was the most energy efficient option to separate ternary mixture (A,B,C) among all other distillation sequences.

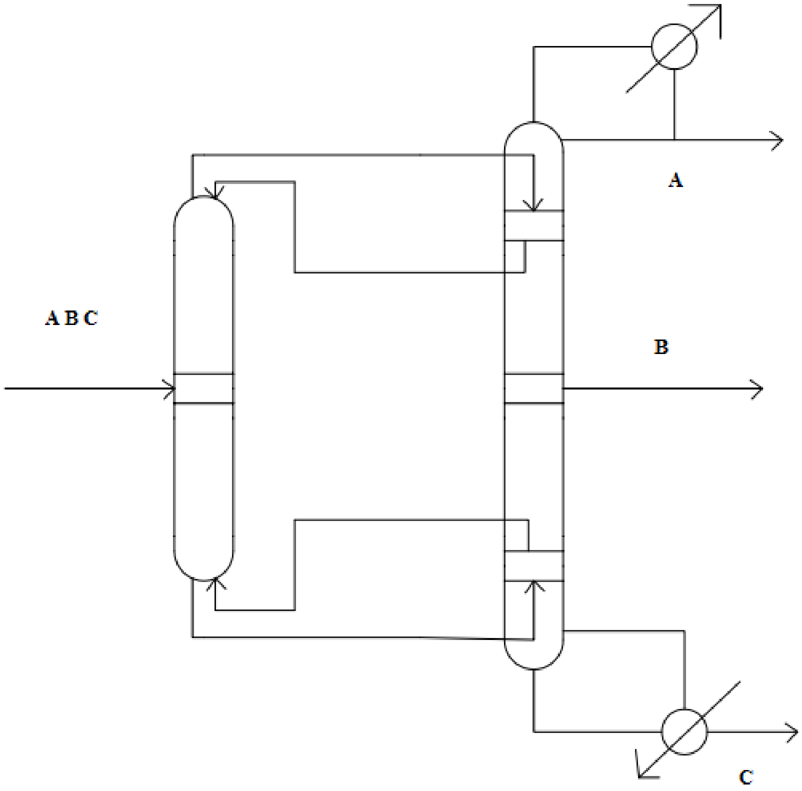

Figure 2.2: Schematic Representation of a Petlyuk Column

Tedder and Rudd (1978) presented the economic comparison of eight sequences of distillation columns using computer design model for the separation of ternary mixtures. The designs included conventional distillation sequences and some new designs of vapour and liquid recycles in order to replace some condensers and reboilers.

Alatiqi and Luyben (1986) gave the quantitative comparison of dynamic response between conventional distillation sequences and thermally coupled distillation columns. Their results showed that the side draw rate is to be manipulated in order to maintain energy efficiency. They found that the load responses of both the systems are not significantly different but in thermally coupled distillation columns the recycling and coupling nature reduces the effect of disturbances.

In order to minimize the vapour flow rate, Fidkowski and Krolikowski (1986) used an optimization technique formulated as a non-linear mathematical problem. The main motive behind this optimization task was to minimize the energy requirement which is proportional to vapour flow rate of the thermally coupled distillation column. They performed the optimization for four different sequences for four different feed compositions for the calculation of minimal vapour flow rate. In the comparative analysis, it was found that the thermally coupled distillation column gave significant savings to achieve the desired separation of the ternary mixture.

Later on a modified form of DWC column was presented by Kaibel(1987). This Kaibel column consisted of two side streams and was capable of separating the feed into four high purity products using a single shell, a single reboiler and a single condenser . The column presented by Kaibel was thermodynamically equivalent to a Petlyuk column with the condition that no heat should pass across the dividing wall. The schematic representation of his design is shown in Figure 2.3.

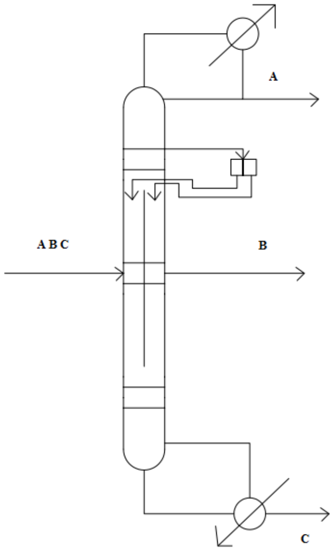

Figure 2.3: Schematic Representation of a Kaibel Column

The separation of multicomponent feed streams is generally performed with the help of several distillation sequences. Floudas and Anastasiadis (1988) gave the mathematical formulation for the proposed sequences and their solution for the optimal configuration of distillation sequences that can perform the desired separation task.

As mentioned earlier, a DWC is the most cost- efficient distillation option for the separation of a ternary mixture. Lockett et al. (1994) used the DWC for the cryogenic distillation of air. Their distillation system consisted of two columns: the first prefractionator and a second partitioned column which was separated by a partition that extended through the length of the partitioned column. The fluid passes from the first column to the second by means of reflux fluids. The system was more or less similar to a divided wall distillation carrying out cryogenic distillation of air using cryogenic rectification method. The products obtained in the process were nitrogen, oxygen and a waste fluid, mainly consisting of argon. Nitrogen of 99% purity, oxygen of 98% purity was withdrawn from the column, and the waste fluid was withdrawn from the partitioned section having 70 % argon.

Woff and Skogestad (1995) considered the three or four product Petlyuk design for their operation and control. They reported that the Petlyuk design offers savings to both capital and energy cost. The Pelyuk design for the four component feed mixture is complex with multiple internal distributors and holes in the operating range for the design leading to infeasible operation and control. The Petlyuk design is to be avoided if two side streams are required. However, the Petlyuk design seems to be more efficient for the three component feed mixture providing feasible operation and control.

The Fenske-Underwood-Gilliland method is generally used as a short cut method to design a simple distillation column. Finn (1996) showed that the above short cut method can also be applied to thermally coupled distillation columns. They provided the easy comparison of thermally coupled distillation column with conventional distillation sequence and showed the thermal coupling as the more appropriate means for energy efficient distillation systems.

In their seminal paper *"Are thermally coupled distillation columns always thermodynamically more efficient for ternary distillation?"* Agrawal and Fidkowski (1998a) showed that there is a finite range of values of feed composition and relative volatility under which the process is thermodynamically efficient. However, even for those values of feed composition and relative volatility for which the process has lower values of thermodynamic efficiencies, these values are much higher when the middle key has low concentration in the feed.

Later on, Agrawal and Fidkowski (1998b) worked on the difficulty in controlling of vapour flows at certain rates and proportions in a fully thermally coupled distillation column (Figure 2.4a). The difficulties were overcome by rearranging the distillation sections as shown in Figure 2.4b. This new arrangement results in two physically separated distillation columns operating at different pressures. The column with slightly high pressure contains a reboiler while that with a slightly lower pressure contains a condenser. The new arrangements are almost equivalent to thermally coupled columns but they do not retain the minimum energy demand as that of thermally coupled columns.

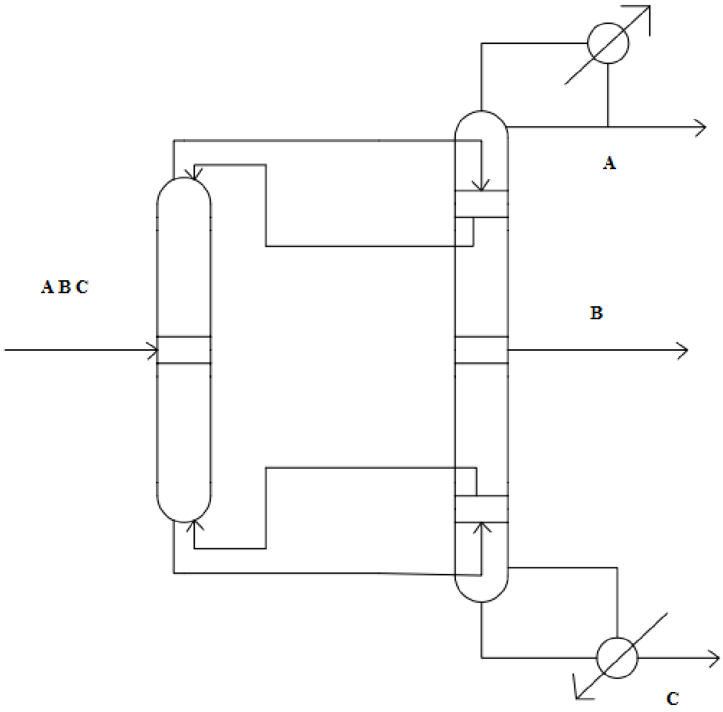

Figure 2.4a: Thermally coupled distillation column (Agrawal and Fidkowski,1998b)

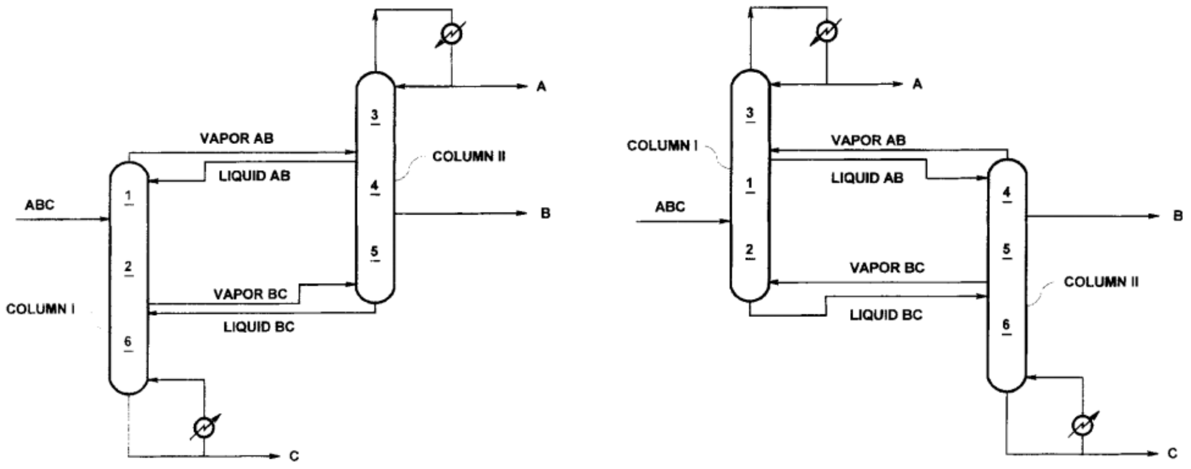

Figure 2.4b: Rearrangement of distillation columns (Agrawal and Fidkowski,1998b)

In a succeeding paper, Agrawal and Fidkowski (1999)_discussed a new thermally coupled scheme for the separation of ternary mixtures. As the Petlyuk design consists of two way connections between the columns, the new design consists of one-way or one two-way connection between the columns. This new design can replace the Petlyuk design of thermally coupled columns as it does not require any increase in energy demand. These systems are as energy efficient as that of Petlyuk design. In other way, it also increases the feasibility of the control system as the number of connecting streams gets reduced. The schematic representation of fully coupled Petlyuk design (FC), side stripper column (SS), side rectifier column (SR) and a system with side draw stream and prefractionating column (SC) is shown in Figure 2.5. The configuration mentioned above fits best for the specified composition of ternary mixture.

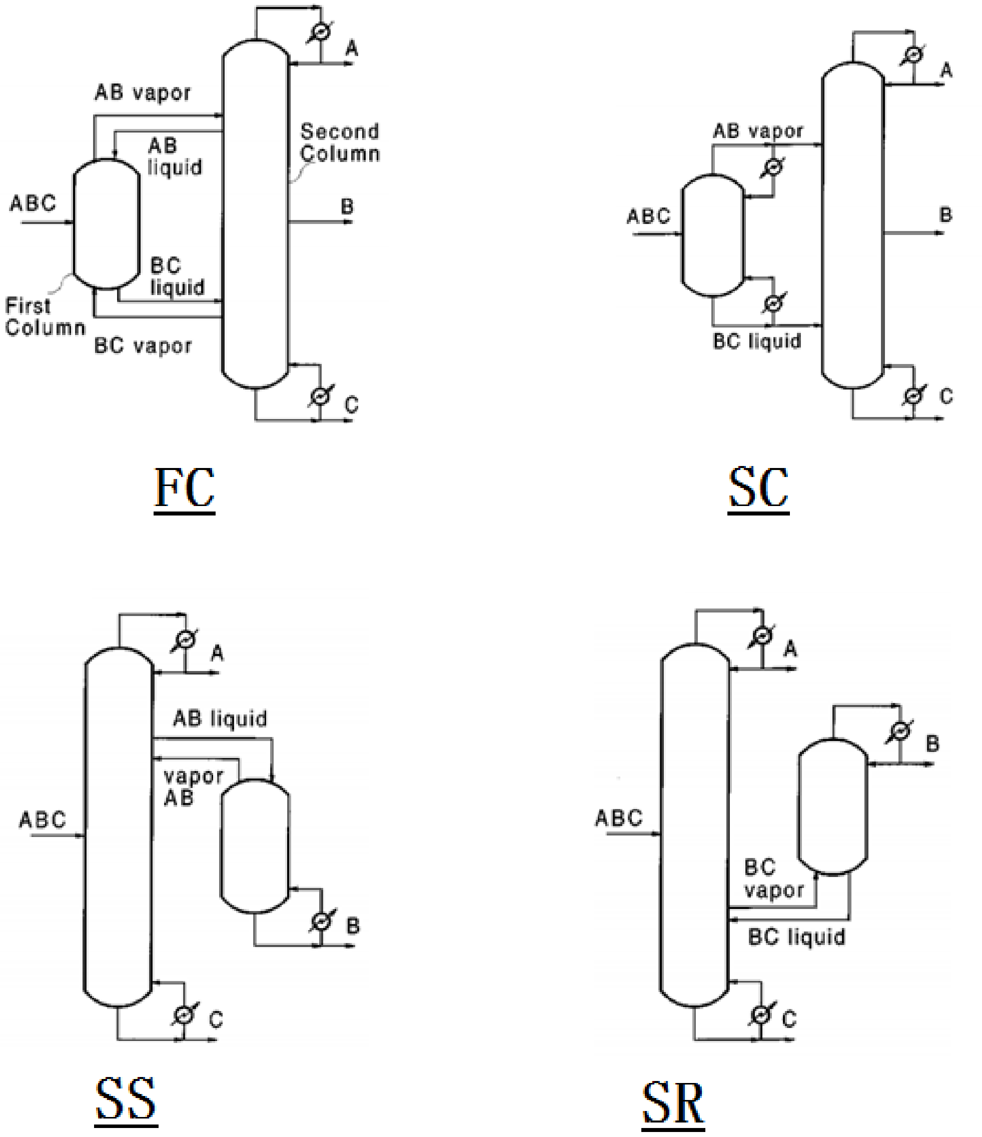

FC SC

SS SR

Figure 2.5: Petlyuk design (FC), side stripper column (SS), side rectifier column (SR) and a system with side draw stream and prefractionating column (SC) (Agrawal and Fidkowski,1999)

Several researchers have reported on the optimal behaviour of Petlyuk column under steady state conditions. Halvorsen and Skogestad (1999) developed the relationships between the measurements obtained from composition profile and the optimal operation of the DWC system. The result achieved by “self-optimizing control” has been compared with nonlinear model based optimization methods and the evaluation was done for the complexity and the performance of the DWC.

Agrawal (2001),_in a patented note, presented an easier and more efficient distillation sequences for the separation of two or more component feed mixtures. He showed that the one way communication between distillation columns was an improvement on two way communication in thermally coupled distillation systems. He proposed that either the distillation section is added to one of the two distillation columns or a new distillation column is added. He proposed the design for the transfer of only liquid stream from one distillation column to the other, thus removing the transfer of vapour stream to the same tray of the two columns. In his design either the more volatile component or the least volatile component is obtained simultaneously in both the distillation columns. The schematic representation of his design is shown in Figure 2.6.

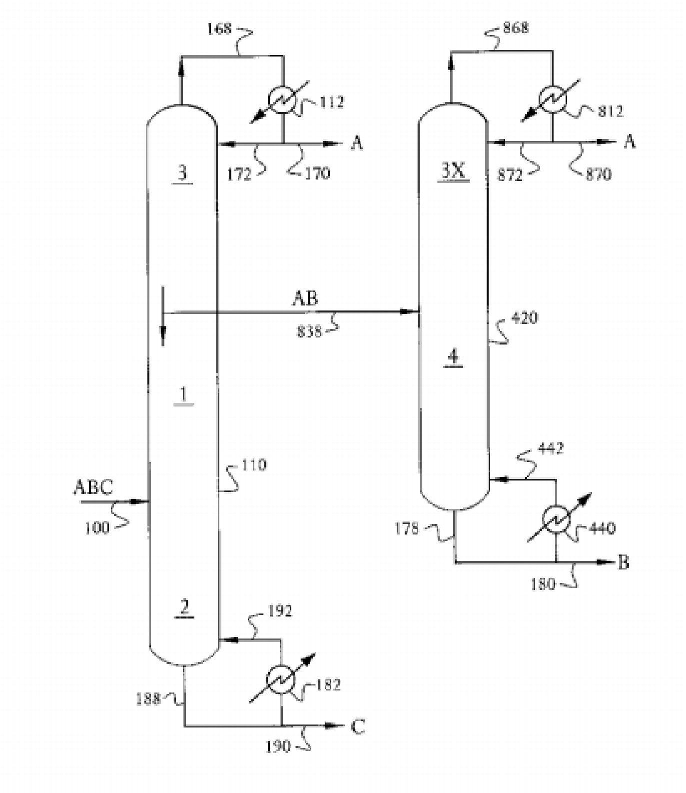

Figure 2.6: Design patented by Agrawal (2001)

(Refrence: US Patent US62,863,35B1)

In another paper, Agrawal(2001b) discussed multicomponent distillation in multi- partitioned distillation columns using multiple reboilers and condensers. The total number of components in the feed mixture leads to the total count of reboilers and condensers used in the process. This leads to better control of liquid and vapour flow ratio which makes the process feasible with better control over product purities. In this paper, he resolved several configurations of distillation columns with partition walls and multiple reboilers and condensers. Some of the configurations are shown in Figure 2.7. The single distillation column configuration as shown below are comparable to side stripper and side rectifier configuration, their heat duty demand is as low as that of the conventional scheme, but single distillation column configuration seems to be beneficial in several concepts. While the configuration reduces the number of distillation columns, reboilers and condensers, it also lowers the heat duty demand as compared to direct and indirect conventional schemes. The concept of single distillation column with multiple reboiler and condenser is impressive as it increases the operability with a marginal increase in operating cost.

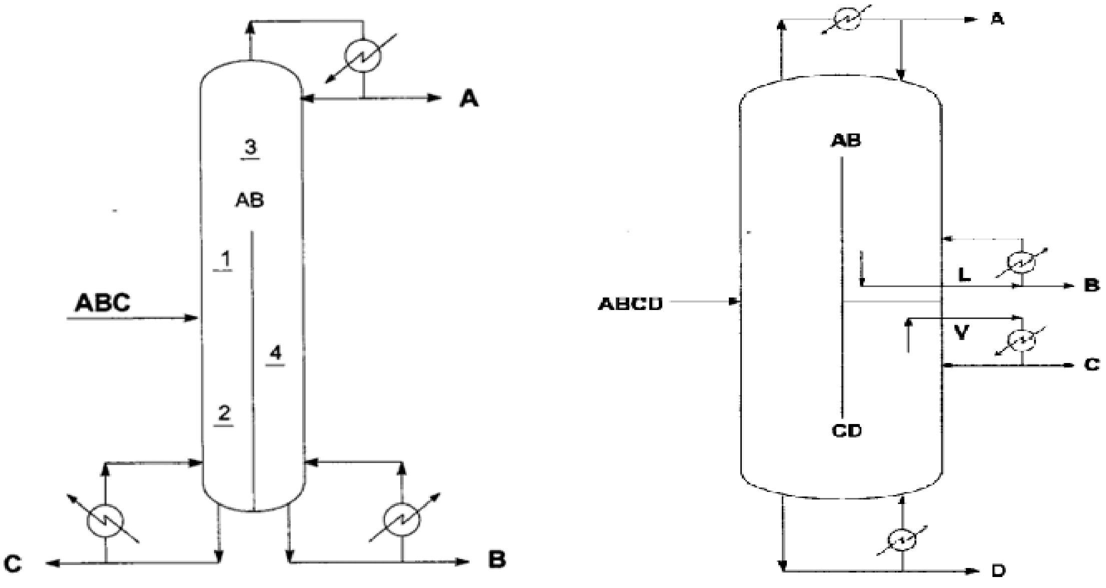

Three Component Feed Mixture

Four Component Feed Mixture

Figure 2.7: Configurations presented by Agrawal(2001)

Earlier in 1986, Fidkowski and Krolikowski gave calculations for the minimum vapour flow rate for the separation of ternary mixtures with the motive to minimize the energy cost. Fidkowski and Agrawal (2001) established the method further for the separation of four component feed mixtures in fully thermally coupled distillation columns. The optimized result for quaternary feed showed less energy requirement as that in conventional system. Various feed and relative volatility were considered at the minimum vapour flow rate conditions. The results showed about 20% savings in half of the cases and about 50% savings in a quarter of cases.

Tung (2002) examined the behaviour of hydraulically balanced fully thermally coupled distillation columns in his patent. The design includes the fractionating apparatus operating at several feed rates, feed compositions and product specifications for the purpose of hydraulic balance and least energy requirement. The system comprises 4 zones - zone D, zone S, zone F and zone B. Zone D comprises the section where distillate product is obtained, zone S is where side stream product is withdrawn, zone F is the feed zone which acts as an inlet to the column and zone B is where the bottom product is obtained. The fractionation column consists of at least one condenser and one reboiler with the aim to give the innovative design for hydraulic balance and energy efficient design at enormous variation in independent variables such as feed rate, composition and product specifications. The schematic representation of the design is as shown in Figure 2.8.

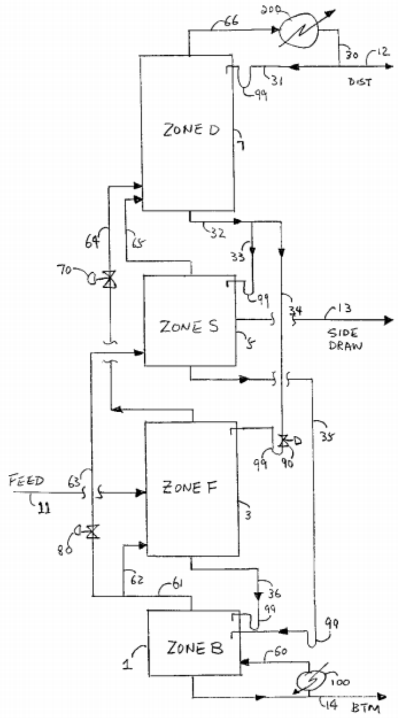

Figure 2.8: Design patented by Tung (2002)

(Refrence: US Patent: US 6,347,533B1)

Muralikrishna et al. (2002) discussed the problems related to the design of a DWC for a specified separation. The shortcut design method of Fenske-Underwood-Gilliland was used to determine the space for efficient design of the column. In this method they represented all the possible designs of DWC in a 2-dimensional plot, which helps in visualizing the design and point out the optimum design required for the specified separation.

Heydrich et al. (2006) worked on the separation of a ternary mixture comprising components, namely 1,1,2,2-tetramethoxymethane, glyoxal dimethyl acetal and methanol. The separation was carried out in an energy efficient DWC. The column was divided into 6 major parts consisting of upper common column region, lower common column region, feed section with rectifying and stripping, and the side stream section with rectifying and stripping regions. The authors considered several variations in independent variables such as feed tray location and number of theoretical plates and obtained different compositions of products. The motive was the requirement of purity of products as heavy key, middle key and light key from the withdrawals of the DWC.

Strandsberg and Skogestad (2006) worked on a laboratory pilot plant of Kaibel column erected by them with the objective to examine the operational performance and its control functions. The work was intended to increase the energy efficiency of the column keeping the product purity as specified. Manipulation of vapour flow on each side of the dividing wall at optimal conditions was also examined. They discussed the operation of the Kaibel distillation column for the separation of a four component feed mixture. Kaibel column was found to be more energy efficient with savings in capital investment in comparison to conventional distillation column sequences. The minimum singular method has been used to find the optimal location of temperature measurement for stabilizing control.

Sotudeh and Shahraki (2007) presented a method for the design of a DWC for the separation of ternary mixtures. They used Fenske equation, Gilliland correlation and pinch composition at the connection points to design the DWC. In the previous literature, all these methods were used. They introduced Underwood equation too for making their calculations. They also showed that the proposed design method can be extended for the separation of more than three components of a feed mixture.

Isopescu et al. (2008) studied the influence of feed composition on energy saving as compared to conventional scheme of multicomponent separation by analyzing the thermodynamic efficiency of a DWC. They carried out a case study of hydrocarbon mixture comprising benzene, toluene, ethyl benzene and o-xylene separation and reported 40% energy saving by using a DWC. They propounded that the DWC was more efficient in energy saving when the middle key was in high concentration in the feed.

Rangaiah et al. (2009) considered six industrial examples for developing the general procedure for the quick design of a DWC through simulation and optimization. The results showed that the vapour and liquid split ratios have significant effect on the energy requirement, and that they have lower impact on the condenser and reboiler duties when the column is operated in the optimum region. For the optimization of a DWC, vapour or liquid splits were varied in the optimum region for rigorous simulation of HYSIS simulator. On an average, about 20 % reduction in the annual cost was obtained. They also examined whether the location of the feed tray, side draw and prefractionator have any effect on the energy requirement and thereby on the total annual cost. They found that the contribution of feed tray location in reducing the total annual cost is very finite: ~ 1% in five of the six examples examined. They proposed that the quick design procedure for a DWC can create a significant impact on process industry leading to a decrease in energy requirement and an alleviation of the environmental concerns.

Premkumar and Rangaiah (2009) examined the capability of DWCs in comparison to conventional distillation columns for the separation of ternary mixtures. For this purpose, they considered six examples of industrial importance that were assumed to be in operation in the plants. They reported impressive savings in annual cost, about 30% reduction in operating cost, and lower energy requirements by retrofitting conventional distillation columns to convert them in to DWCs.

Butler (2010) studied the separation of hydrocarbon mixtures being carried out in a DWC. They related the impurity removal from hydrocarbon mixtures and the production of several demanding compounds in DWCs. The operations comprised separation of compounds from such mixtures as ethylbenzene and polyethylbenzenze from an alkylation process, ethylbenzene, xylenes and styrene from styrene or polystyrene production process and benzene, toluene and xylene from BTX mixture.

Shah and Agrawal (2010) described a simple matrix method for finding out multicomponent distillation sequences. This provides the opportunity to rank-list the configuration according to the criteria of requirement. For this method, the only information needed is the number of components in the feed. Using this method, the authors developed the configuration for eight component feed mixture.

Lee et al. (2011) carried out a study on the separation of crude n-butanol in to pure n-butanol and several by products in a DWC. They varied the values of the operating variables to work for an energy efficient process giving high purity n-buatanol. They modelled the operation of a DWC for the separation of a BTX ternary mixture and used the BBD under RSM to optimize the structural and process parameters for increasing the energy efficiency of the DWC. Multifrac model of ASPEN plus simulator was used to carry out the simulation of the design. The optimization was performed by considering that there is zero pressure difference between both the sides of the wall of DWC. It was found that the process parameters like liquid split, vapour split, reflux rate, and feed composition have significant effect on the energy efficiency of aDWC. The effect of structural parameters was found to be insignificant in comparison to operating variables.

Sangal et al. (2012b) carried out the simulation of a DWC for the separation of C4-C6 normal paraffin ternary mixture to increase the product purity and the energy efficiency. They used Multifrac model of the ASPEN plus^{TM} software for the simulation purposes and BBD for the optimization of the process. The functional values of the product quality and energy efficiency were found by rigorous simulations of the domain variables such as reflux ratio, liquid split and vapour split. It was observed that by optimization with BBD, the number of simulation runs get significantly reduced. The authors predicted that the results obtained by this technique are almost similar to that obtained with rigorous simulation.

The pressure in the column changes very little from the condenser to the reboiler in a conventional distillation column. This spurred that there is no use in considering the pressure change in the column for simulation purposes. This little change in pressure shows insignificant effect on the vapour-liquid equilibrium in the column. The pressure drop is calculated for the flow of vapour and liquid inside the column. For DWC, the pressure drop on the both sides of the wall should be equal and the vapour split ratio will get adjusted naturally. Sangal et al. (2012c) studied the effect of pressure drop on the operation and performance of a DWC. They studied the feasible vapour split as a function of reflux ratio and liquid split. The results showed that the liquid rate has insignificant effect on the feasible vapour rate and that significantly different pressure profiles are obtained on the two sides of the wall. The vapour flow rate led to a large variation in the concentration profile in a DWC.

2.2 Reactive Divided Wall Distillation Column

Hauan and Lien (1998) analyzed the effect of phenomena vectors in the RD process which included reactive and separation processes simultaneously. They showed that the change in the process parameters such as pressure, temperature and composition changes their relative positions and interactions to allow for the reaction and separation to occur in the same physical shell.

Huss et al. (1999) discussed the computer aided tools for the design of RD systems. They carried out the survey of available techniques for the design, emphasized on the geometric methods for the design and explored the opportunities for further research. They pointed out the conceptual design of RD for methyl acetate production from methanol. In this method, they used simple equilibrium model which acts as a starting point for the design of kinetically controlled RD process.

Reactive DWC is an important example of process intensification. While the DWC decreases the energy demand for distillation processes; further process intensification is done by carrying out the reaction in the DWC. Reactive DWC can lead to further reduction in the operating cost. Daniel et al. (2006) presented a novel approach for the design of a RDWC. The methodology depends on the graphical boundary value method (BVM). A reaction system is analyzed with four components. Chemical equilibrium is assumed at each stage. This procedure generates the cost function which is used to rank the design from several designs being proposed in the design procedures.

Mueller and Kenig (2007) proposed a novel rate- based approach to model the reactive and unreactive DWC. This model has been applied to several industrial processes and successfully verified. It has been applied to non-reactive ternary mixture of methanol, isopropanol and butanol and the results were completely validated. Transesterification of carbonantes has been the successful example for the reactive DWC. The reaction used is equilibrium limited and synthesized to high conversions. For the first case, the results showed that the vapour flow rate ratio can be set equal to cross sectional area ratio due to similarity of vapour resistances at both sides of the divided wall in the RDWC. In the second case, the results showed that the process parameters should be set such that the conversion and selectivity increase significantly. At the same time, it offered good separation between products and non-reactive compounds within the same apparatus.

Bumbac et al. (2007) worked on the modelling and simulation of a RDWC using different simulators such ASPEN DISTIL^{TM} and ASPEN HYSIS^{TM}. The feasibility of separation scheme was carried out using ASPEN DISTIL ^{TM} and simulation of flowsheet configuration was performed using ASPEN HYSIS^{TM} using two columns model. The reactive zone in prefractionator section was assumed to be modelled as two backflow CSTRs in series. A case study of isoamylenes etherification with ethanol to obtain tert-amylethylether was examined in RDWC using structured packing. Based on the results, it was recommended that the reaction zone should be placed much closer to the prefractionator top and the feed inlet be kept below the reaction zone, in order to increase the production of tert-amyl ethyl ether in the RDWC.

Hern´andez et al. (2008) carried out the steady state and dynamic simulation of reactive Petlyuk column considering an equivalent RDWC. The simulation was carried out for an RDWC and implemented in a pilot plant. The reaction between ethanol and acetic acid, catalyzed by sulfuric acid was taken as the case study for producing ethyl acetate and water. The results showed that the changes can be achieved to two set points and disturbances in the compositions of feed streams can be eliminated. The dynamic simulation results showed that either the composition of the top or bottom product or the temperature of the two streams can be controlled by handling reboiler heat duty or reflux rate of the column.

Groten et al. (2008) reported on the RD which comprised the contact of first component alone or with a second component passed through the catalytic distillation structure resulting in a decrease in the amount of the first component leading to the formation of products through catalytic reaction. The reaction leads to the formation of two types of mixtures, first consists of first component and the product and the other mixture consists of first component, second component and the product, thus separation of the second mixture requires a ternary mixture separation which is to be fulfilled by a DWC. In this process, the column is divided by the wall separating the zone into two comprising reaction zone and non-reaction zone or fractionation zone. The etherification of iso-olefins was carried out by reaction of C_5iso-olefins with methanol producing tertiary amyl methyl ether (TAME). On one side, the TAME is being separated from C5 iso-olefins and methanol, and on the other side other unreacted C5 iso-olefins and methanol are reacted leading to shifting of equilibrium of the reaction and providing greater conversion of the reactants to products. The schematic representation of the proposed design is shown in Figure 2.9.

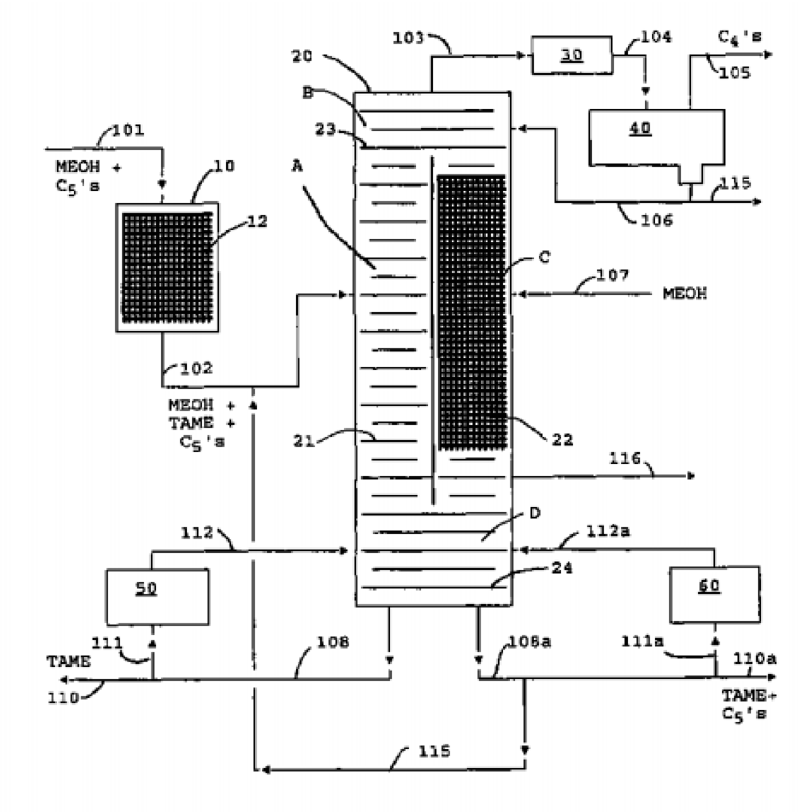

Figure 2.9: Schematic representation of the proposed design of Groten et al. (2008).

(Reference: US Patent : US7,410,555)

Miranda-Galindo et al. (2009) proposed the design of a RD for the production of biodiesel using multi-objective genetic algorithm with restrictions. Biodiesel production was carried out by esterification of lauric acid and methanol in which sulfuric acid acted as the catalyst, being processed in thermally coupled distillation sequences involving a side rectifier. The results showed that the biodiesel obtained in the above system is of high purity resulting in a drastic decrease in energy consumption for the column.

Kiss et al. (2009) posed a question "*Reactive Dividing-Wall Columns—How to Get More with Less Resources?"* and answered it with the study of Akzo Nobel chemical industry giving a first reported industrial application of a RDWC. The purpose of the design was to reduce the production rate of the by product at the expense of the main product. They proposed a novel integrated design approach to examine the reactive and separation processes in a DWC, simultaneously leading to reduce a capital investment by 35% and energy cost by 15% as compared to a base case design.

Santander et al. (2010) presented their work on the production of biodiesel from RD operation using castor oil. The simulation was carried out using Aspen Plus simulator and SRM. They concluded that high yield percentage in the transesterification reaction can be achieved using an oil feed rate of 20.52 g/min, an ethanol: oil molar ratio of 13, a molar reflux rate of 3.51 and a distillate: feed ethanol ratio of 0.84. The results showed that the oil to ethanol molar ratio is reduced by 31.6% as compared to standard conventional processes.

Delgado-Delgado et al. (2011) provided a brief review on reactive DWC. Although the thermally coupled distillation column and sequences design and control have been explained in the late 1940's, the real industrial usage of DWC started only in the middle of 1980's. They carried out experiments for the production of ethyl acetate using reactive DWC. The results obtained were compared with simulation results obtained by using Aspen One- Aspen plus simulator. These results verified the previous simulation studies about design and control of reactive DWC, evolving as a new concept of experimental study of RD with a step to enhance the philosophy of process intensification.

Kiss et al. (2012) analyzed the synthesis of dimethyl ether by dehydration of methanol through different processes and systems. They carried out several simulations for synthesis which forms the ternary system of methanol, dimethyl ether and water. They carried out the calculations on two systems such as conventional RD and RDWCs. Macroporous sulphonic acid resin was used as the catalyst. The process was optimized using sequential quadratic programming combined with Aspen PLUS simulator. The results clearly validate the energy savings of 12-58% of RDWC than that of conventional RD system. The RDWC operation led to a 60% reduction in CO_2 emission as well as 30% reduction in capital cost.

CHAPTER- 3

PROBLEM STATEMENT

3.1 Problem

Distillation is an operation which is best governed by the concept of vapor-liquid equilibrium. For simulation purposes, the minor change in pressure does not affect the equilibrium significantly. So the change in pressure (plate by plate) is usually neglected and it is assumed to be constant or having a constant pressure drop. Whether the pressure difference is more or it is less, acts as the deciding factor for total molar vapor or liquid flows across the trays, especially in the case of a DWC or a reactive DWC. Reactive DWC can be divided into three parts such as the upper zone or the rectifying section, the lower zone or the stripping section, and the middle zone of the column, which is divided into two parallel sections with left zone acting as the reactive zone and the right zone as the fractionation zone. For the feasible operation, the process parameters such as vapor split ratio, liquid split ratio and the reflux rate are adjusted in such a way that the difference in pressure drops across both the sides of the dividing wall is zero. The basic material, equilibrium, summation and heat balance equations taken together are known as MESH equations, and are used to model the system. In the case of reaction and separation processes occurring in the same column system, the MESH equations get transformed into MESHR equations, where R represents the reaction rate equation. The addition of difference in pressure drop equations transforms the MESHR equation to MESHRD equation, where D represents the pressure difference equation. Before performing the simulation analysis is done about the process independent variables and dependent variables involved in the system, for that purpose the degree of freedom analysis is to be done. Several simulations are to be performed using two thermally coupled RADFRAC columns of the Aspen Plus in order to verify the above formed MESHRD equations. The RADFRAC model is capable of solving MESHR equations and the difference in pressure drop equation is verified by performing several simulations with different values of process parameters, and the optimized results are obtained. The system is to be optimized for multiple responses such as the product purities at all the streams, reboiler duty, condenser duty and the difference in pressure drops at both the sides of the wall. After getting the optimized process parameters a simulation run is performed to obtain the reaction yield and product composition at all streams for the system. Dimethyl ether (DME) is a fuel of industrial importance, it is a clean fuel used in diesel engines, act as a predecessor for organic compounds, and as a replacement for chloro-fluoro carbons (CFC) with the property of green aerosol propellant. DME is produced by dehydration of methanol which is obtained by catalytic reaction of synthesis gas. In the present analysis the system is taken as dehydration of methanol over macroporous sulphonic acid resin catalyst producing DME as the main product and water as the by-product. Optimization is to be performed using BBD operated under multiple response surface methodology (RSM).

3.2: OBJECTIVE

Several researchers [Kiss et al. (2012), Delgado-Delgado et al. (2011)] analyzed the reactive DWC without considering the pressure drop equalization on both the sides of the dividing wall. The objective of the present dissertation is to analyze and optimize the effect of process parameters over multiple responses such as the product purity at all the streams, reboiler duty, condenser duty and pressure drop equalization.

CHAPTER- 4

MATHEMATICAL MODELING AND DEGREE OF FREEDOM ANALYSIS

Mathematical modeling is an approach to quantify the material, energy and momentum output as a function of input parameters with the help of material, energy and momentum balance equations along with some constitutive relationships to describe the physical properties of the material as well as the system. The above mentioned statement is illustrated in Figure 4.1.

Figure 4.1: Basic schematic diagram for the first step to design a system

The functional relationship is written as

Output= f (Input)

This function f can be of several types such as:

1. Relation obtained by material, energy and momentum balance equations.
2. Constitutive relationships.
3. Empirical relationships.

A complete mathematical modeling of the reactive plus separation process requires material, energy and momentum balance equations along with the reaction rate equations for each individual tray of the column. Most of the existing models [37-41] ignore momentum balances and try to model the system using material balance, equilibrium relationship, summation and heat balance equations. These equations are together known as basic MESH equations. For reaction and separation process to occur simultaneously reaction rate equations are also included for the analysis and the equations together are called as MESHR equations. Consider an equilibrium stage i as shown in Figure 4.2, where several material and heat inputs and outputs are also shown. This is the basic diagram for mathematical modeling of a fractionating column.

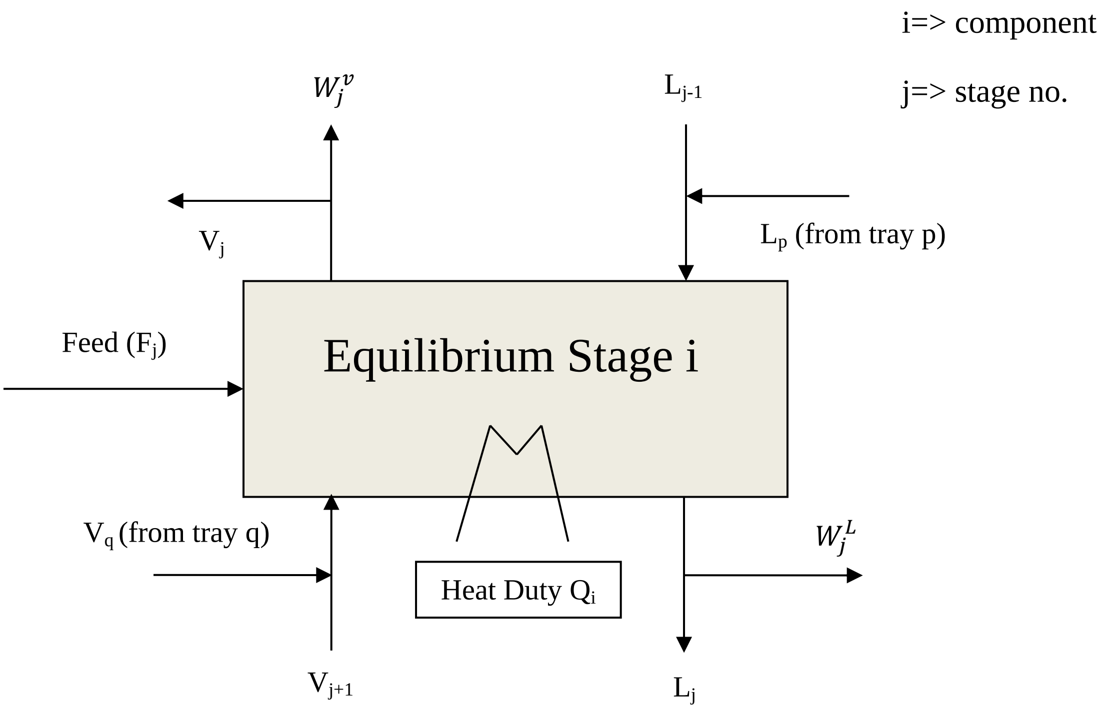

Figure 4.2: Equilibrium based approach for modeling

Considering reaction and the separation processes taken together, the first step is to model the RD system followed by modeling of the reactive DWC system.

4.1:Reactive distillation

It operates efficiently for binary systems such as

1) A → P with excess moles of A
2) A → B + C with limited moles of A
3) A + B → C with one of the reactants in excess

In this process, some plates are set as reactive zone in which the reaction and separation processes take place simultaneously. The upper part of the reactive zone consists of some plates which are termed as rectification section, and the lower part of the reactive zone is called the stripping section.

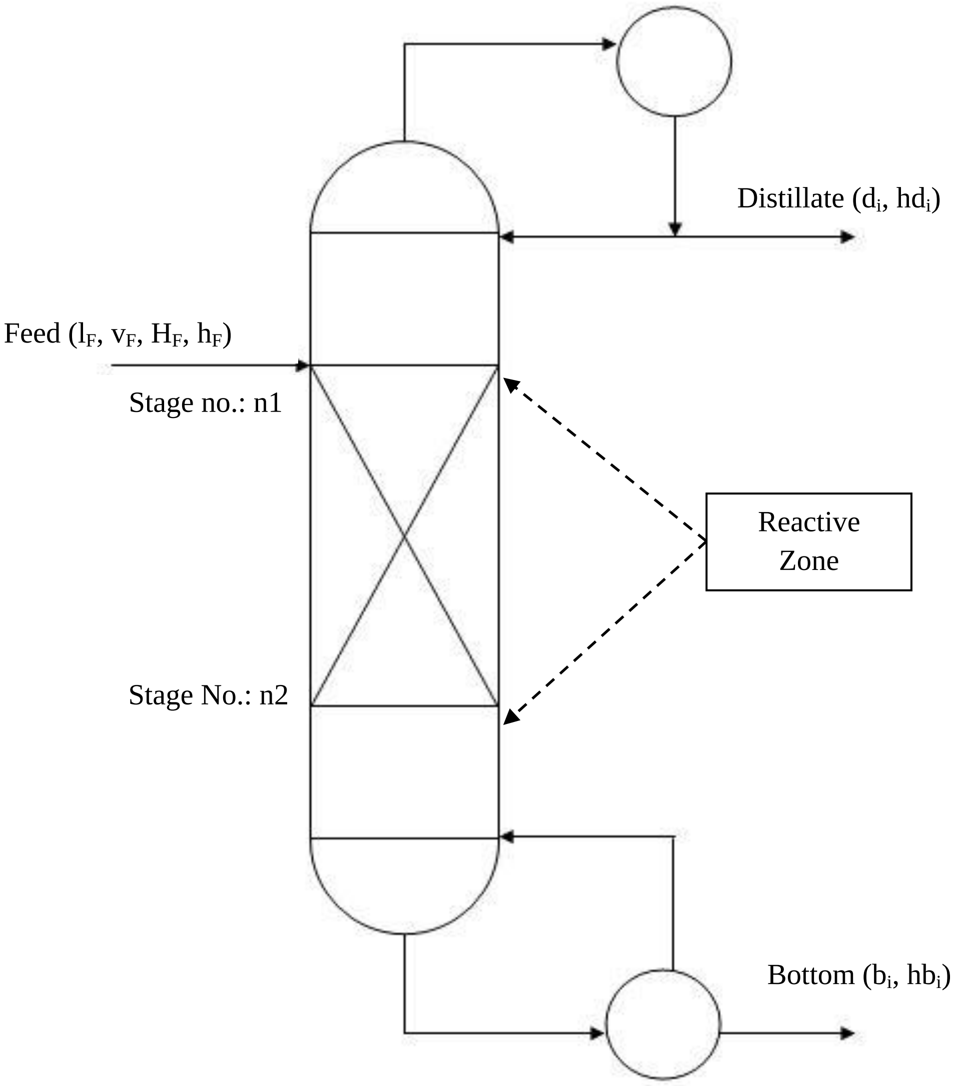

Figure 4.3: RD system

Material Balance

$v_{1,i} - l_{0,i} - v_{0,i} = 0$……………(4.1) for j=0

$v_{j+1,i} - l_{j-1,i} - v_{j,i} - l_{j,i} = 0$……………(4.2) for $1 \leq j \leq n1-2$

$v_{n1,i} - l_{n1-2,i} - v_{n1-1,i} - l_{n1-1,i} = -v_{F,i}$ (4.3) for j=n1-1

$v_{n1+1,i} - l_{n1-1,i} - v_{n1,i} - l_{n1,i} \pm r_i V'_{n1} = -l_{F,i}$ (4.4) for j=n1

$v_{j+1,i} - l_{j-1,i} - v_{j,i} - l_{j,i} \pm r_i V'_j = 0$ (4.5) for $n1+1 \leq j \leq n2$

$v_{j+1,i} - l_{j-1,i} - v_{j,i} - l_{j,i} = 0$ (4.6) for n2+1 $\leq$ j $\leq$ n

$l_{n,i} - v_{n+1,i} - l_{n+1,i} = 0$ (4.7) for j=n+1

Summation Equation

$L_j = \sum_{i=1}^{c} l_{j,i}$ (4.8)

$V_j = \sum_{i=1}^{c} v_{j,i}$ (4.9)

Equilibrium Relationship

$y_{j,i} = K_{j,i}\, x_{j,i}$ (4.10a)

$K_{j,i} = f(T_j, P_j)$ (4.10b)

Heat Balance

$\sum_{i=1}^{c} v_{1,i}H_{1,i} - \sum_{i=1}^{c} l_{0,i}h_{0,i} - \sum_{i=1}^{c} v_{0.i}H_{0,i} - Q_C = 0$ (4.11) for j=0

$\sum_{i=1}^{c} v_{j+1,i}H_{j+1,i} + \sum_{i=1}^{c} l_{j-1,i}h_{j-1,i} - \sum_{i=1}^{c} v_{j,i}H_{j,i} - \sum_{i=1}^{c} l_{j,i}h_{j,i} = 0$ (4.12) for 1 $\leq$ j $\leq$ n1-2

$\sum_{i=1}^{c} v_{n1,i}H_{n1,i} + \sum_{i=1}^{c} l_{n1-2,i}h_{n1-2,i} - \sum_{i=1}^{c} v_{n1-1,i}H_{n1-1,i} + \sum_{i=1}^{c} l_{n1-1,i}h_{n1-1,i} = -\sum_{i=1}^{c} v_{F,i}H_{F,i}$
(4.13) for j=n1-1

$\sum_{i=1}^{c} v_{n1+1,i}H_{n1+1,i} + \sum_{i=1}^{c} l_{n1-1,i}h_{n1-1,i} - \sum_{i=1}^{c} v_{n1,i}H_{n1,i} + \sum_{i=1}^{c} l_{n1,i}h_{n1,i} \pm r_i\,\Delta H_r = -\sum_{i=1}^{c} l_{F,i}h_{F,i}$ (4.14) for j=n1

$\sum_{i=1}^{c} v_{j+1,i}H_{j+1,i} + \sum_{i=1}^{c} l_{j-1,i}h_{j-1,i} - \sum_{i=1}^{c} v_{j,i}H_{j,i} - \sum_{i=1}^{c} l_{j,i}h_{n1,i} \pm r_i\,\Delta H_r = 0$……………(4.15) for n1+1 $\leq$ j $\leq$ n2

$\sum_{i=1}^{c} v_{j+1,i}H_{j+1,i} + \sum_{i=1}^{c} l_{j-1,i}h_{j-1,i} - \sum_{i=1}^{c} v_{j,i}H_{j,i} + \sum_{i=1}^{c} l_{j,i}h_{j,i} = 0$……………(4.16) for n2+1 $\leq$ j $\leq$ n

$\sum_{i=1}^{c} l_{N,i}h_{N,i} - \sum_{i=1}^{c} v_{N+1,i}H_{N+1,i} - \sum_{i=1}^{c} l_{N+1,i}h_{N+1,i} = 0$……………(4.17) for j=n+1

$r_i = f(C_1, C_2, C_3, \dots\dots, C_i, \dots\dots, C_c)$ ……………(4.18)

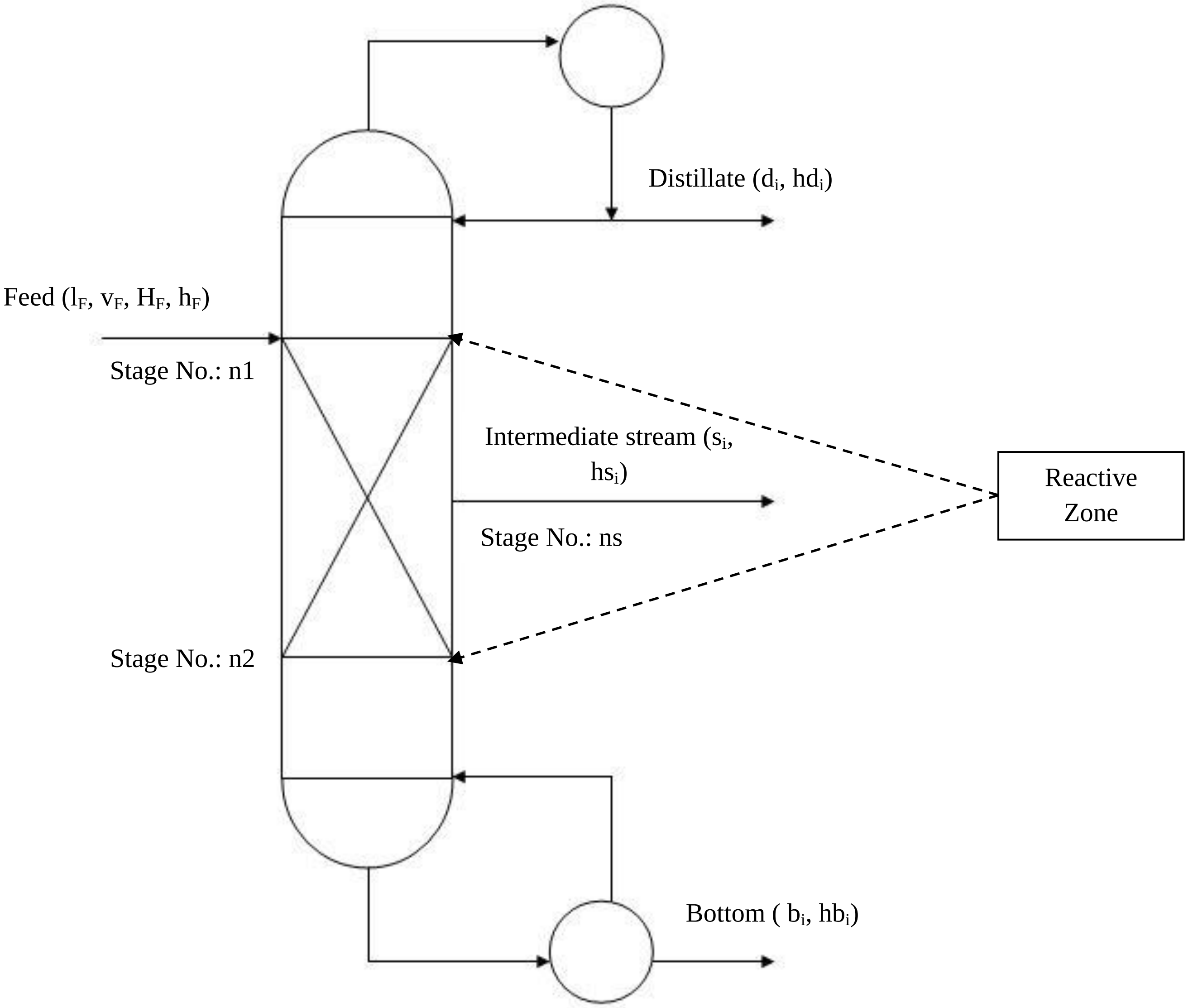

Figure 4.4: RD system with an intermediate side draw

Suppose at j=ns, an intermediate product is withdrawn as a side draw, then the material and energy balance equations tend to be

$v_{ns,i} + l_{ns-2,i} - v_{ns-1,i} - l_{ns-1,i} \pm r_i V'_{ns-1} = l_{s,i}$ ……………(4.19) for j=ns-1

$\sum_{i=1}^{c} v_{ns,i} H_{ns,i} + \sum_{i=1}^{c} l_{ns-2,i} h_{ns-2,i} - \sum_{i=1}^{c} v_{ns-1,i} H_{ns-1,i} - \sum_{i=1}^{c} l_{ns-1,i} h_{ns-1,i} \pm r_i \, \Delta H_r = 0$ ……………(4.20) for j=ns-1

$v_{ns+1,i} + l_{ns-1,i} - v_{ns,i} - l_{ns,i} \pm r_i V'_{ns} = v_{s,i}$ ……………(4.21) for j=ns

$\sum_{i=1}^{c} v_{ns+1,i}H_{ns+1,i} + \sum_{i=1}^{c} l_{ns-2,i}h_{ns-2,i} - \sum_{i=1}^{c} v_{ns-1,i}H_{ns-1,i} - \sum_{i=1}^{c} l_{ns-1,i}h_{ns-1,i} \pm r_i \Delta H_r = 0$……………(4.22) for j=ns

4.2:Reactive divided wall distillation column

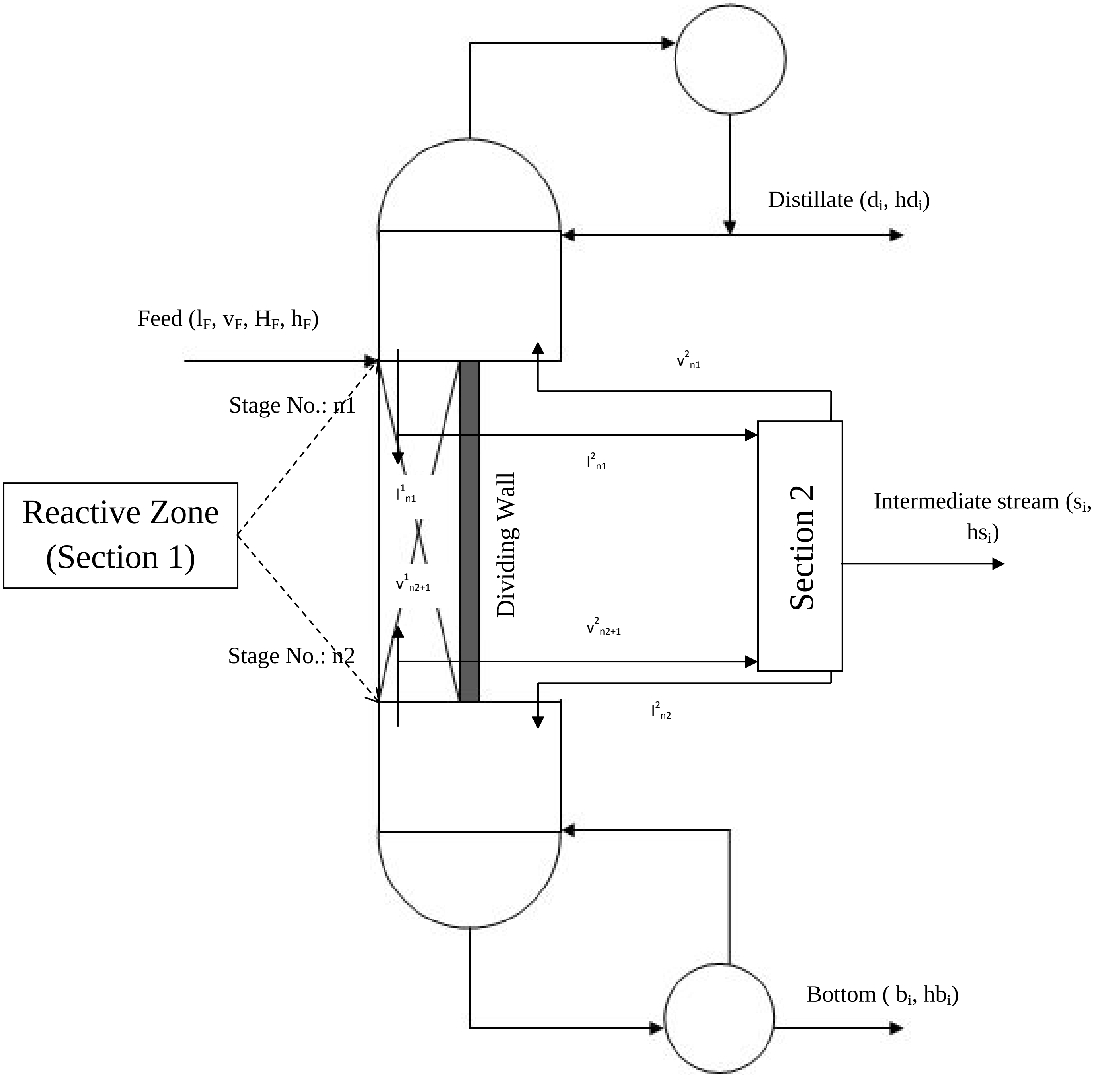

Figure 4.5: Reactive DWC system

Reactive DWC operates efficiently for ternary systems such as:

1) A → B + C with moles of A in excess
2) A + I → B + C with limited moles of A and inert added with the reactants
3) A + B → C with both A and B in excess
4) A + B → C + D with one of the reactants in excess

Material Balance:

For condenser

$v_{1,i} - l_{0,i} - v_{0,i} = 0$……………(4.23) for j=0

For column above the wall

$v_{j+1,i} + l_{j-1,i} - v_{j,i} - l_{j,i} = 0$……………(4.24) for 1 ≤ j ≤ n1-1

Plate at which dividing wall originates

$v^{1}_{n1+1,i} + v^{2}_{n1+1,i} + l_{n1-1,i} - l^{1}_{n1,i} - l^{2}_{n1,i} - v_{n1,i} = -v_{F,i}$……………(4.25) for j=n1

For column 1 section:

$v^{1}_{n1+2} + l^{1}_{n1,i} - v^{1}_{n1+1,i} - l^{1}_{n1+1,i} \pm rV'^{1}_{n1+1} = -l_{F,i}$……………(4.26) for j=n1+1

$v^{1}_{j+1,i} + l^{1}_{j-1,i} - v^{1}_{j,i} - l^{1}_{j,i} \pm rV'^{1}_{j} = 0$……………(4.27) for n1+2 ≤ j ≤ n2-1

For column 2 section:

$v^{2}_{j+1,i} + l^{2}_{j-1,i} - v^{2}_{j,i} - l^{2}_{j,i} = 0$……………(4.28) for n1+1 ≤ j ≤ ns-2

$v^{2}_{ns,i} + l^{2}_{ns-2,i} - v^{2}_{ns-1,i} - l^{2}_{ns-1,i} = l_{s,i}$……………(4.29) for j=ns-1

$v^{2}_{ns+1,i} + l^{2}_{ns-1,i} - v^{2}_{ns,i} - l^{2}_{ns,i} = v_{s,i}$……………(4.30) for j=ns

$v^{2}_{j+1,i} + l^{2}_{j-1,i} - v^{2}_{j,i} - l^{2}_{j,i} = 0$……………(4.31) for ns+1 ≤ j ≤ n2-1

Plate at which the dividing wall ends

$v^1_{n2+1,i} + v^2_{n2+1,i} + l^1_{n2-1,i} + l^2_{n2-1,i} - v^1_{n2,i} - v^2_{n2,i} - l^1_{n2,i} - l^2_{n2.i} \pm rV'^1_{n2,i} = 0$……………(4.32) for j=n2

For the column below the dividing wall

$v_{j+1,i} + l_{j-1,i} - v_{j,i} - l_{j,i} = 0$……………(4.33) for n2+1 ≤ j ≤ n

For reboiler

$l_{n,i} - v_{n+1,i} - l_{n+1,i} = 0$……………(4.34) for j=n+1

Summation equation

$L_j = \sum_{i=1}^{c} l_{j,i}$……………(4.35)

$V_j = \sum_{i=1}^{c} v_{j,i}$……………(4.36)

Equilibrium relationship

$y_{j,i} = K_{j,i}x_{j,i}$……………(4.37a)

$K_{j,i} = f\,(T_j, P_j)$ ……………(4.37b)

Heat Balance

For condenser

$\sum_{i=1}^{c} v_{1,i}H_{1,i} - \sum_{i=1}^{c} l_{0,i}h_{0,i} - \sum_{i=1}^{c} v_{0.i}H_{0,i} - Q_C = 0$……………(4.38) for j=0

For column above the wall

$\sum_{i=1}^{c} v_{j+1,i}H_{j+1,i} + \sum_{i=1}^{c} l_{j-1,i}h_{j-1,i} - \sum_{i=1}^{c} v_{j,i}H_{j,i} - \sum_{i=1}^{c} l_{j,i}h_{j,i} = 0$……………(4.39) for 1 ≤ j ≤ n1-1

Plate at which dividing wall originates

$\sum_{i=1}^{c} v_{n1+1,i}^{1} H_{n1+1,i}^{1} + \sum_{i=1}^{c} v_{n1+1,i}^{2} H_{n1+1,i}^{2} + \sum_{i=1}^{c} l_{n1-1,i} h_{n1-1,i} - \sum_{i=1}^{c} l_{n1,i}^{1} h_{n1,i}^{1} - \sum_{i=1}^{c} l_{n1,i}^{2} h_{n1,i}^{2} - \sum_{i=1}^{c} v_{n1,i} H_{n1,i} = -\sum_{i=1}^{c} v_{F,i} H_{F,i}$……………(4.40) for j=n1

For column 1 section:

$\sum_{i=1}^{c} v_{n1+2,i}^{1} H_{n1+2,i}^{1} + \sum_{i=1}^{c} l_{n1,i}^{1} h_{n1,i}^{1} - \sum_{i=1}^{c} v_{n1+1,i}^{1} H_{n1+1,i}^{1} - \sum_{i=1}^{c} l_{n1+1,i}^{1} h_{n1+1,i}^{1} \pm r_i V'^{1}_{n1+1} \Delta H_{r_{n1+1}} = -\sum_{i=1}^{c} l_{F,i} h_{F,i}$……………(4.41) for j=n1+1

$\sum_{i=1}^{c} v_{j+1,i}^{1} H_{j+1,i}^{1} + \sum_{i=1}^{c} l_{j-1,i}^{1} h_{j-1,i}^{1} - \sum_{i=1}^{c} v_{j,i}^{1} H_{j,i}^{1} - \sum_{i=1}^{c} l_{j,i}^{1} h_{j,i}^{1} \pm r_i V'^{1}_{j} \Delta H_{r_j} = 0$……………(4.42) for n1+2 $\leq$ j $\leq$ n2-1

For column 2 section:

$\sum_{i=1}^{c} v_{j+1,i}^{2} H_{j+1,i}^{2} + \sum_{i=1}^{c} l_{j-1,i}^{2} h_{j-1,i}^{2} - \sum_{i=1}^{c} v_{j,i}^{2} H_{j,i}^{2} - \sum_{i=1}^{c} l_{j,i}^{2} h_{j,i}^{2} = 0$……………(4.43) for n1+1 $\leq$ j $\leq$ ns-2

$\sum_{i=1}^{c} v_{ns,i}^{2} H_{ns,i}^{2} + \sum_{i=1}^{c} l_{ns-2,i}^{2} h_{ns-2,i}^{2} - \sum_{i=1}^{c} v_{ns-1,i}^{2} H_{ns-1,i}^{2} - \sum_{i=1}^{c} l_{ns-1,i}^{2} h_{ns-1,i}^{2} = \sum_{i=1}^{c} l_{S,i} h_{S,i}$……………(4.44) for j=ns-1

$\sum_{i=1}^{c} v_{ns+1,i}^{2} H_{ns+1,i}^{2} + \sum_{i=1}^{c} l_{ns-1,i}^{2} h_{ns-1,i}^{2} - \sum_{i=1}^{c} v_{ns,i}^{2} H_{ns,i}^{2} - \sum_{i=1}^{c} l_{ns,i}^{2} h_{ns,i}^{2} = \sum_{i=1}^{c} v_{S,i} H_{S,i}$……………(4.45) for j=ns

$\sum_{i=1}^{c} v_{j+1,i}^{2} H_{j+1,i}^{2} + \sum_{i=1}^{c} l_{j-1,i}^{2} h_{j-1,i}^{2} - \sum_{i=1}^{c} v_{j,i}^{2} H_{j,i}^{2} - \sum_{i=1}^{c} l_{j,i}^{2} h_{j,i}^{2} = 0$……………(4.46) for ns+1 $\leq$ j $\leq$ n2-1

Plate at which the dividing wall ends

$\sum_{i=1}^{c} v_{n2+1,i}^{1} H_{n2+1,i}^{1} + \sum_{i=1}^{c} v_{n2+1,i}^{2} H_{n2+1,i}^{2} + \sum_{i=1}^{c} l_{n2-1,i}^{1} h_{n2-1,i}^{1} + \sum_{i=1}^{c} l_{n2-1,i}^{2} h_{n2-1,i}^{2} - \sum_{i=1}^{c} v_{n2,i}^{1} H_{n2,i}^{2} - \sum_{i=1}^{c} v_{n2,i}^{2} H_{n2,i}^{2} - \sum_{i=1}^{c} l_{n2,i}^{1} h_{n2,i}^{1} - \sum_{i=1}^{c} l_{n2,i}^{2} h_{n2,i}^{2} \pm r_i V'^{1}_{n2} \Delta H_{r_{n2}} = 0$……………(4.47) for j=n2

For the column below the dividing wall

$\sum_{i=1}^{c} v_{j+1,i}H_{j+1,i} + \sum_{i=1}^{c} l_{j-1,i}h_{j-1,i} - \sum_{i=1}^{c} v_{j,i}H_{j,i} - \sum_{i=1}^{c} l_{j,i}h_{j,i} = 0$……………(4.48)
for n2+1 $\leq$ j $\leq$ n

For reboiler

$\sum_{i=1}^{c} l_{N,i}h_{N,i} - \sum_{i=1}^{c} v_{N+1,i}H_{N+1,i} - \sum_{i=1}^{c} l_{N+1,i}h_{N+1,i} = 0$……………(4.49) for j=n+1

$r_i = f(C_1, C_2, C_3, \dots\dots, C_i, \dots\dots, C_c)$ ……………(4.50)

For several systems of RDC, the pressure at the plates are assumed to be constant as the operating pressure or the top condenser pressure, or it can be assumed to be constant pressure drop across each plate. In the present analysis, we have considered the pressure drop relation [42]. Here, the pressure drop is considered to comprise weir height pressure drop, over weir height pressure drop, dry plate pressure drop and residual head pressure drop. The equation is as shown below:

$(P_j - P_{j-1}) - \rho_L\, g\, h_{tj} = 0$……….(4.51) for j=1, 2, 3,……..,(n+1)

Where h_{tj}= (h_w + h_{ow} + h_d + h_r)…………..(4.52a)

h_{tj} denotes the liquid head between the j'th plate and (j-1)'th plate, h_w is the pressure head created by weir height, h_{ow} is the pressure head created by over weir height, h_d is the dry plate pressure drop and h_r is the residual head pressure drop.

These heads can be calculated by equations given below as presented by Lockett:

$h_{ow} = f1(L_j, W_L)$ ……….(4.52b)

$h_d = f2(V_j, t_p, d_h)$ ……….(4.52c)

$h_r = f3(\sigma_L, t_p, d_h)$ ……….(4.52d)

Where W_L is the weir length, d_H is the hole diameter, t_p is the plate thickness and σ_L is the surface tension of the liquid.

In the case of the reboiler such as n to n+1 plates, the pressure drop equation transforms into

$(P_{N+1} - P_N) - \Delta P_{Re} = 0$………(4.53a)

Where ΔPre is the reboiler pressure drop and is given by the following equation:

$$\Delta P_{Re} = \frac{f^0\ G_S^2\ D_S\ (N_{pass}+1)}{2g\rho D_e \varphi_S}\text{………(4.53b)}$$

Where f^o is the friction factor, D_s is the shell side diameter, N_{pass} is the number of passes, ρ is the density, D_e is the equivalent diameter and φ_s is the ratio of viscosity of liquid to the viscosity of water.

4.3: Degree of freedom analysis

Table 4.1: Degree of freedom analysis table for RD system

Equation No.	Total Variables	Independent Variables	Dependent Variables	Total No. of Independent Variables	Total No. of Independent Equations
4.1 to 4.7	$v_{j,i}$, $l_{j,i}$, $v_{F,I}$, r_i, V'_j, $l_{F,i}$	$v_{j,I}$, $l_{j,I}$, $v_{F,I}$, ,V'_j	$l_{F,I}$, r_i	2(n+2)C+C+(n2-n1+1)	(n+2)C
4.8 to 4.9	L_j, V_j	-	L_j, V_j	-	-
4.10a and 4.10b	T_j, P_j, $K_{j,I}$, $y_{j,I}$, $x_{j,i}$	T_j,P_j (j=2….(N+2)	$K_{j,I}$, $y_{j,I}$, $x_{j,i}$	2(n+2) -2	(n+2)C-C
4.11 to 4.17	R, Q_c, P_0, T_F, Q_b, $h_{j,I}$, $H_{j,I}$, $h_{F,I}$, $H_{F,I}$, ΔH_{rj}	R, Q_c, P_0, T_F, Q_b	$h_{j,I}$, $H_{j,I}$, $h_{F,I}$, $H_{F,I}$, ΔH_{rj}	5	(n+2)+C
Total				2(n+2)(C+1)+C+3+ (n2-n1+1)	2(n+2)C +(n+2)

Degree of freedom (DOF) = (Total No. of Independent Variables) – (Total No. of Independent Equations) = (n+2) + C +3+ (n2-n1+1)

Considering n+2 independent equations, the DOF of the system tends to be C+3. Feed compositions and feed temperature are taken as input parameters which provide C+1 independent variables and DOF of the system get reduced to ((C+3)-(C+1)) = 2+ (n2-n1+1)

Considering RD with one intermediate product, one new independent variable is added such as total side draw flow (S) which increases the DOF to 3+ (n2-n1+1).

Table 4.2: Degree of freedom analysis table for reactive DWC system

Equation No.	Total Variables	Independent Variables	Dependent Variables	Total No. of Independent Variables	Total No. of Independent Equations
4.23 to 4.34	$v_{j,i}$, $l_{j,i}$, $v_{F,i}$, $l_{F,i}$, r_i, V'_j, $L2_{n1}$, $V2_{n2+1}$, S	$v_{j,i}$, $l_{j,i}$, $v_{F,i}$, $L2_{n1}$, $V2_{n2+1}$, S, V'_j	$l_{F,i}$, r_i	2(n+2)C+C+3+(n2-n1+1)	(n+2)C
4.35 to 4.36	L_j, V_j	-	L_j, V_j	-	-
4.37a and 4.37b	T_j, P_j, $K_{j,i}$, $y_{j,i}$, $x_{j,i}$	T_j,P_j (j=2….(N+2))	$K_{j,i}$, $y_{j,i}$, $x_{j,i}$	2(n+2) -2	(n+2)C-C
4.38 to 4.49	R, Q_c, P_0, TF, Q_b, $h_{j,i}$, $H_{j,i}$, $h_{F,i}$, $H_{F,i}$, ΔH_{rj}	R, Q_c, P_0, T_F, Q_b	$h_{j,i}$, $H_{j,i}$, $h_{F,i}$, $H_{F,i}$, ΔH_{rj}	5	(n+2)+C
Total				2(n+2)(C+1)+C+6+ (n2-n1+1)	(n+2)(2C+1)

Degrees of freedom = (Total Number of Independent Variables) - (Total Number of Independent Equations) = (n+2) + C + 6+ (n2-n1+1)

Considering n+2 independent equations, the DOF of the system tends to be C+3. Feed compositions and feed temperature are taken as input parameters which provide C+1 independent variables, and the DOF of the system get reduced to ((C+6)-(C+1)) = 5+ (n2-n1+1)

If condenser pressure (P_0) is known, then the DOF decreases to 4+ (n2-n1+1).

CHAPTER- 5

METHODOLOGY

5.1: Process Simulations

This chapter describes the simulation procedure for DME synthesis in a reactive DWC. The total number of stages in a R-DWC unit were taken to be 35, and were divided into three sections: an upper rectification zone, a central reactive zone, and a lower stripping zone. The reactive zone was consisted of the stages numbering stage 8 to 31 on the feed side, a common stripping section (stages 32 to 35) and a common rectifying zone (stages 1 to 7). The stages are numbered from the top to the bottom, with stage 1 as the condenser and stage 35 as the reboiler. Methanol is fed in the rectifying section at stage 8, i.e. at the top of the reactive zone. Dividing wall is placed at stage 8 and extends up to stage 31. The DWC is operated at 10 bar pressure. DME and water rich streams (products) are obtained in column 1. The purity of the recovered methanol stream that is recycled is high (95 mole %) and is obtained at stage 22 in the post-fractionator. The reaction takes place in liquid phase.

Fig. 5.1 shows the residue curve of the mixture DME-MeOH-H_2O. Residue curve analysis is quite useful in studying ternary system. The ternary mixture of components MeOH, DME, and H_2O, has constant relative volatiles of DME (=4), MeOH (=3), and H_2O (=2). The initial composition of the liquid feed stream is X_{MeOH}=1.0, X_{DME}= 0 and X_{H2O}= 0

The residue curves start at the lightest component and move toward the heaviest component.

The light components go out from the top, and the heavy components, go out from the bottom. Residue curve gives the feasible separation in a column and is satisfied that the distillate compositions x_{Dj} and the bottoms compositions x_{Bj} lie near a residue curve and lie on a straight line through the feed composition point z_j.

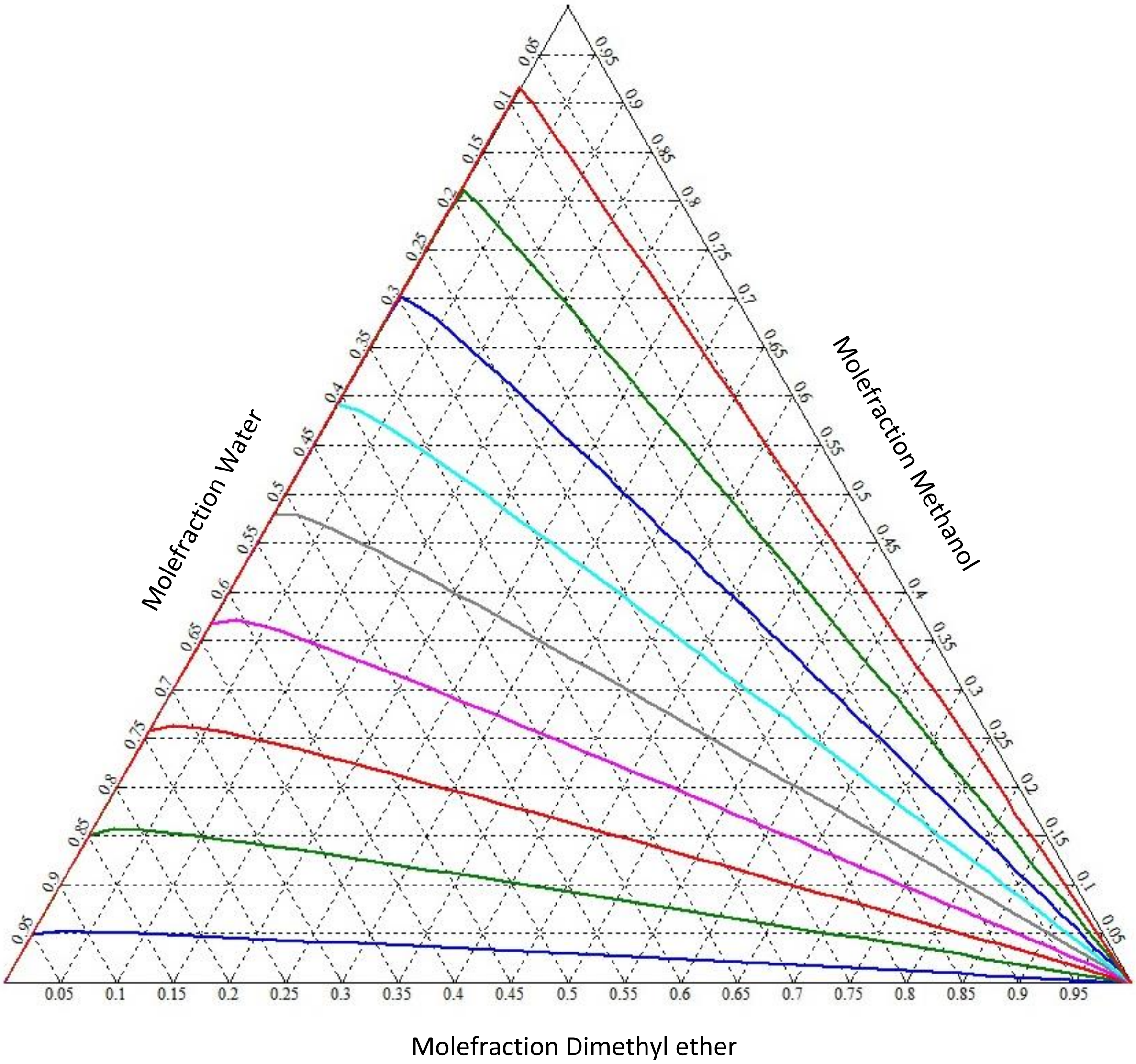

Figure 5.1: Residue curve for Dimethyl ether, Methanol and Water

For simulation, the two thermally coupled RADFRAC units are used as a reactive DWC system (Figure 5.2)

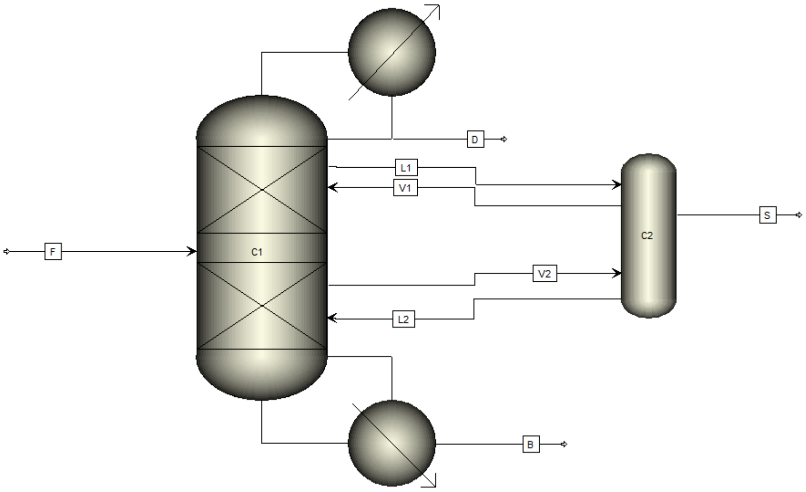

Figure 5.2: Two thermally coupled RADFRAC units

The UNIQUAC- REDLICH-KWONG model is used for the calculation of VLE data and physical properties.
Redlich-Kwong equation of state (EOS):

The Redlich-Kwong EOS can calculate vapor phase thermodynamic properties for the following property methods: NRTL-RK,UNIFAC, UNIF-LL, UNIQ-RK, VANL-RK, and WILS-RK. It is applicable for systems at low to moderate pressures (maximum pressure 10 atm) for which the vapor-phase non-ideality is small. The Hayden-O'Connell model is recommended for a more nonideal vapor phase, such as in systems containing organic acids. It is not recommended for calculating liquid phase properties.

The RK EOS is:

$$P = \frac{RT}{V_m - b} - \frac{a/T^{0.5}}{V_m(V_m + b)} \text{……….(5.1)}$$

Where

$$\sqrt{a} = \sum_i x_i \sqrt{a_i} \text{…….. (5.2a)}$$

$$b = \sum_i x_i b_i \text{…….. (5.2b)}$$

$a_i = {}^{0.42748023\, R^2 T_{ci}^{2.5}}\!/_{P_{ci}}$ …….. (5.2c)

$b_i = {}^{0.08664035\, R\, T_{ci}}\!/_{P_{ci}}$ …….. (5.2d)

UNIQUAC Activity Coefficient model:

The UNIQUAC model calculates liquid activity coefficients for the property methods: UNIQUAC, UNIQ-2, UNIQ-HOC, UNIQ-NTH, and UNIQ-RK. It is recommended for highly non-ideal chemical systems, and can be used for VLE and LLE applications. This model can also be used in the advanced EOS mixing rules, such as Wong-Sandler and MHV2.

The equation for the UNIQUAC model is:

$\ln \gamma_i = \ln \frac{\varphi_i}{x_i} + \frac{z}{2}\, q_i' \ln \frac{\theta_i}{\varphi_i} - q_i' \ln t_i' - q_i' \sum_j {}^{\theta_j' \tau_{i,j}}\!/_{t_j'} + \; l_i + q_i' - \frac{\varphi_i}{x_i} \sum_j x_j l_j$ …….(5.3)

Where:

$\theta_i = {}^{q_i x_i}\!/_{q_T}\,;\; q_T = \sum_k q_k x_k$ ……..(5.4a)

$\theta_i' = {}^{q_i' x_i}\!/_{q_T'}\,;\; q_T' = \sum_k q_k' x_k$ ……..(5.4b)

$\varphi_i = {}^{r_i x_i}\!/_{r_T}\,;\; r_T = \sum_k r_k x_k$ ……..(5.4c)

$l_i = \frac{z}{2}(r_i - q_i) + 1 - \; r_i$ ……..(5.4d)

$t_i' = \sum_k \theta_k' \tau_{ki}$ ……..(5.4e)

$\tau_{ij} = \exp(a_{ij} + {}^{b_{ij}}\!/_{T} + C_{ij} \ln T + d_{ij} T + {}^{e_{ij}}\!/_{T^2})$ ……..(5.4f)

$z = 10$ ……..(5.4g)

Here, aij, bij, cij, and dij are unsymmetrical. That is, aij may not be equal to aji, etc. Absolute temperature units are assumed for the binary parameters a_{ij}, b_{ij}, c_{ij}, d_{ij}, and e_{ij} can be determined from VLE and/or LLE data regression. The Aspen Physical Property System has a large number of built-in parameters for the UNIQUAC model. The binary parameters have been regressed using VLE and LLE data from the Dortmund Databank of Gmehling. The binary parameters for VLE applications were regressed using the ideal gas, Redlich-Kwong, and Hayden-O'Connell EOS.

Aspen PLUS provides its own data bank which consists of several physical property data for different pure components at every temperature and pressure. During component specifications, the chemical components that are to be used for simulation purposes are provided.
The snapshot (Figure 5.3) below clearly explains the situation.

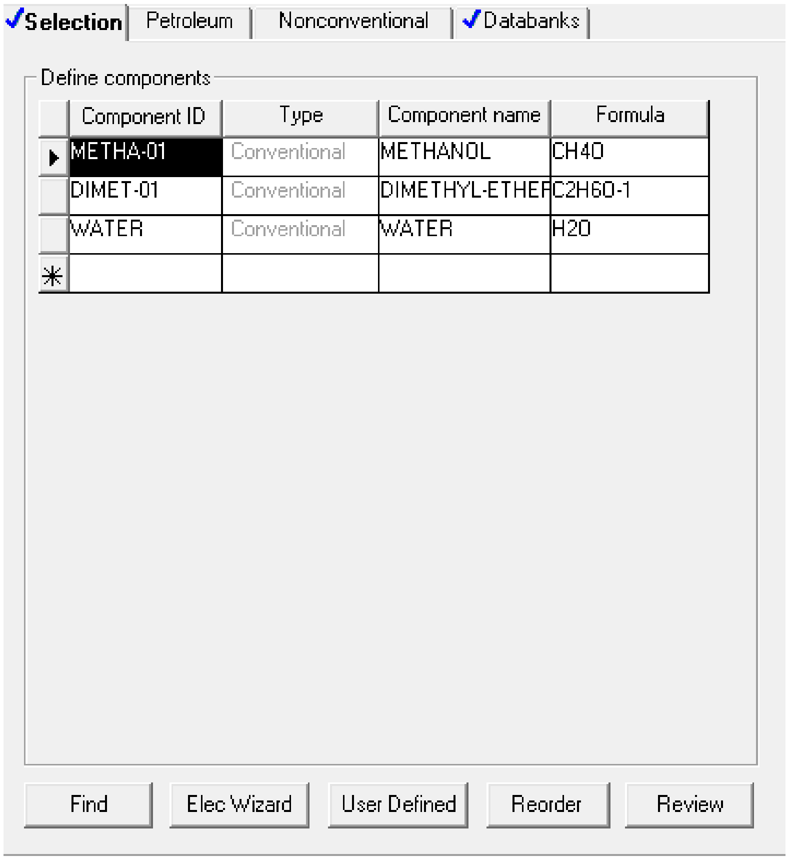

Component ID	Type	Component name	Formula
METHA-01	Conventional	METHANOL	CH4O
DIMET-01	Conventional	DIMETHYL-ETHER	C2H6O-1
WATER	Conventional	WATER	H2O

Figure 5.3: Aspen PLUS window to define component specifications

Aspen PLUS calculates itself the degrees of freedom for the process as given in the flow sheet (Figure 5.4) and takes input to perform the simulation. For input to the column, the stream property is to be defined by us consisting of several inputs such as temperature, pressure, total flow and component flow or flow fraction. The snapshot below (Figure 5.5) clearly explains the scenerio.

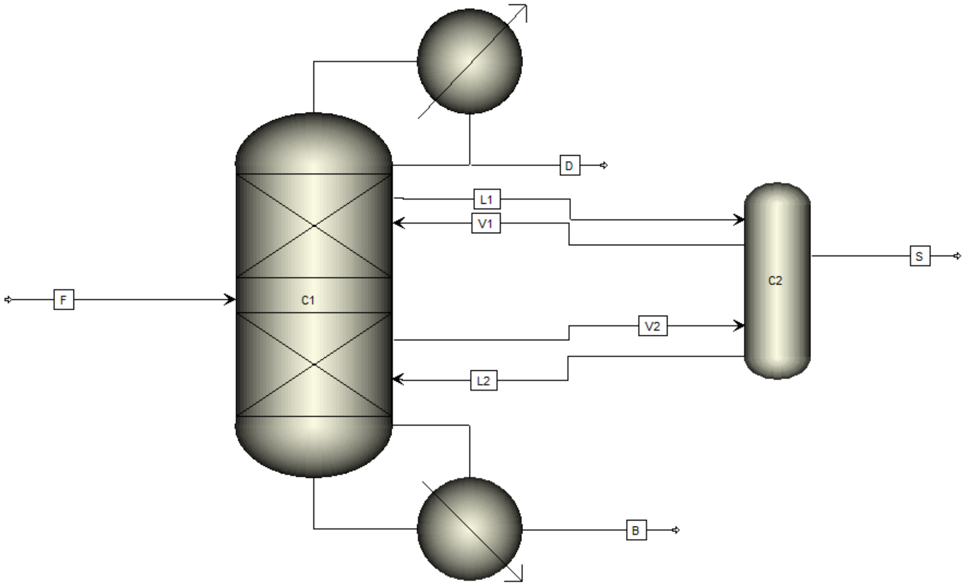

Figure 5.4: Aspen PLUS system of reactive DWC

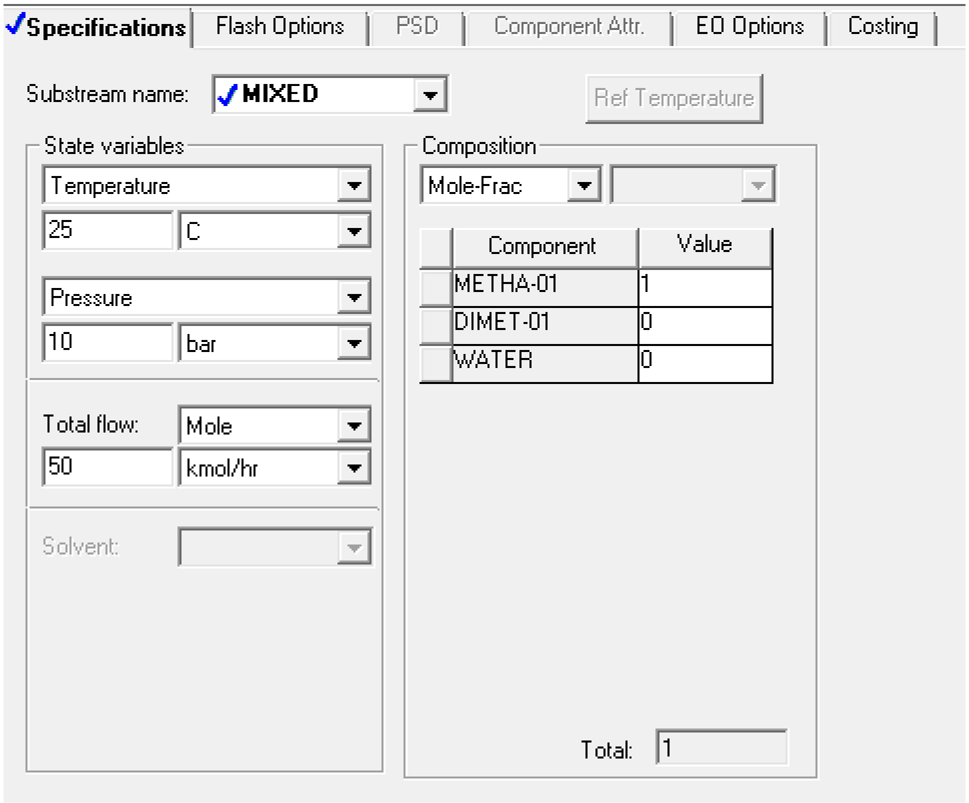

Substream name: MIXED

State variables

Temperature: 25 C

Pressure: 10 bar

Total flow: Mole 50 kmol/hr

Solvent:

Composition: Mole-Frac

Component	Value
METHA-01	1
DIMET-01	0
WATER	0

Total: 1

Figure 5.5: Aspen PLUS window to define feed specification

As shown in the flow diagram above, it consists of two Radfrac columns C1 and C2, thermally coupled to give thermodynamically equivalent system of a DWC. Aspen PLUS takes input to both the columns which consists of the number of stages, feed tray location stage, product stream flow rates and their stages, operating pressure and many others. The snapshots below (Figure 5.6) clearly explain this matter

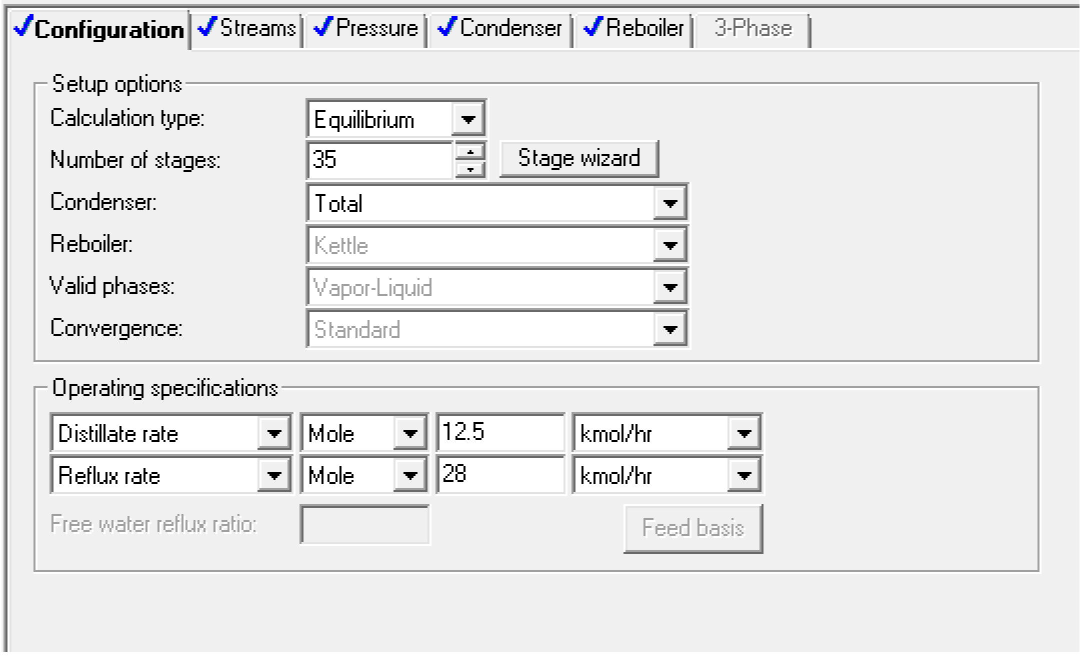

Setup options

Calculation type: Equilibrium
Number of stages: 35
Condenser: Total
Reboiler: Kettle
Valid phases: Vapor-Liquid
Convergence: Standard

Operating specifications

Distillate rate	Mole	12.5	kmol/hr
Reflux rate	Mole	28	kmol/hr

Free water reflux ratio:

Figure 5.6a: Aspen PLUS window to define column 1 specifications

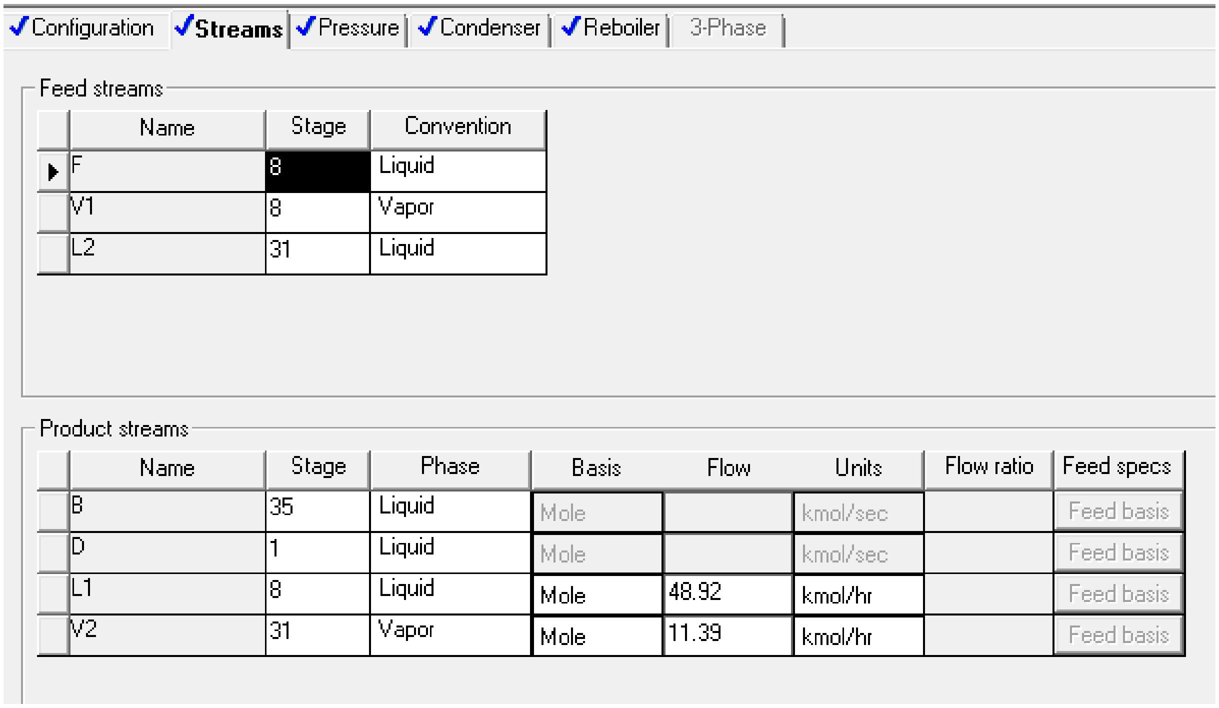

Feed streams

Name	Stage	Convention
F	8	Liquid
V1	8	Vapor
L2	31	Liquid

Product streams

Name	Stage	Phase	Basis	Flow	Units	Flow ratio	Feed specs
B	35	Liquid	Mole		kmol/sec		Feed basis
D	1	Liquid	Mole		kmol/sec		Feed basis
L1	8	Liquid	Mole	48.92	kmol/hr		Feed basis
V2	31	Vapor	Mole	11.39	kmol/hr		Feed basis

Figure 5.6b: Aspen PLUS window to define column 1 specifications

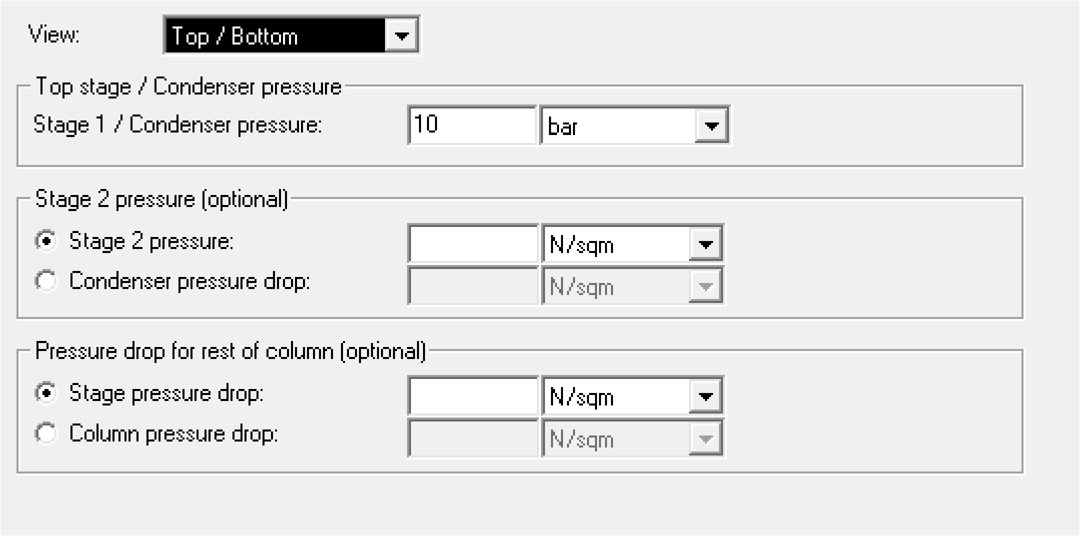

View: Top / Bottom

Top stage / Condenser pressure
Stage 1 / Condenser pressure: 10 bar

Stage 2 pressure (optional)
● Stage 2 pressure: N/sqm
○ Condenser pressure drop: N/sqm

Pressure drop for rest of column (optional)
● Stage pressure drop: N/sqm
○ Column pressure drop: N/sqm

Figure 5.6c: Aspen PLUS window to define column 1 specifications

For column 1, some trays are set as reactive zone which process RD to perform separation and reaction process simultaneously. The snapshots below (Figure 5.7) exhibit this scenario:

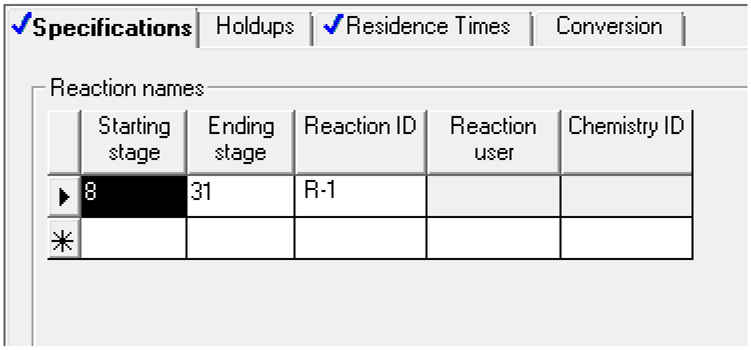

Reaction names

Starting stage	Ending stage	Reaction ID	Reaction user	Chemistry ID
8	31	R-1		

Figure 5.7: Aspen PLUS window to define column 1 reaction specifications

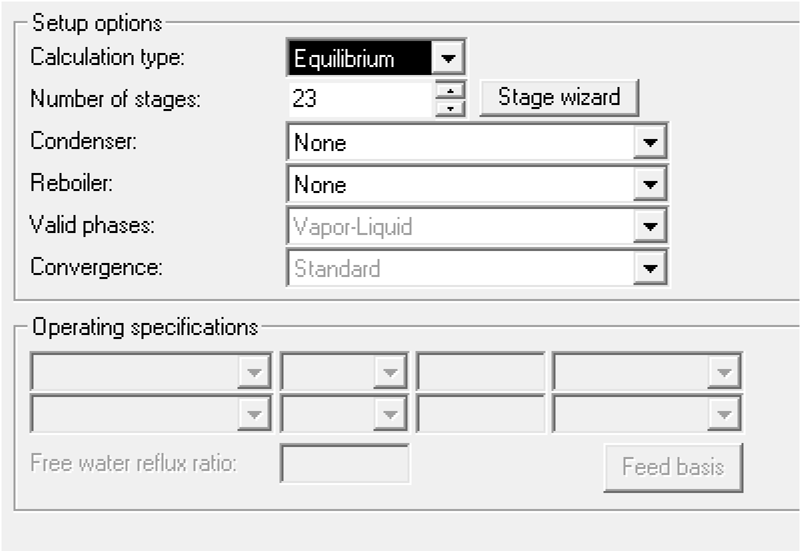

Setup options
Calculation type: Equilibrium
Number of stages: 23
Condenser: None
Reboiler: None
Valid phases: Vapor-Liquid
Convergence: Standard

Operating specifications
Free water reflux ratio:

Figure 5.8a: Aspen PLUS window to define column 2 specifications

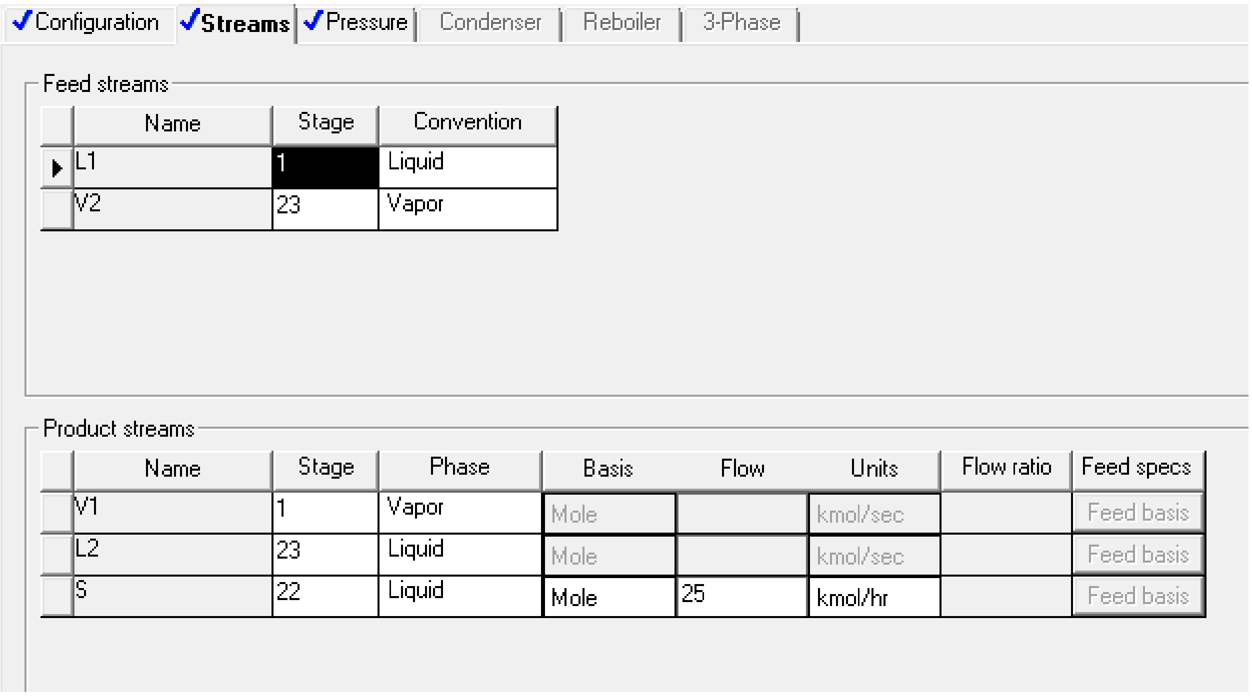

Feed streams

Name	Stage	Convention
L1	1	Liquid
V2	23	Vapor

Product streams

Name	Stage	Phase	Basis	Flow	Units	Flow ratio	Feed specs
V1	1	Vapor	Mole		kmol/sec		Feed basis
L2	23	Liquid	Mole		kmol/sec		Feed basis
S	22	Liquid	Mole	25	kmol/hr		Feed basis

Figure 5.8b: Aspen PLUS window to define column 2 specifications

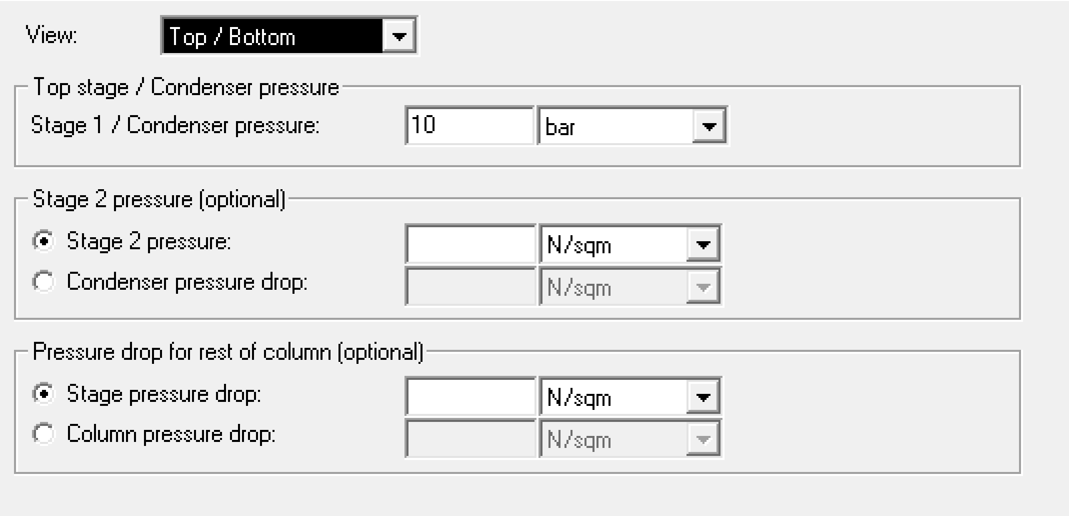

View: Top / Bottom

Top stage / Condenser pressure

Stage 1 / Condenser pressure: 10 bar

Stage 2 pressure (optional)

● Stage 2 pressure: N/sqm

○ Condenser pressure drop: N/sqm

Pressure drop for rest of column (optional)

● Stage pressure drop: N/sqm

○ Column pressure drop: N/sqm

Figure 5.8c: Aspen PLUS window to define column 2 specifications

In Aspen PLUS, one can provide the reaction scheme to calculate its molar conversion such as the disappearance for the reactant and the formation of the products. The snapshots below (Figure 5.9) shows this situation.

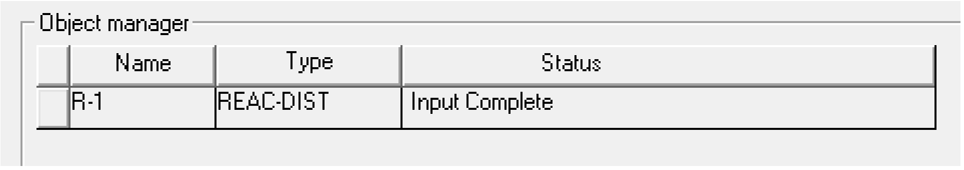

Object manager

Name	Type	Status
R-1	REAC-DIST	Input Complete

Figure 5.9: Aspen PLUS window to define RD system

REAC-DIST specifies the RD process.

The reaction that is to be used is as shown in Figure 5.10

Rxn No.	Reaction type	Stoichiometry
1	Kinetic	2 METHA-01 --> DIMET-01 + WATER

Figure 5.10: Aspen PLUS window to define the reaction

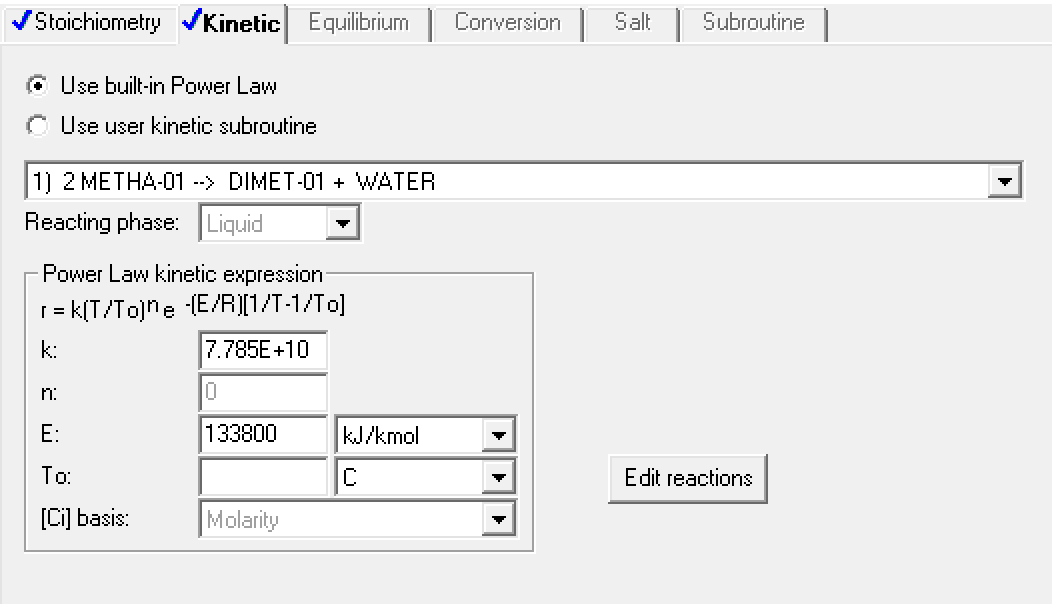

● Use built-in Power Law
○ Use user kinetic subroutine

1) 2 METHA-01 --> DIMET-01 + WATER

Reacting phase: Liquid

Power Law kinetic expression

$r = k(T/To)^n e^{-(E/R)[1/T-1/To]}$

k: 7.785E+10
n: 0
E: 133800 kJ/kmol
To: C
[Ci] basis: Molarity

Figure 5.11: Aspen PLUS window to define kinetic parameters for the reaction

The built-in power law expression can be used to provide the kinetic parameters and the rate of formation of product for the reaction. In case the rate expression is quite complex, one has to use the kinetic subroutine for calculation of kinetic parameters or rate expression. The power law expression depends on the concentration basis one selects in the [Ci] Basis list box:

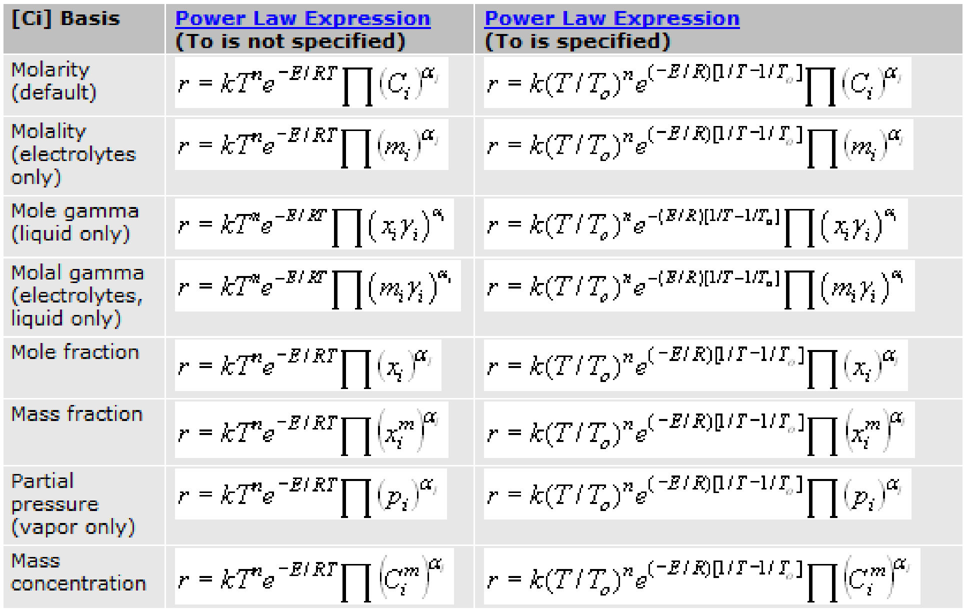

[Ci] Basis	Power Law Expression (To is not specified)	Power Law Expression (To is specified)
Molarity (default)	$r = kT^n e^{-E/RT} \prod (C_i)^{\alpha_i}$	$r = k(T/T_o)^n e^{(-E/R)[1/T - 1/T_o]} \prod (C_i)^{\alpha_i}$
Molality (electrolytes only)	$r = kT^n e^{-E/RT} \prod (m_i)^{\alpha_i}$	$r = k(T/T_o)^n e^{(-E/R)[1/T - 1/T_o]} \prod (m_i)^{\alpha_i}$
Mole gamma (liquid only)	$r = kT^n e^{-E/RT} \prod (x_i \gamma_i)^{\alpha_i}$	$r = k(T/T_o)^n e^{-(E/R)[1/T - 1/T_o]} \prod (x_i \gamma_i)^{\alpha_i}$
Molal gamma (electrolytes, liquid only)	$r = kT^n e^{-E/RT} \prod (m_i \gamma_i)^{\alpha_i}$	$r = k(T/T_o)^n e^{-(E/R)[1/T - 1/T_o]} \prod (m_i \gamma_i)^{\alpha_i}$
Mole fraction	$r = kT^n e^{-E/RT} \prod (x_i)^{\alpha_i}$	$r = k(T/T_o)^n e^{(-E/R)[1/T - 1/T_o]} \prod (x_i)^{\alpha_i}$
Mass fraction	$r = kT^n e^{-E/RT} \prod (x_i^m)^{\alpha_i}$	$r = k(T/T_o)^n e^{(-E/R)[1/T - 1/T_o]} \prod (x_i^m)^{\alpha_i}$
Partial pressure (vapor only)	$r = kT^n e^{-E/RT} \prod (p_i)^{\alpha_i}$	$r = k(T/T_o)^n e^{(-E/R)[1/T - 1/T_o]} \prod (p_i)^{\alpha_i}$
Mass concentration	$r = kT^n e^{-E/RT} \prod (C_i^m)^{\alpha_i}$	$r = k(T/T_o)^n e^{(-E/R)[1/T - 1/T_o]} \prod (C_i^m)^{\alpha_i}$

Figure 5.12: Aspen PLUS power law expressions used for the calculation

The units of the reaction rate and the pre-exponential factor depend on the:

- Order of the reaction
- Holdup basis used by the distillation block
- Concentration basis selected in the [Ci] Basis list box

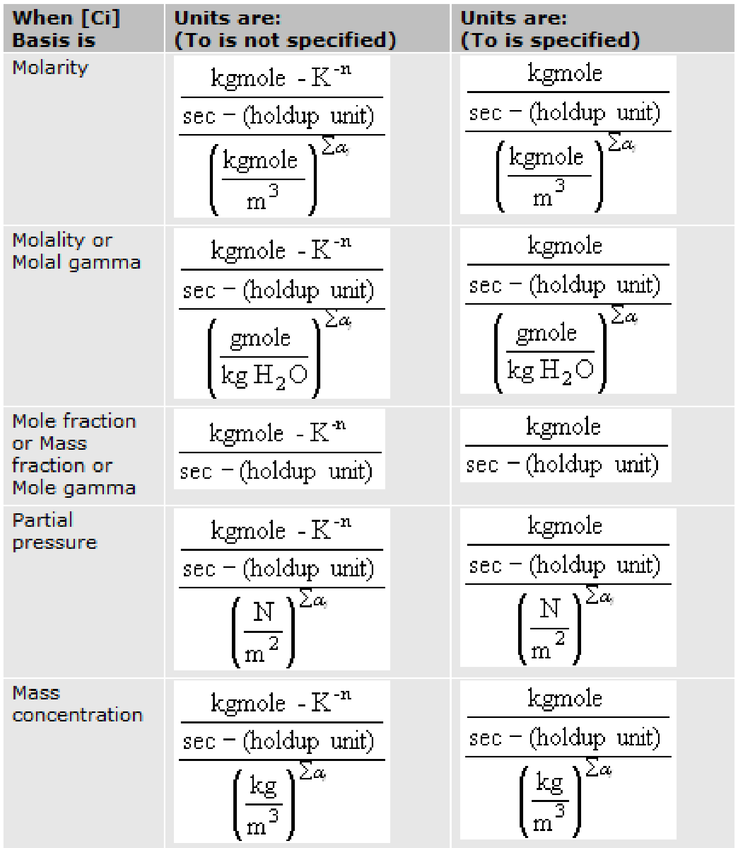

When [Ci] Basis is	Units are: (To is not specified)	Units are: (To is specified)
Molarity	$\frac{\text{kgmole - K}^{-n}}{\text{sec} - (\text{holdup unit}) \left(\frac{\text{kgmole}}{\text{m}^3}\right)^{\Sigma\alpha}}$	$\frac{\text{kgmole}}{\text{sec} - (\text{holdup unit}) \left(\frac{\text{kgmole}}{\text{m}^3}\right)^{\Sigma\alpha}}$
Molality or Molal gamma	$\frac{\text{kgmole - K}^{-n}}{\text{sec} - (\text{holdup unit}) \left(\frac{\text{gmole}}{\text{kg H}_2\text{O}}\right)^{\Sigma\alpha}}$	$\frac{\text{kgmole}}{\text{sec} - (\text{holdup unit}) \left(\frac{\text{gmole}}{\text{kg H}_2\text{O}}\right)^{\Sigma\alpha}}$
Mole fraction or Mass fraction or Mole gamma	$\frac{\text{kgmole - K}^{-n}}{\text{sec} - (\text{holdup unit})}$	$\frac{\text{kgmole}}{\text{sec} - (\text{holdup unit})}$
Partial pressure	$\frac{\text{kgmole - K}^{-n}}{\text{sec} - (\text{holdup unit}) \left(\frac{\text{N}}{\text{m}^2}\right)^{\Sigma\alpha}}$	$\frac{\text{kgmole}}{\text{sec} - (\text{holdup unit}) \left(\frac{\text{N}}{\text{m}^2}\right)^{\Sigma\alpha}}$
Mass concentration	$\frac{\text{kgmole - K}^{-n}}{\text{sec} - (\text{holdup unit}) \left(\frac{\text{kg}}{\text{m}^3}\right)^{\Sigma\alpha}}$	$\frac{\text{kgmole}}{\text{sec} - (\text{holdup unit}) \left(\frac{\text{kg}}{\text{m}^3}\right)^{\Sigma\alpha}}$

Figure 5.13: Aspen PLUS power law expression units

The units for the pre-exponential factor are as follows:

Where holdup unit is	When this is specified in the distillation block that uses the reactions
kgmole	Mole holdup or residence time
kg	Mass holdup
m^3	Volume holdup

The Catalyst System and the Reaction Rate Expression:

In the present problem, we use the macroporous sulphonic acid ion exchange resin as the catalyst and the rate expression as given by researchers [43] in power law rate expression form:

$r = kWcat[MeOH]^m[H2O]^n$

where, A is the Arrhenius factor (A = 5.19×109m^3 kg cat^{-1} s^{-1}), Ea is the activation energy (133.8 kJ mol^{-1}), and m and n are the orders of reaction with respect to methanol and water, respectively (m = 1.51 and n = −0.51). The reaction takes place only in the liquid phase. 15 kg catalyst is being used for the simulation purposes.

For the complex rate equation such as that of dehydration of methanol to dimethyl ether over gamma-alumina catalyst, one requires user kinetic subroutine to perform the simulation process. The rate expression is

$$-r_m = \frac{kK_m{}^2[P_m{}^2 - (P_w P_d/K_{eq})]}{[1 + 2(K_m P_m)^{1/2} + K_w P_w]^4}$$

The subroutine code is written in FORTRAN programming background which calculates the rate of different compositions for RD process. The code is verified using programming in C++. The code is given in the Appendix.

The simulation is run for a number of variations in the input parameters giving different results with the constraint of material and energy balances for the each and every unit involved in the process.

For the feasible operation of a DWC, the pressure drop on both the sides of the dividing wall should be equal [44] such as

$\Delta P_{C1} - \Delta P_{C2} = 0$

If this law is followed for the DWC, then it can also be performed for a reactive DWC. To implement this operation, the tray sizing and tray rating feature of Aspen PLUS were used and at several input process parameters the pressure drop for both the sections were calculated. The snapshots below (Figure 5.14 and Figure 5.15) clearly explain the procedure.

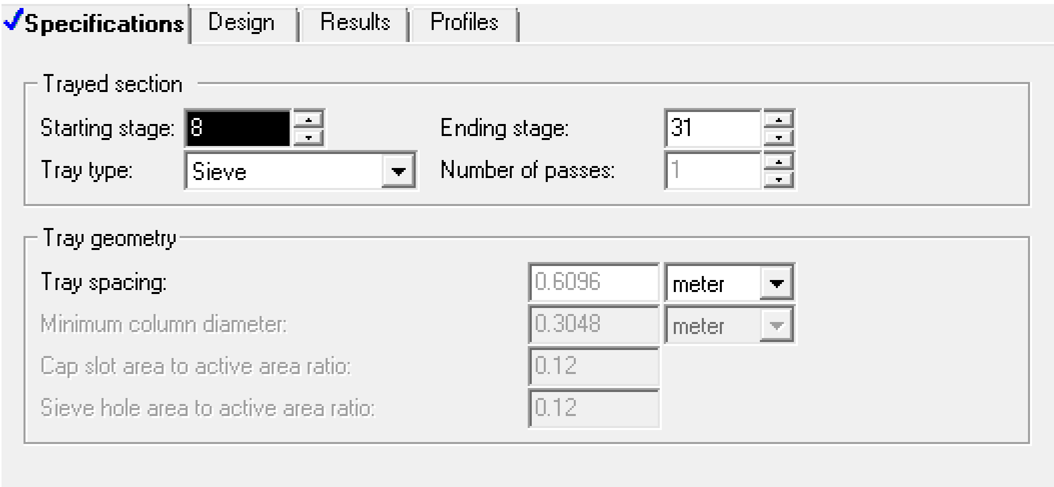

Trayed section

Starting stage: 8

Ending stage: 31

Tray type: Sieve

Number of passes: 1

Tray geometry

Tray spacing: 0.6096 meter

Minimum column diameter: 0.3048 meter

Cap slot area to active area ratio: 0.12

Sieve hole area to active area ratio: 0.12

Figure 5.14a: Aspen PLUS window to define tray sizing feature of column 1

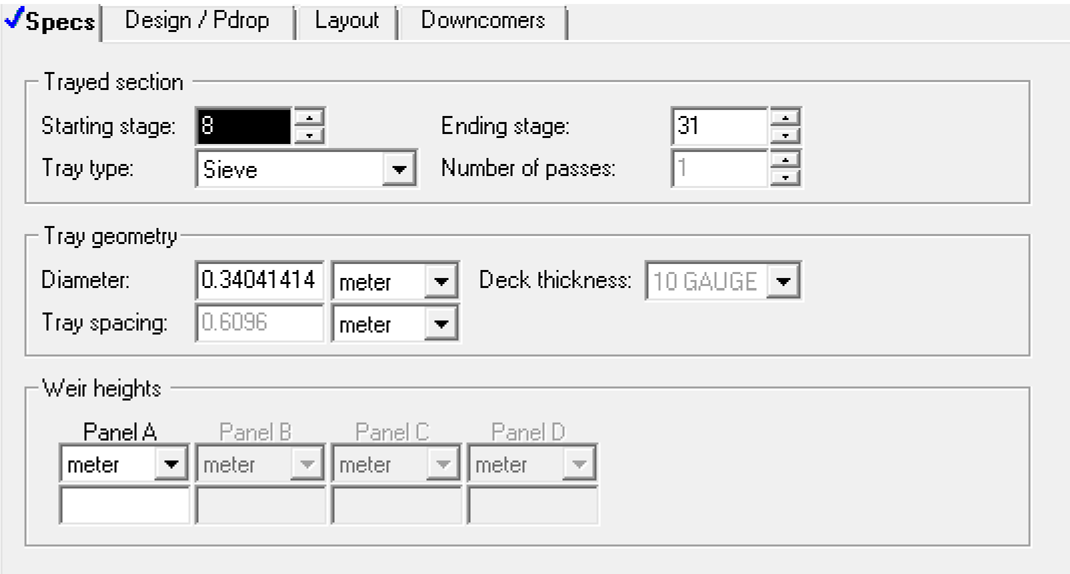

Trayed section

Starting stage: 8

Ending stage: 31

Tray type: Sieve

Number of passes: 1

Tray geometry

Diameter: 0.34041414 meter

Deck thickness: 10 GAUGE

Tray spacing: 0.6096 meter

Weir heights

Panel A	Panel B	Panel C	Panel D
meter	meter	meter	meter

Figure 5.14b: Aspen PLUS window to define tray rating feature of column 1

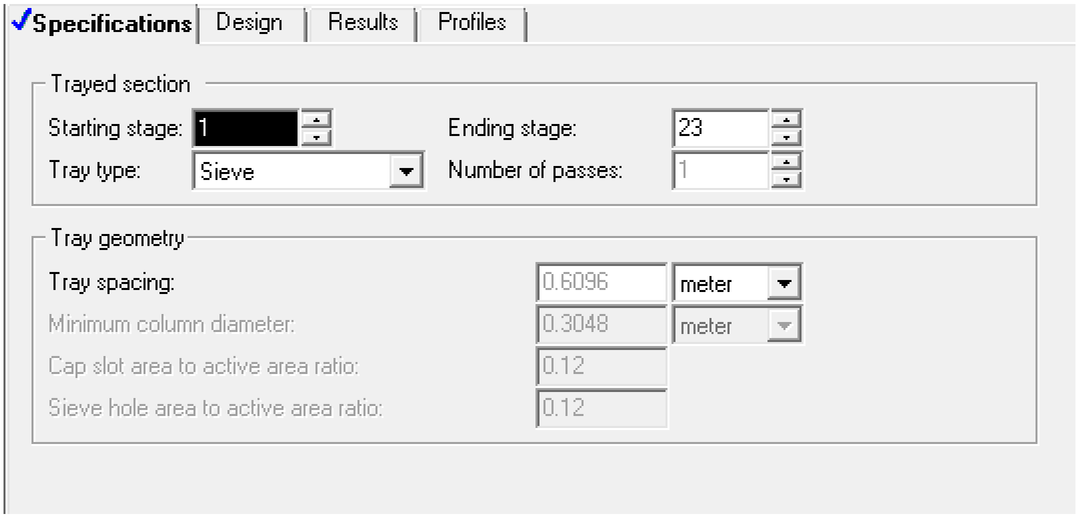

Trayed section

Starting stage: 1

Ending stage: 23

Tray type: Sieve

Number of passes: 1

Tray geometry

Tray spacing: 0.6096 meter

Minimum column diameter: 0.3048 meter

Cap slot area to active area ratio: 0.12

Sieve hole area to active area ratio: 0.12

Figure 5.15a: Aspen PLUS window to define tray sizing feature of column 1

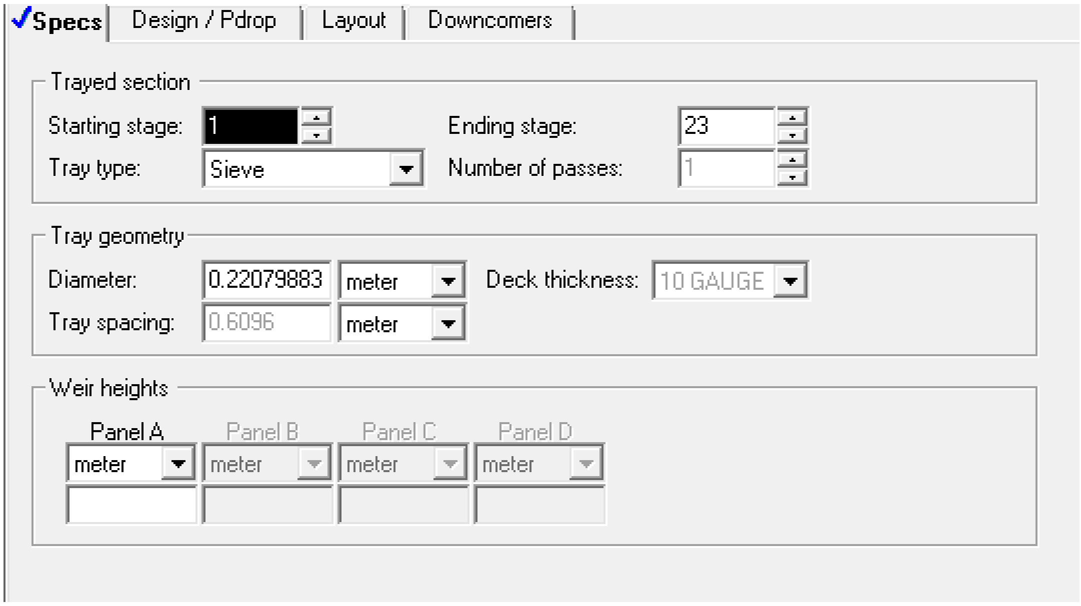

Trayed section

Starting stage: 1

Ending stage: 23

Tray type: Sieve

Number of passes: 1

Tray geometry

Diameter: 0.22079883 meter

Deck thickness: 10 GAUGE

Tray spacing: 0.6096 meter

Weir heights

Panel A	Panel B	Panel C	Panel D
meter	meter	meter	meter

Figure 5.15b: Aspen PLUS window to define tray rating feature of column 1

Now the setup is completed and the simulation can be performed to obtain the desired results.

5.2: Optimization

Box Behnken Design and Multi response optimization:

Box Behnken design (BBD) is used to provide optimum results of responses on account of the number of simulation runs required for the operation. The number of runs for the BBD are calculated by the equation 5.1 given below:

$\mathrm{N} = \mathrm{f}^2 + \mathrm{f} + \mathrm{r}_{\mathrm{cp}}$............(5.1)

Where

F is the number of input factors or number of independent variables which affect the response, and

r_{cp} is the replicate number of central points as explained by researchers [45]

BBD is a spherical revolving design and consists of a central point and middle points of the boundaries of the cube circumscribed on the sphere.

The process responses Y_i which are the functions of input factors $x_1, x_2, \ldots\ldots x_i, \ldots\ldots x_f$, are obtained from the following relationship:

$\mathrm{Y_i} = \varphi(\mathrm{x}_1, \mathrm{x}_2, \mathrm{x}_3, \ldots \ldots \ldots \ldots \ldots, \mathrm{x}_\mathrm{i}, \ldots \ldots \ldots \ldots \ldots, \mathrm{x}_\mathrm{f})$............(5.2)

The above relation between responses and the input factors are considered as quadratic response model. The relevant model terms are identified using non- linear regression analysis to fit the responses according to simulated results or input factors. The model being used is best related as given by equation 5.3.

$Y_i = \gamma_0 + \sum_{i=1}^{f} \gamma_i x_i + \sum_{i=1}^{f} \gamma_{ii} x_i^2 + \sum\sum_{i<j} \gamma_{ij} x_i x_j + \epsilon$............... (5.3)

Where

γ_0 is constant parameter, γ_i is the slope or linear effect of input factor x_i, γ_{ij} is the linear effect of interaction between x_i and x_j, and γ_{ii} is the quadratic effect of factor x_i. [45].

For the present case, a multi response optimization is used due to involvement of six responses (product purity at distillate, side draw and bottom product streams, reboiler duty, condenser duty and difference in pressure drop on both sides of the wall) for three process parameters, namely vapour split ratios, liquid split ratios and reflux rate. Desirability function approach is the most-used method for multiple response optimizations [46]. In the present case, the one sided desirability function for each and every response is calculated using a set of equations 5.4 and an overall desirability is predicted using equation 5.5.

$$d_i = 0 \text{ for } Y_i \leq Y_{i\text{-min}}$$

$$= \left(\frac{Y_i - Y_{i-min}}{Y_{i-max} - Y_{i-min}}\right)^r \text{ for } Y_{i\text{-min}} < Y_i < Y_{i\text{-max}} \ldots\ldots\ldots\ldots\ldots\ldots\ldots\ldots\ldots\ldots(5.4)$$

$$= 1 \text{ for } Y_i \geq Y_{i\text{-max}}$$

Where Yi are response values, Yi-max and Yi-min are the maximum and minimum acceptable values of the response i, r is the used scale of the desirability and acts as a weight for the desirability. The desirability lies between 0 and 1, quantifying the fitting of responses over the simulations data. All the desirability functions are combined to predict the overall desirability function with the motto to convert multiple responses to one single response.

$$D_O = \left(\prod_i d_i\right)^{\frac{1}{k}} \ldots\ldots\ldots\ldots\ldots\ldots (5.5)$$

If all the desirability values approach to an ideal condition such as 1, the overall desirability will be equal to 1 and if anyone of the desirability is less than 1 the overall desirability will lie between 0 and 1.

In the present work, the three levels, three factorial BBD is used to provide optimum process parameters with the given target for the responses. The three input factors consist of reflux rate (kmol/h), liquid split (kmol/h) and vapor split (kmol/h) which provide six responses such as distillate purity, side draw purity, bottom purity, reboiler duty, condenser duty and difference in pressure drops across the two sides of the dividing wall.

For the regression analysis of simulated data, the statistical Design-Expert software version 6.06 (STAT-EASE Inc., Minneapolis, US) was used.

CHAPTER- 6

RESULTS AND DISCUSSION

After performing several simulations using the post-fractionator system as discussed in previous chapter, a number of results were obtained. The input parameters (Table 6.1) were taken from the work of Kiss et al. (2011), but with an increased feed flow rate and the other process parameters were varied according to the Table 6.3.

Table 6.1: Input process parameters

Parameters	Kiss et al. (2011)	
	Value	Unit
Flow rate of feed Stream	50	kmol/h
Feed Composition		
Methanol	100%	
Dimethyl ether	0%	
Water	0%	
Temperature of feed stream	25	^{o}C
Pressure of feed stream	10	Bar
Number of stages	35	
Stages of reactive zone (from/ to stage number)	8 to 31	
Feed stage number	8	
Wall Position (From/to Stage number)	8 to 31	
Distillate to feed ratio	0.25	kmol/kmol
Operating pressure	10	Bar
Side draw stream flow rate	25	kmol/h

The following nomenclatures have been used in the analysis:

r: reflux rate of the system (kmol/h)

l: liquid split (kmol/h)

v: vapor split (kmol/h)

D: dimethyl ether (DME) composition in the distillate

S: methanol composition in the side draw

B: water composition in the bottoms

Qb: reboiler duty

Qc: condenser duty

Del P: difference in pressure across the dividing wall in the two sections

Table 6.2: Design summary

Study Type	Response Surface Methodology		No. of calculation runs=17				
Initial Design	Box Behnken		No. of Blocks =1				
Design Model	Quadratic						
Response	Name	Units	Obs	Minimum	Maximum	Trans	Model
Y1	D		17	0.96972	0.99999	None	Quadratic
Y2	S		17	0.85774	0.95025	None	Quadratic
Y3	B		17	0.96506	0.99831	None	Quadratic
Y4	Qb	Watt	17	275478	305400	None	Quadratic
Y5	Qc	Watt	17	-213249	-184150	None	Quadratic
Y6	Del P		17	-0.02729	0.008834	None	Quadratic

Factor	Name	Units	Type	Low Actual	High Actual	Low Coded	High Coded
A	r	kmol/hr	Numeric	26	32	-1	1
B	l	kmol/hr	Numeric	46	54	-1	1
C	v	kmol/hr	Numeric	8	16	-1	1

Table 6.3: Results at several input process parameters

Run	Reflux Rate (kmol/h)	Liquid Split (kmol/h)	Vapor Split (kmol/h)	Dimethyl ether composition in Distillate stream (Mol fraction)	Methanol composition in Side draw stream (Mol fraction)	Water composition in Bottom stream (Mol fraction)	Reboiler Duty (W)	Condenser Duty (W)	ΔP1-ΔP2 (bar)
	r	l	v	D	S	B	Qb	Qc	Del P
1	32	50	16	0.99999	0.88657	0.9983	299173	-212846	-0.02345
2	29	46	8	0.99972	0.91096	0.99703	289154	-198613	0.007769
3	32	50	8	0.9991	0.90044	0.9947	302530	-213249	0.008834
4	29	54	16	0.99998	0.95025	0.98699	292784	-198501	-0.0168
5	26	54	12	0.98948	0.93619	0.96506	282269	-188258	-0.00278
6	26	46	12	0.99998	0.92233	0.99735	275992	-184153	-0.00293
7	32	46	12	0.99999	0.91288	0.99831	303737	-212848	-0.00099
8	29	50	12	0.99997	0.9342	0.99452	291223	-198507	-0.00164
9	26	50	16	0.99999	0.91419	0.99641	275478	-184150	-0.02108
10	29	46	16	0.99999	0.85774	0.99785	280059	-198496	-0.02729
11	29	54	8	0.97183	0.88824	0.9768	297515	-210276	0.008004
12	29	50	12	0.99997	0.9342	0.99452	291223	-198507	-0.00164
13	29	50	12	0.99997	0.9342	0.99452	291223	-198507	-0.00164
14	26	50	8	0.96972	0.90383	0.99073	284516	-195879	0.00686
15	29	50	12	0.99997	0.9342	0.99452	291223	-198507	-0.00164
16	29	50	12	0.99997	0.9342	0.99452	291223	-198507	-0.00164
17	32	54	12	0.99996	0.92889	0.98749	305400	-212863	-0.00019

The model F- value define the best fitting of the model, if F-value is greater than 5 indicates tthat the model is significant. Values “Prob>F” defines the significant model terms, if it is less than 0.05 the model terms are significant and value greater than 0.1 indicate insignificant model terms. Adequate precision measures the signal to noise ratio, ratio value greater than 4 is desirable and it is efficient in navigating the design space.

6.1 Results for response dimethyl ether composition D:

Table 6.4a: Sequential Model Sum of Squares for Response: D

Source	Sum of Squares	Degree of Freedom	Mean Square	F Value	Prob> F		
Mean	16.85945	1	16.85945				
Linear	0.000827	3	0.000276	5.096015	0.0150		
2 Factor Interaction	0.000438	3	0.000146	5.488304	0.0172	Suggested	
Quadratic	0.000182	3	6.08E-05	5.113969	0.0348	Suggested	
Cubic	8.33E-05	3	2.78E-05	63660000	<0.0001	Aliased	
Residual	0	4	0				
Total	16.86098	17	0.991822				

Table 6.4b: Model Summary Statistics for Response D

Source	Std. Dev.	Adjusted		Predicted		
		R-Squared	R-Squared	R-Squared	PRESS	
Linear	0.007355	0.540442	0.43439	0.091314	0.001391	
2FI	0.005155	0.826352	0.722163	0.329348	0.001026	Suggested
Quadratic	0.003449	0.945594	0.875643	0.129502	0.001332	Suggested
Cubic	0	1	1		+	Aliased

Table 6.4c: ANOVA for Response Surface Quadratic Model (for purity of distillate D)

Analysis of variance table [Partial sum of squares]						
Source	Sum of Squares	Degree of Freedom	Mean Square	F Value	` Prob> F	
Model	0.001447	9	0.000161	13.518	0.0012	significant
r	0.000199	1	0.000199	16.70627	0.0046	
l	0.000185	1	0.000185	15.52128	0.0056	
v	0.000444	1	0.000444	37.30679	0.0005	
r^2	1.14E-05	1	1.14E-05	0.962327	0.3593	
l^2	3.95E-06	1	3.95E-06	0.332228	0.5824	
v^2	0.000158	1	0.000158	13.26458	0.0083	
rl	2.74E-05	1	2.74E-05	2.304147	0.1728	
rv	0.000216	1	0.000216	18.14348	0.0037	
lv	0.000194	1	0.000194	16.33813	0.0049	
Residual	8.33E-05	7	1.19E-05			
Lack of Fit	8.33E-05	3	2.78E-05			
Pure Error	0	4	0			
Cor Total	0.00153	16				

Std. Dev.	0.003449		R-Squared	0.945594	
Mean	0.995858		Adjuste R-Squared	0.875643	
C.V.	0.346309		Predicted R-Squared	0.129502	
PRESS	0.001332		Adequate Precision	12.13531	

Final Equation in Terms of Actual Factors:		
	D	=
	0.993624	
	0.008725	* r
	-0.0067	* l
	0.007013	* v
	-0.00018	* r^2
	-6.1E-05	* l^2
	-0.00038	* v^2
	0.000218	* r * l
	-0.00061	* r * v
	0.000436	* l * v

Model F-value = 13.52 model is significant.

In this case r, l, v, v^2, rv and lv are significant model terms.

Adequate Precision = 12.13 indicates an adequate signal.

Figure 6.1(a,b,c,d,e,f) shows the variation of dimethyl ether composition in the distillate (Distillate purity) with respect to process parameters with one factor and two factor variations. Figure 6.1a shows nonlinear variation with respect to reflux rate, figure 6.1b shows more or less linear variation with respect to liquid split and figure 6.1c shows complete non-linear variation with respect to vapor split. Plots in figure 6.1a,b,c show a quite small change in Distillate purity with respect to reflux rate, liquid split and vapor split. Figure 6.1d,e,f shows the three dimensional plot of distillate purity with respect to combinations of any two parameters form process parameters list. Figure 6.1 d shows the variation of distillate purity with respect to liquid split and reflux rate, plot shows that the distillate purity remains constant to unity for many combinations of liquid split and reflux rate but it decreases after certain combination when liquid split increases and reflux rate decreases. Figure 6.1e shows the variation of distillate purity with respect to vapor split and reflux rate, plot shows that the distillate purity is constant to unity for large combinations of vapor split and reflux rate but it decreases when vapor split and reflux rate both decreases. Figure 6.1f shows the variation of distillate purity with respect to vapor split and liquid split, plot shows that the distillate purity is constant to unity for large combinations of vapor split and liquid split but it decreases with decrease in vapor split and increase in liquid split.

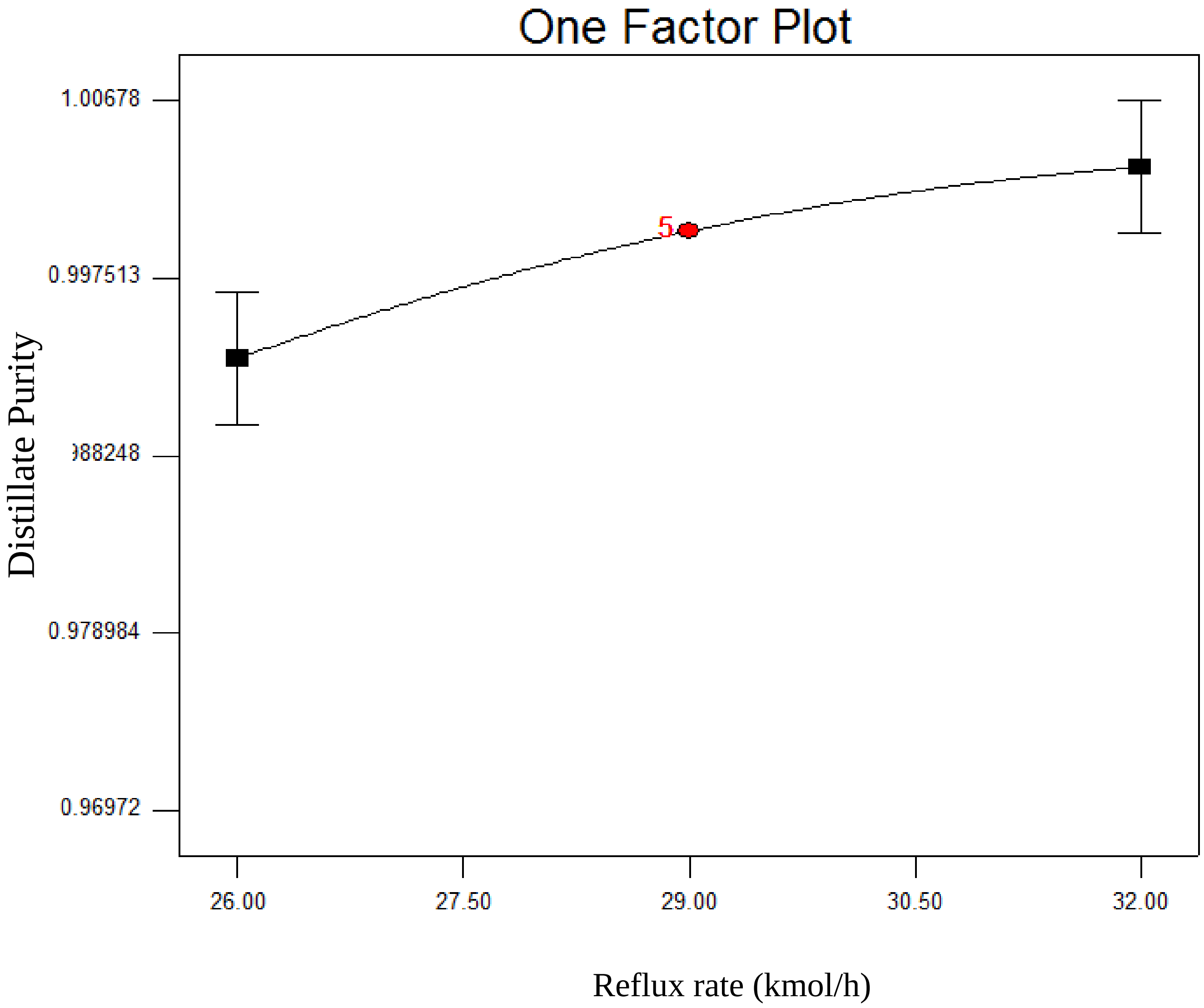

Figure 6.1a: Variation of mole fraction of dimethyl ether in the distillate stream with respect to reflux rate

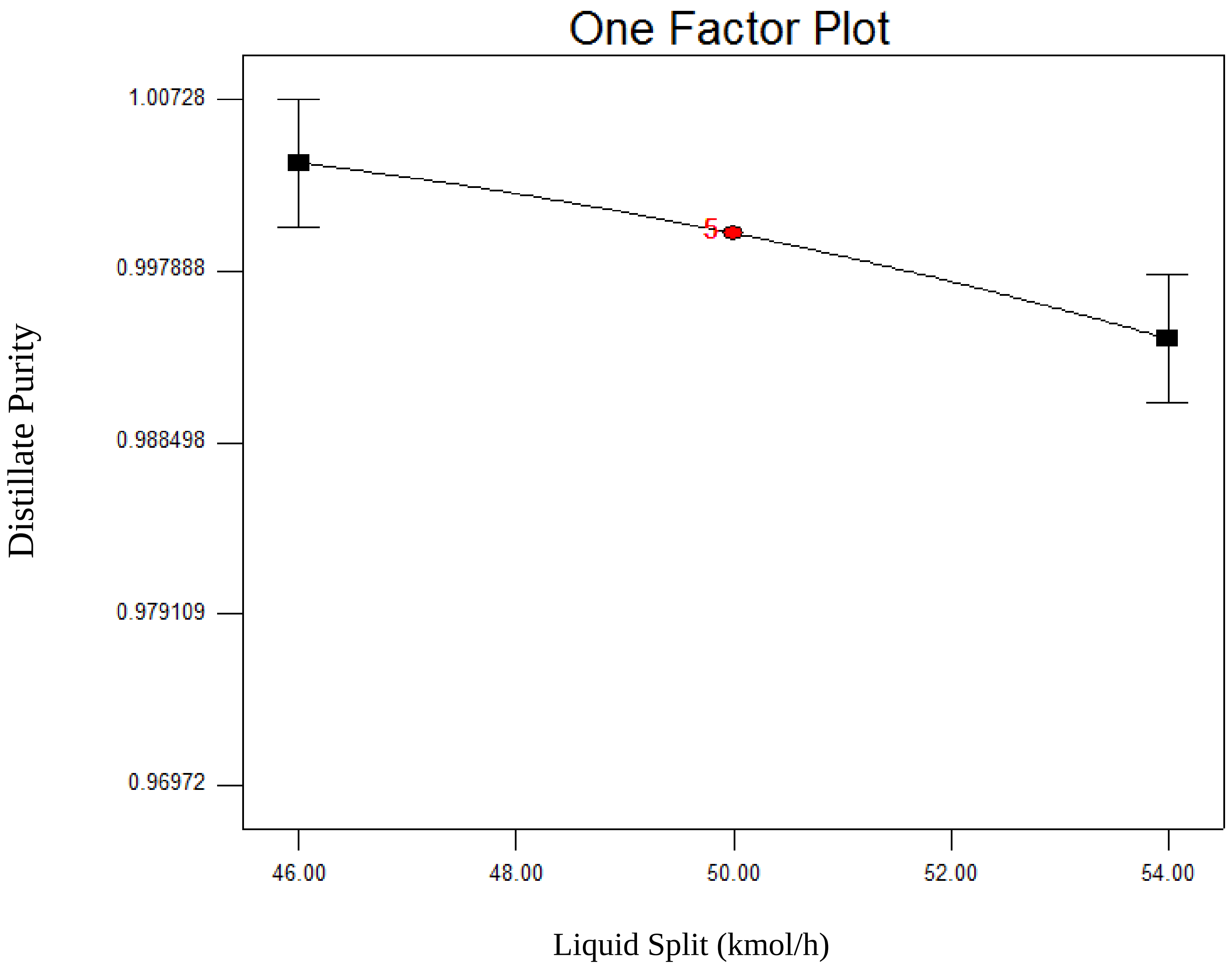

Figure 6.1b: Variation of mole fraction of dimethyl ether in the distillate stream with respect to liquid split

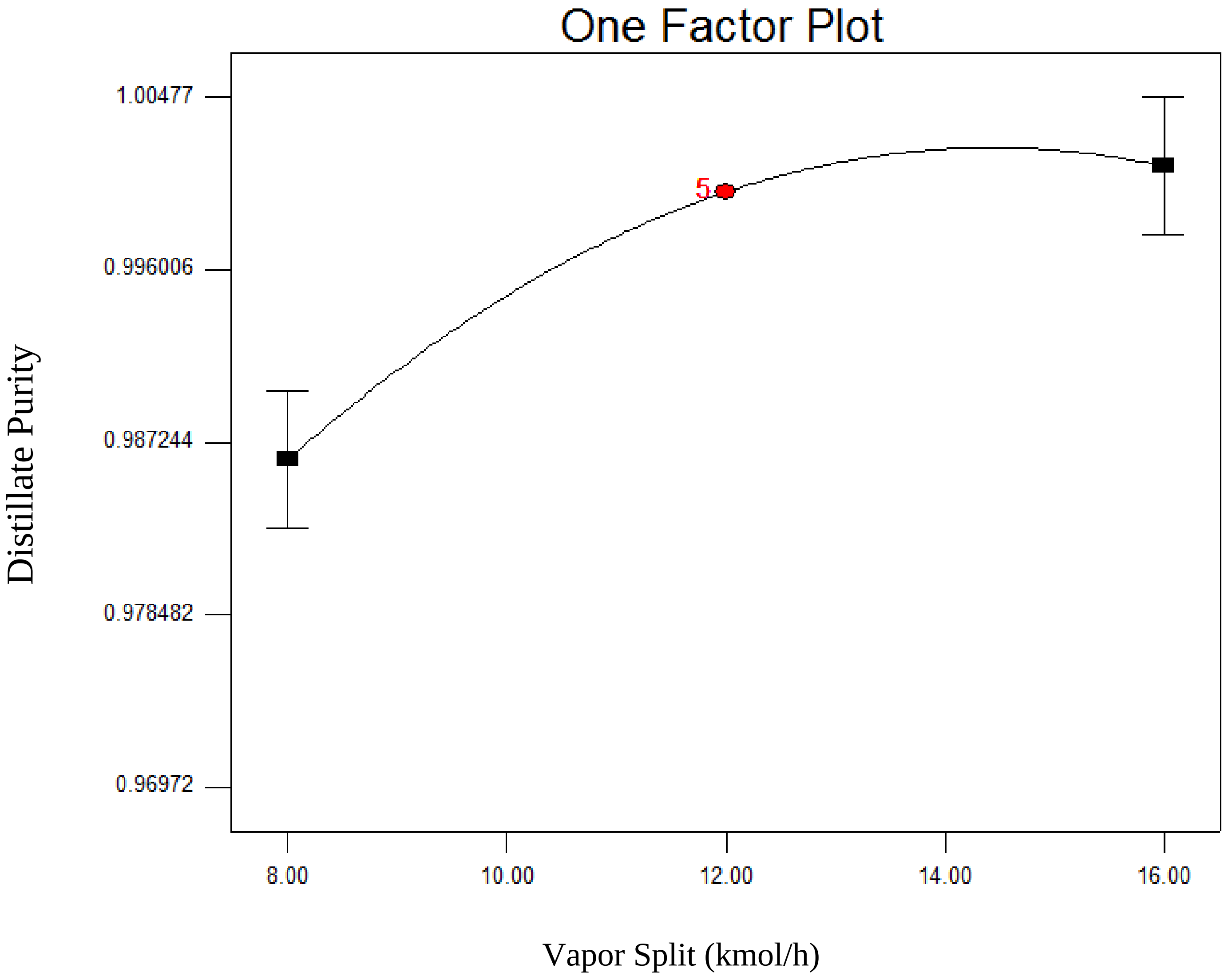

Figure 6.1c: Variation of mole fraction of dimethyl ether in the distillate stream with respect to vapour split

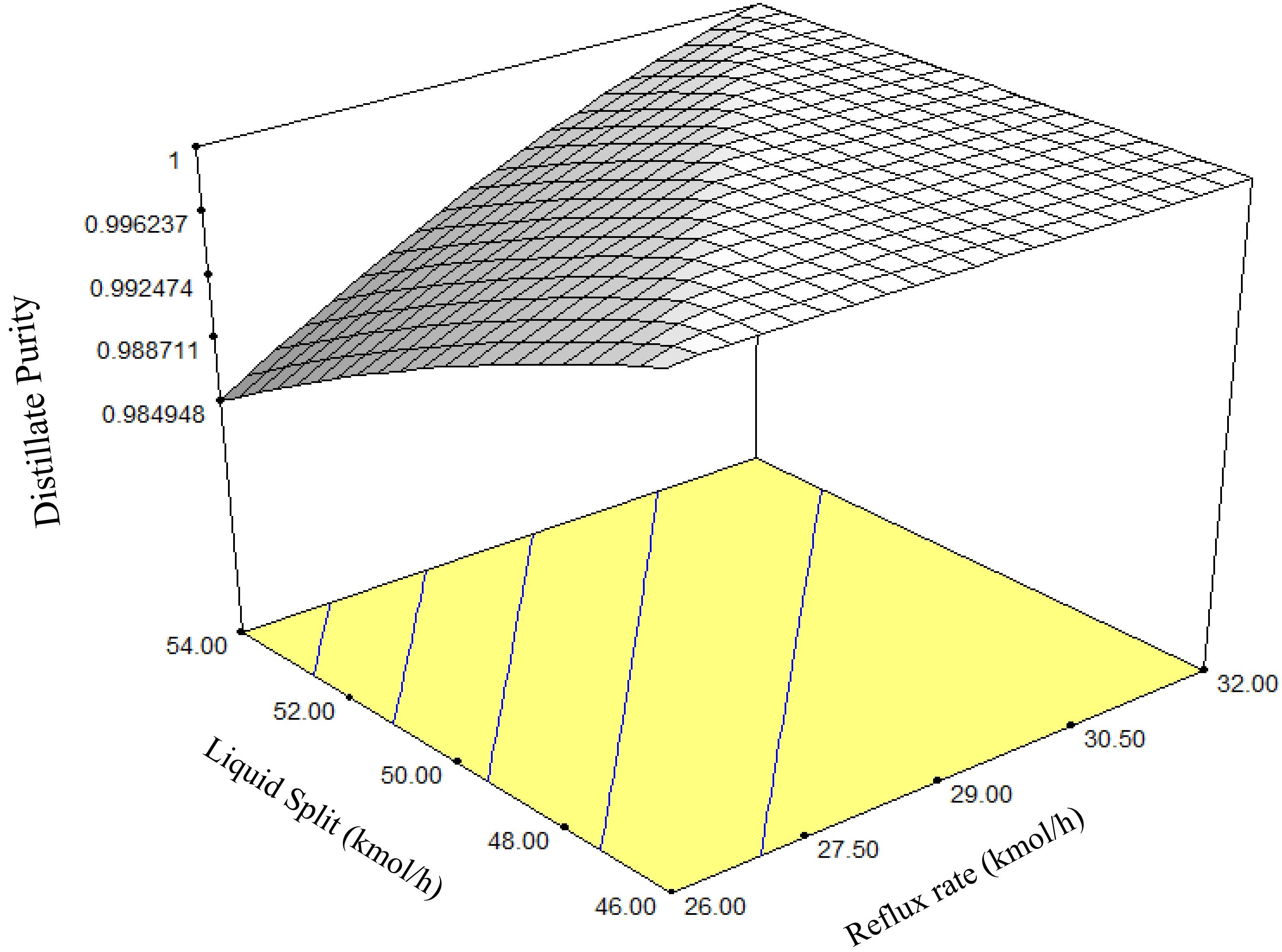

Figure 6.1d: Variation of mole fraction of dimethyl ether in the distillate stream with respect to liquid split and reflux rate

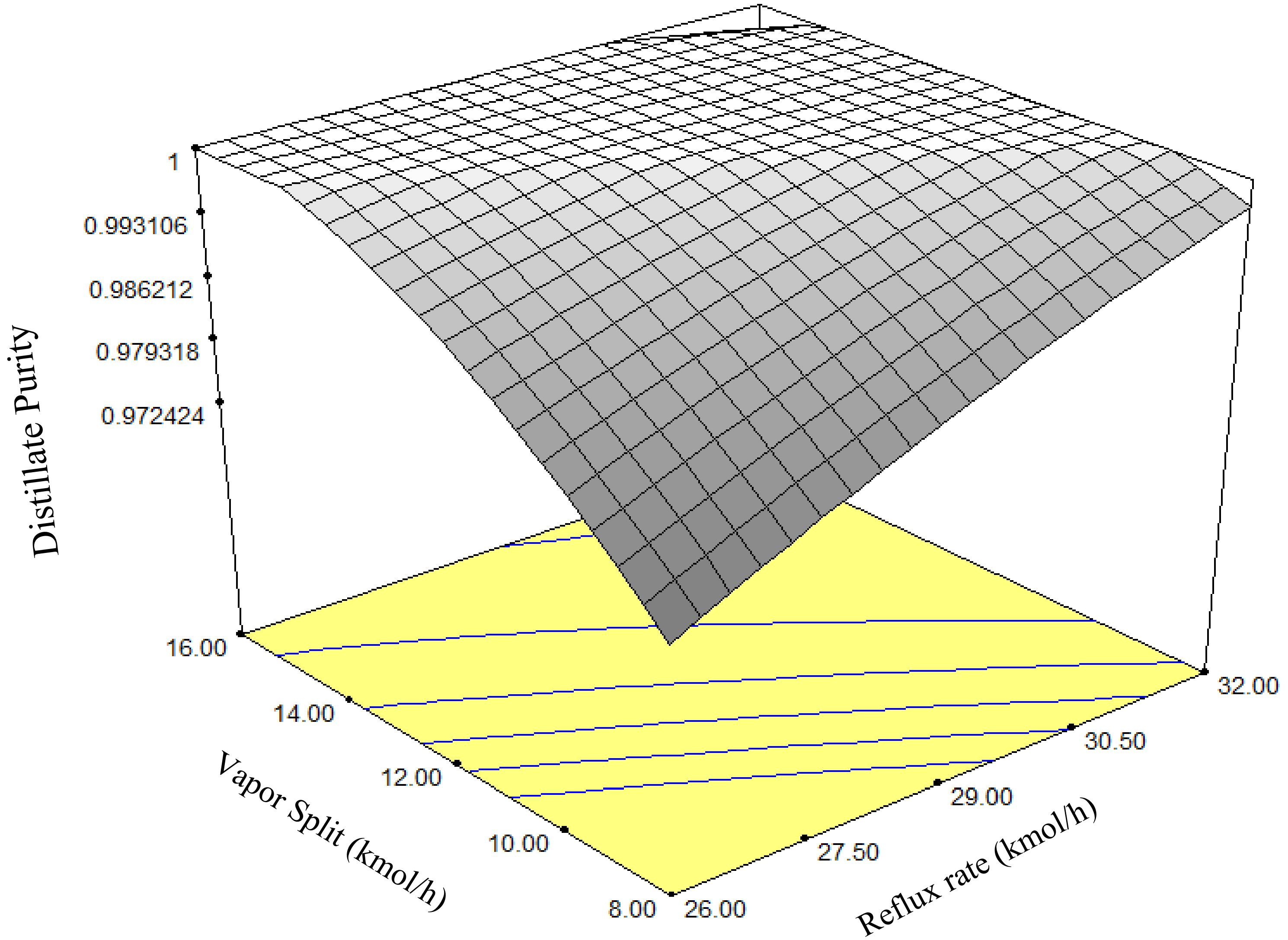

Figure 6.1e: Variation of mole fraction of dimethyl ether in the distillate stream with respect to vapor split and reflux rate

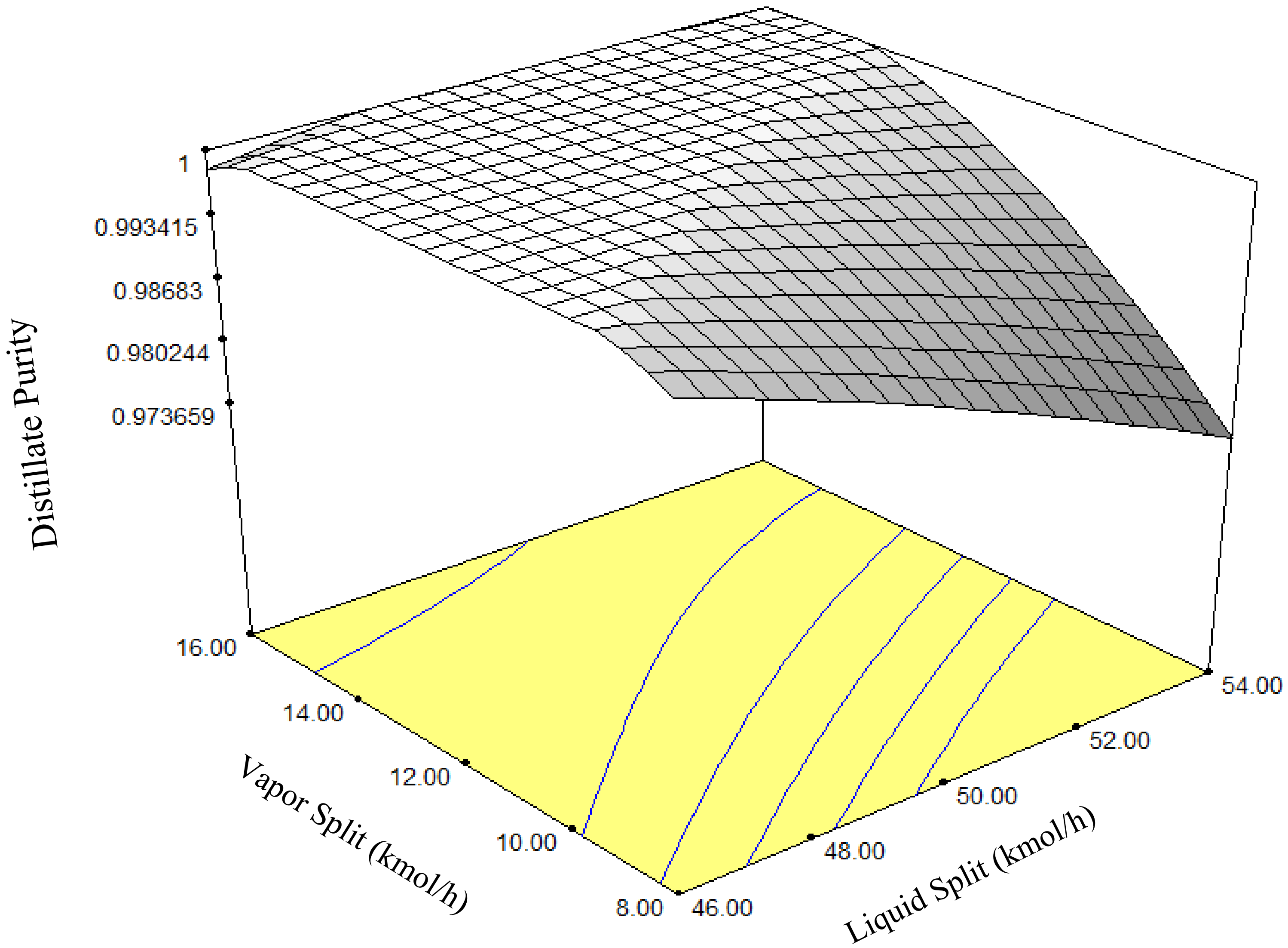

Figure 6.1f: Variation of mole fraction of dimethyl ether in the distillate stream with respect to vapor split and liquid split

6.2: Results for response methanol composition S

Table 6.5a: Sequential Model Sum of Squares for Response: S

Source	Sum of Squares	Degree of Freedom	Mean Square	F Value	Prob> F	
Mean	14.28505	1	14.28505			
Linear	0.00153	3	0.00051	0.900302	0.4674	
2FI	0.003467	3	0.001156	2.965591	0.0838	
Quadratic	0.003654	3	0.001218	35.00862	0.0001	Suggested
Cubic	0.000244	3	8.12E-05	63660000	< 0.0001	Aliased
Residual	0	4	0			
Total	14.29394	17	0.84082			

Table 6.5b: Model Summary Statistics for Response: S

Source	Std. Dev.	Adjusted	Predicted			
		R-Squared	R-Squared	R-Squared	PRESS	
Linear	0.023802	0.172022	-0.01905	-0.56672	0.013936	
2FI	0.019742	0.561842	0.298947	-0.55923	0.013869	
Quadratic	0.005898	0.972621	0.93742	0.561943	0.003896	Suggested
Cubic	0	1	1		+	Aliased

Table 6.5c: ANOVA for Response Surface Quadratic Model (for purity of side draw S)

Analysis of variance table [Partial sum of squares]						
Source	Sum of Squares	Degree of Freedom	Mean Square	F Value	Prob> F	
Model	0.008651	9	0.000961	27.63049	0.0001	significant
r	0.000285	1	0.000285	8.195649	0.0242	
l	0.001242	1	0.001242	35.68588	0.0006	
v	3.48E-06	1	3.48E-06	0.100167	0.7609	
r^2	9.84E-05	1	9.84E-05	2.827805	0.1365	
l^2	7.76E-05	1	7.76E-05	2.231283	0.1789	
v^2	0.003327	1	0.003327	95.62339	< 0.0001	
rl	1.16E-06	1	1.16E-06	0.033217	0.8605	
rv	0.000147	1	0.000147	4.218825	0.0791	
lv	0.003319	1	0.003319	95.41481	< 0.0001	
Residual	0.000244	7	3.48E-05			
Lack of Fit	0.000244	3	8.12E-05			
Pure Error	0	4	0			
Cor Total	0.008895	16				

Std. Dev.	0.005898		R-Squared	0.972621	
Mean	0.916677		Adjusted R-Squared	0.93742	
C.V.	0.643445		Predicted R-Squared	0.561943	
PRESS	0.003896		Adequate Precision	18.24352	

Final Equation in Terms of Actual Factors:		
	S	=
	0.428209	
	0.032979	* r
	0.007046	* l
	-0.03306	* v
	-0.00054	* r^2
	-0.00027	* l^2
	-0.00176	* v^2
	4.48E-05	* r * l
	-0.0005	* r * v
	0.0018	* l * v

Model F-value = 27.63 model is significant.

In this case r, l, v^2 and lv are significant model terms.

Adequate Precision = 18.24 indicates an adequate signal.

Figure 6.2(a,b,c,d,e,f) shows the variation of methanol composition in the side draw (Side draw purity) with respect to process parameters with one factor and two factor variations. Figure 6.2a,b,c shows nonlinear variation of side draw purity with respect to reflux rate, liquid split and vapor split respectively. Figure 6.2a show that the side draw purity is less effected by reflux rate, figure 6.2b show that as liquid split increases the side draw purity also increases and it increases with considerable amount of 0.03 for a given range of liquid split, figure 6.2c shows the parabolic variation of side draw purity with respect to vapor split, as vapor split increases the side draw purity increases up to certain amount of 0.93 and then starts decreasing after vapor split of 12.13 kmol/hr. Figure 6.2d,e,f shows the three dimensional plot of side draw purity with respect to combinations of any two parameters form process parameters list. Figure 6.2 d shows the variation of side draw purity with respect to liquid split and reflux rate, plot shows that the side draw purity remains continuously decreases with decrease in liquid split and increase in reflux rate. Figure 6.2e shows the variation of side draw purity with respect to vapor split and reflux rate, plot shows that the side draw purity is parabolic with respect to vapor split and as the reflux rate increases the concaveness of the plot increases. Figure 6.2f shows the variation of side draw purity with respect to vapor split and liquid split, plot shows that the side draw purity is parabolic with respect to vapor split and concaveness decreases and side draw purity increases with increase in liquid split.

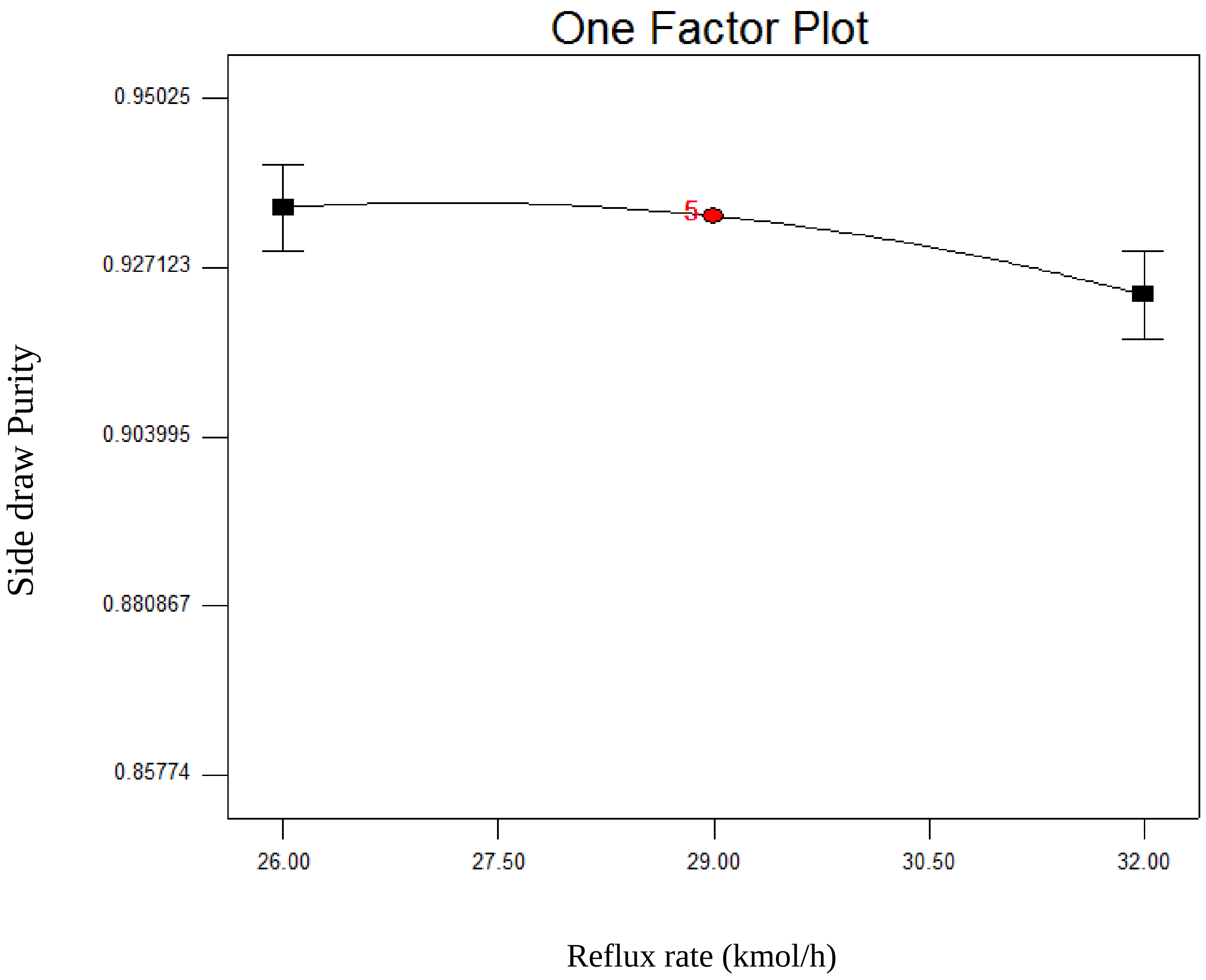

Figure 6.2a: Variation of mole fraction of methanol in the side draw stream with respect to reflux rate

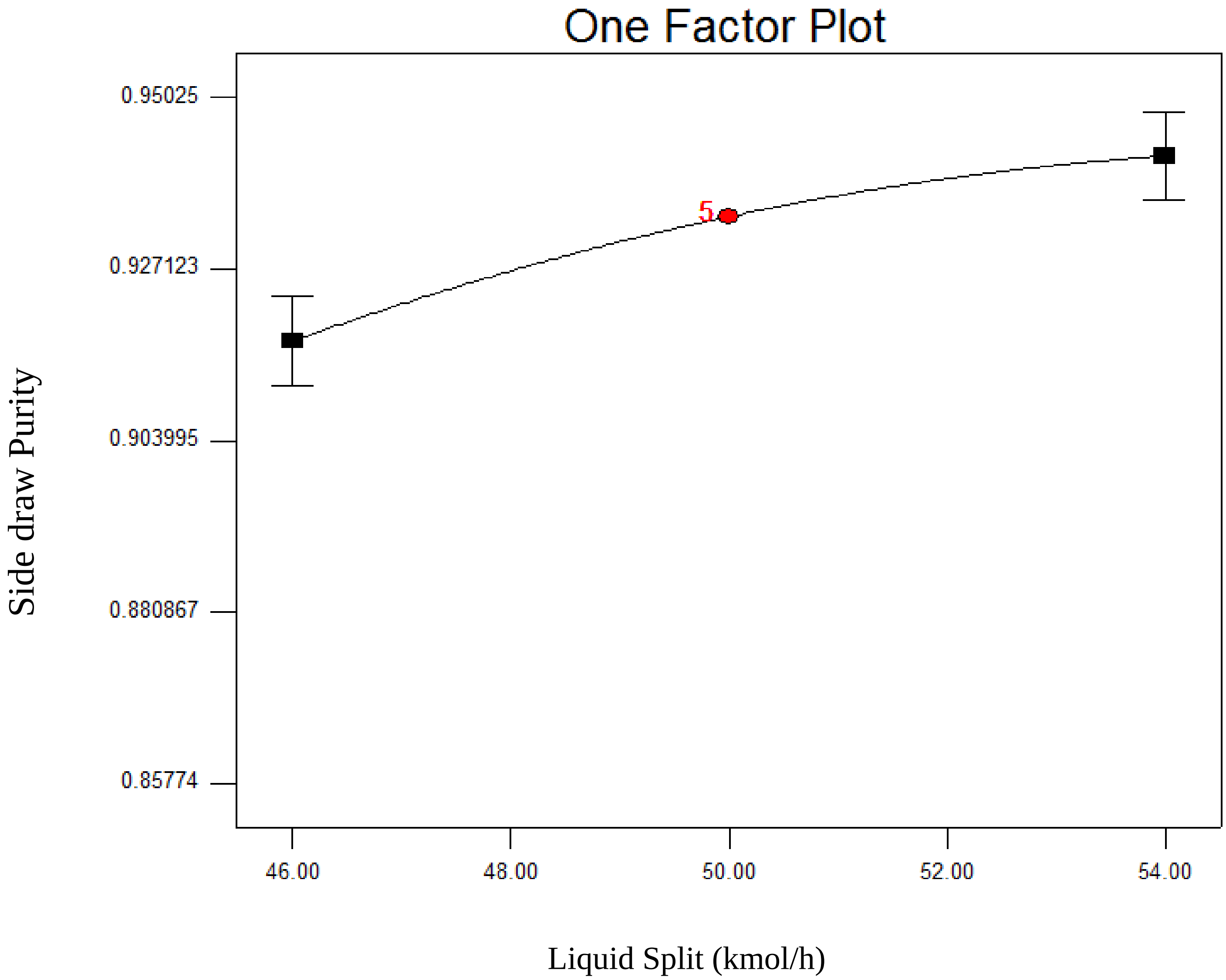

Figure 6.2b: Variation of mole fraction of methanol in the side draw stream with respect to liquid split

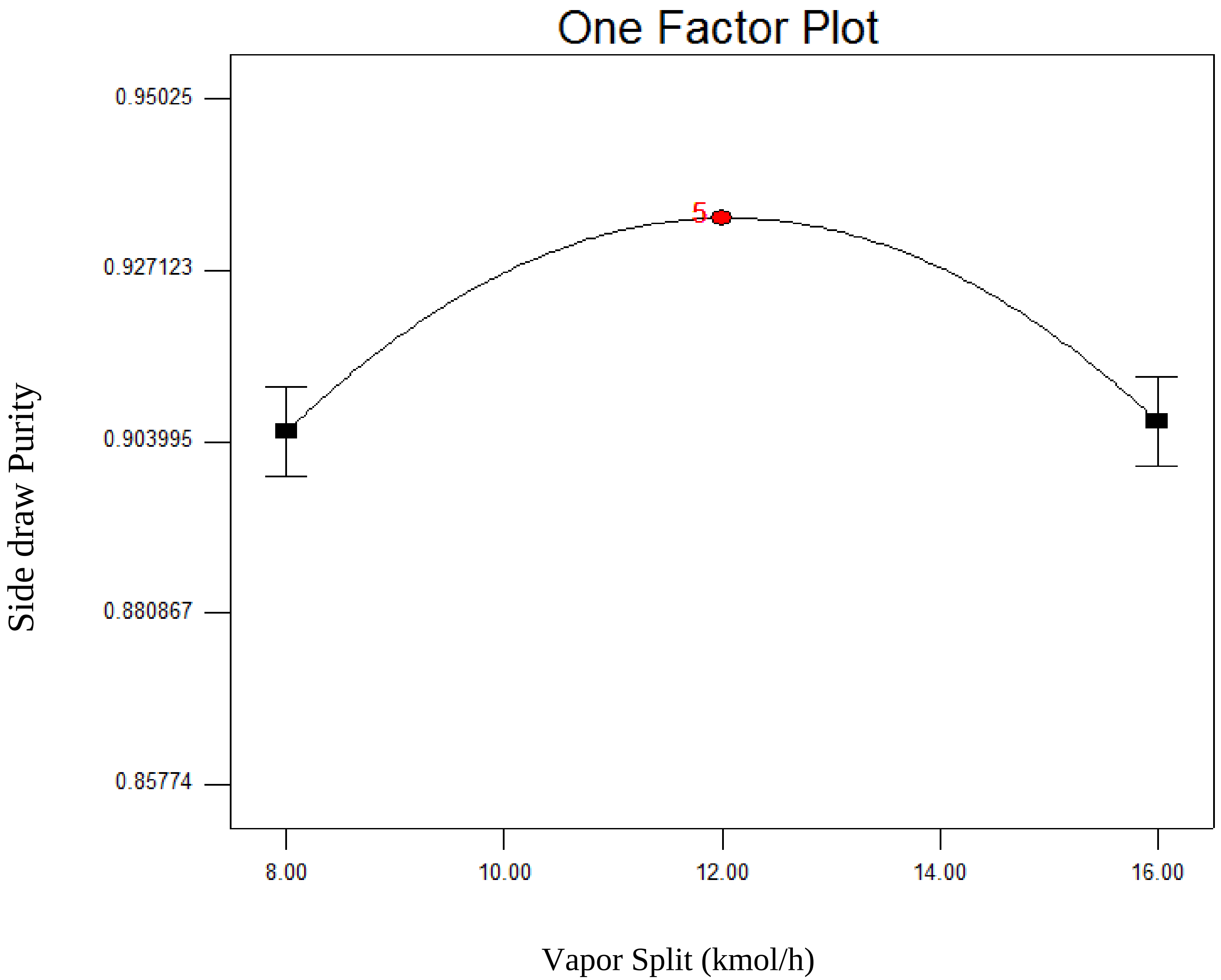

Figure 6.2c: Variation of mole fraction of methanol in the side draw stream with respect to vapor split

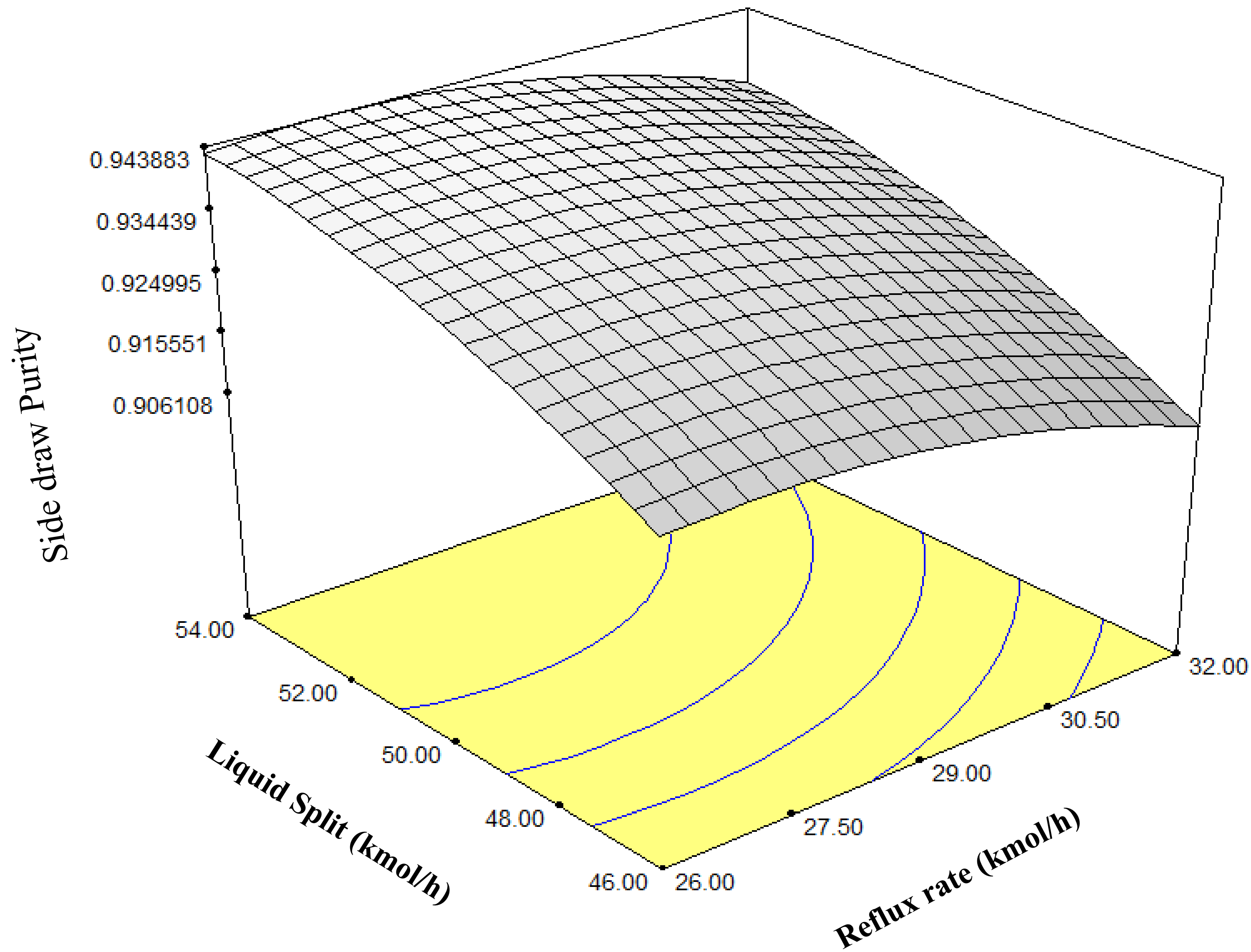

Figure 6.2d: Variation of mole fraction of methanol in the side draw stream with respect to liquid split and reflux rate

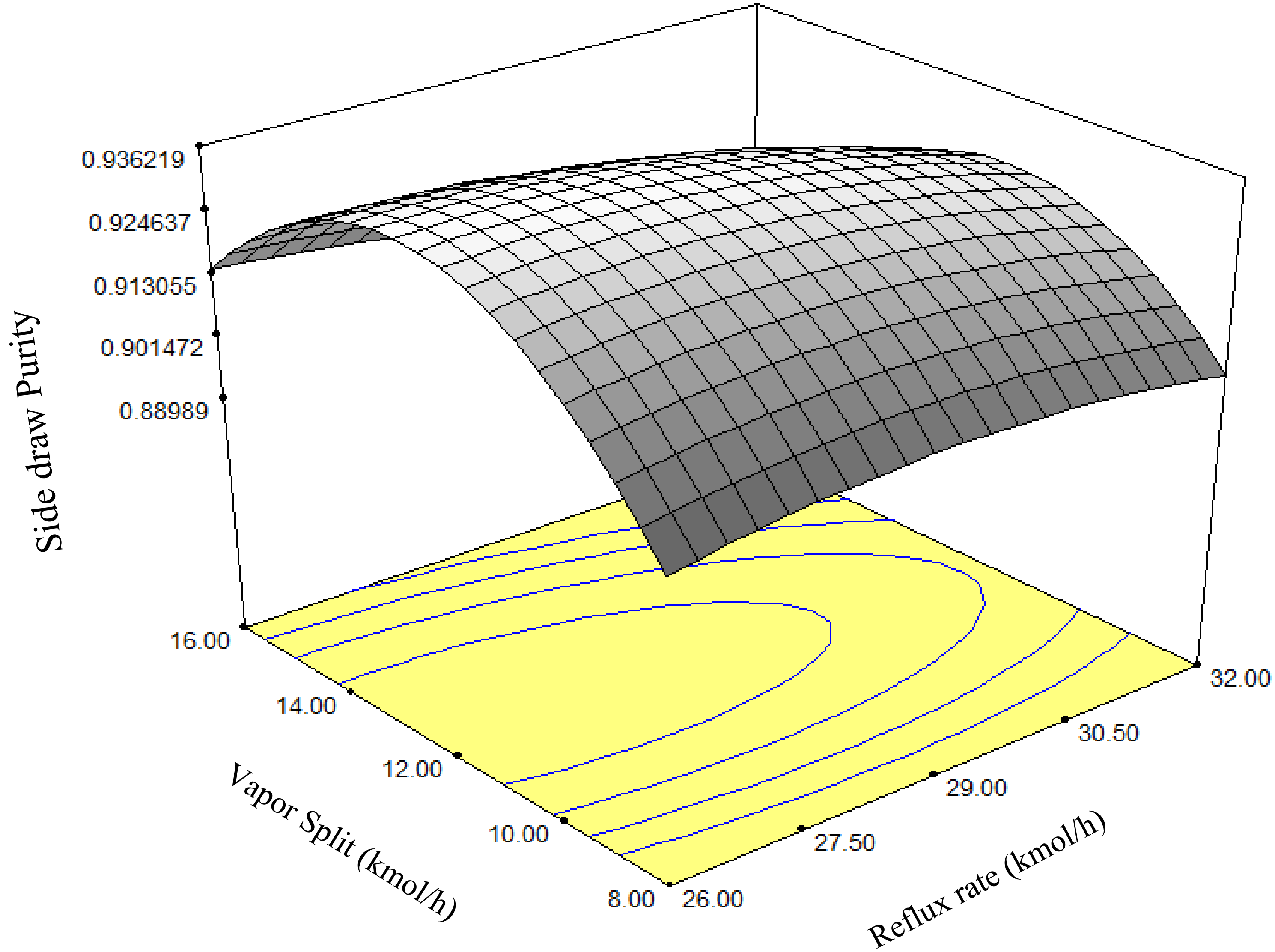

Figure 6.2e: Variation of mole fraction of methanol in the side draw stream with respect to vapor split and reflux rate

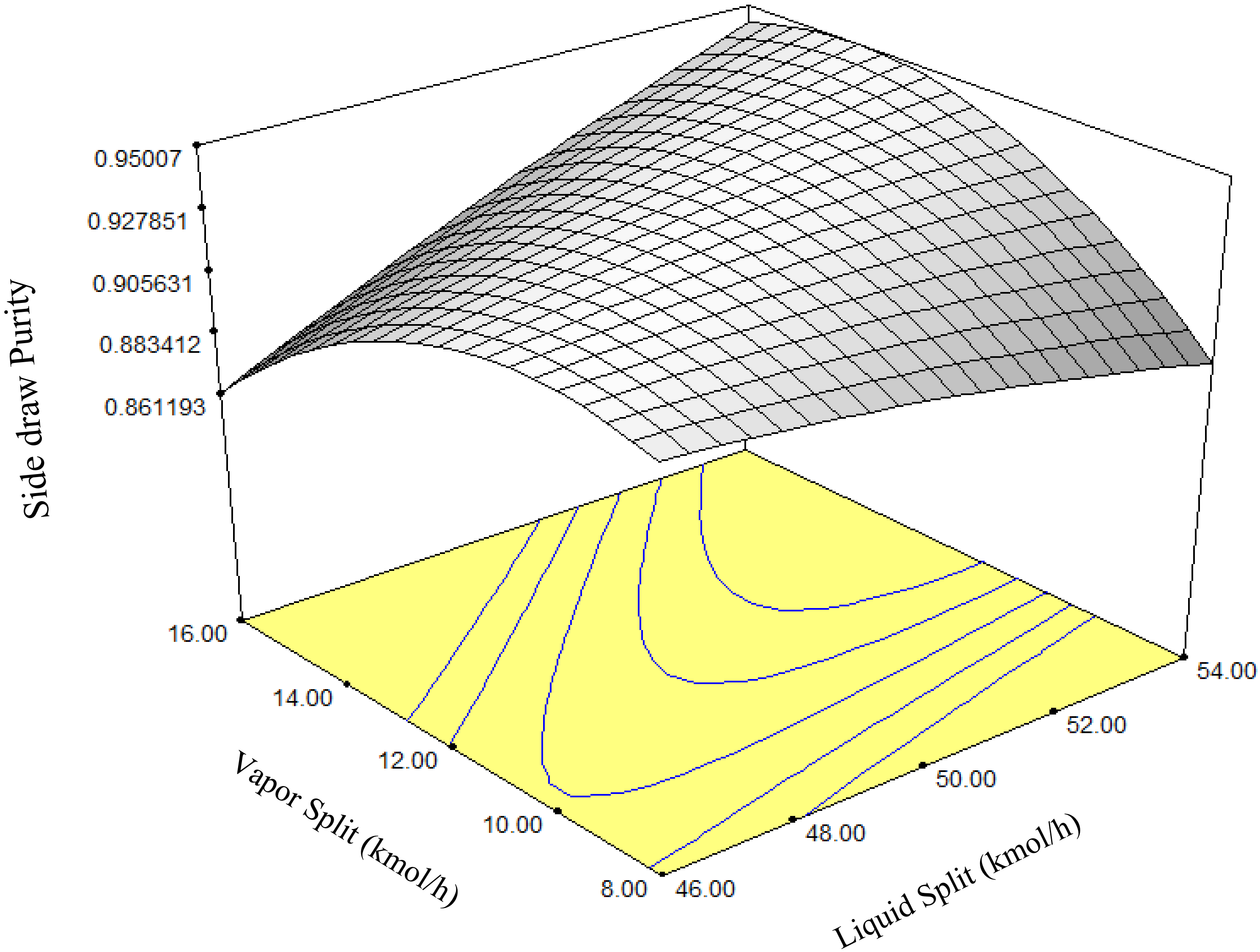

Figure 6.2f: Variation of mole fraction of methanol in the side draw stream with respect to vapor split and liquid split

6.3: Results for response water composition B

Table 6.6a: Sequential Model Sum of Squares for Response: B

Source	Sum of Squares	Degree of Freedom	Mean Square	F Value	Prob> F	
Mean	16.7204	1	16.7204			
Linear	0.000847	3	0.000282	9.597269	0.0013	Suggested
2FI	0.000138	3	4.61E-05	1.889038	0.1954	
Quadratic	0.000187	3	6.24E-05	7.681418	0.0129	Suggested
Cubic	5.68E-05	3	1.89E-05	63660000	< 0.0001	Aliased
Residual	0	4	0			
Total	16.72163	17	0.983625			

Table 6.6b: Model Summary Statistics for Response: B

Source	Std. Dev.	Adjusted		Predicted		
		R-Squared	R-Squared	R-Squared	PRESS	
Linear	0.005423	0.688934	0.61715	0.379133	0.000763	Suggested
2FI	0.00494	0.801453	0.682325	0.105756	0.001099	
Quadratic	0.00285	0.953741	0.894264	0.25985	0.00091	Suggested
Cubic	0	1	1		+	Aliased

Table 6.6c: ANOVA for Response Surface Quadratic Model (for purity of bottom B)

Analysis of variance table [Partial sum of squares]						
Source	Sum of Squares	Degree of Freedom	Mean Square	F Value	Prob> F	
Model	0.001172	9	0.00013	16.03563	0.0007	significant
r	0.000107	1	0.000107	13.16904	0.0084	
l	0.000688	1	0.000688	84.74421	< 0.0001	
v	5.15E-05	1	5.15E-05	6.336746	0.0400	
r^2	4.64E-06	1	4.64E-06	0.57162	0.4743	
l^2	0.000173	1	0.000173	21.35307	0.0024	
v^2	1.03E-05	1	1.03E-05	1.269864	0.2969	
rl	0.000115	1	0.000115	14.19045	0.0070	
rv	1.08E-06	1	1.08E-06	0.133186	0.7259	
lv	2.19E-05	1	2.19E-05	2.702784	0.1442	
Residual	5.68E-05	7	8.12E-06			
Lack of Fit	5.68E-05	3	1.89E-05			
Pure Error	0	4	0			
Cor Total	0.001229	16				

Std. Dev.	0.00285		R-Squared	0.953741
Mean	0.991742		Adjusted R-Squared	0.894264
C.V.	0.287346		Predicted R-Squared	0.25985
PRESS	0.00091		Adequate Precision	14.61983

Final Equation in Terms of Actual Factors:		
	B	=
	0.702076	
	-0.01386	* r
	0.023062	* l
	-0.00778	* v
	-0.00012	* r^2
	-0.0004	* l^2
	9.78E-05	* v^2
	0.000447	* r * l
	-4.3E-05	* r * v
	0.000146	* l * v

Model F-value = 16.04 model is significant.

In this case r, l, v, l^2, and rl are significant model terms.

Adequate Precision = 14.62 indicates an adequate signal.

Figure 6.3(a,b,c,d,e,f) shows the variation of water composition in the bottom stream (Bottom purity) with respect to process parameters with one factor and two factor variations. Figure 6.3a,b,c shows nonlinear variation of bottom purity with respect to reflux rate, liquid split and vapor split respectively. Figure 5.3a show that the bottom purity is less affected by reflux rate, figure 6.3b show that as liquid split increases the bottom purity decreases and it decreases with considerable amount for a given range of liquid split, figure 6.3c shows the monotonically increasing attitude of bottom purity with increase in vapor split in a defined range. Figure 6.3d,e,f shows the three dimensional plot of bottom purity with respect to combinations of any two parameters form process parameters list. Figure 6.3d shows the variation of bottom purity with respect to liquid split and reflux rate, plot shows that the bottom purity is high up to 0.99 for low liquid split and reflux rate, it maintains up to that limit for wide combinations of liquid split and reflux rate and then decreases with increase in both liquid split and reflux rate. Figure 6.3e shows the variation of bottom purity with respect to vapor split and reflux rate, plot shows that the bottom purity is unity at 16 kmol/hr of vapor split and reflux rate of 32kmol/hr to 31.25 kmol/hr after that the bottom purity decreases with decrease in liquid split and reflux rate. Figure 6.3f shows the variation of bottom purity with respect to vapor split and liquid split, plot shows that the bottom purity doesn’t show any significant variation with vapor split but it decreases as liquid split increases.

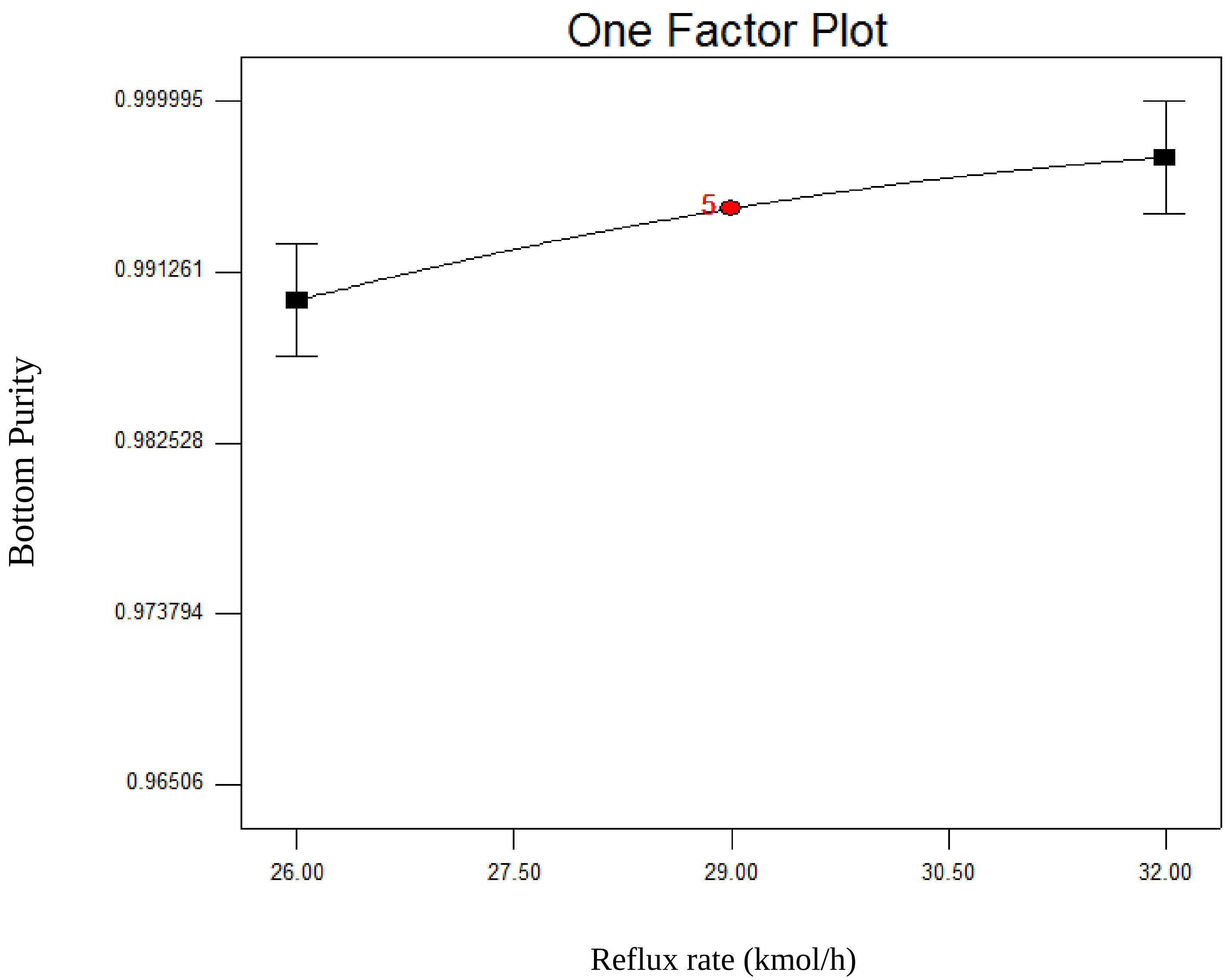

Figure 6.3a: Variation of mole fraction of water in the bottom stream with respect to reflux rate

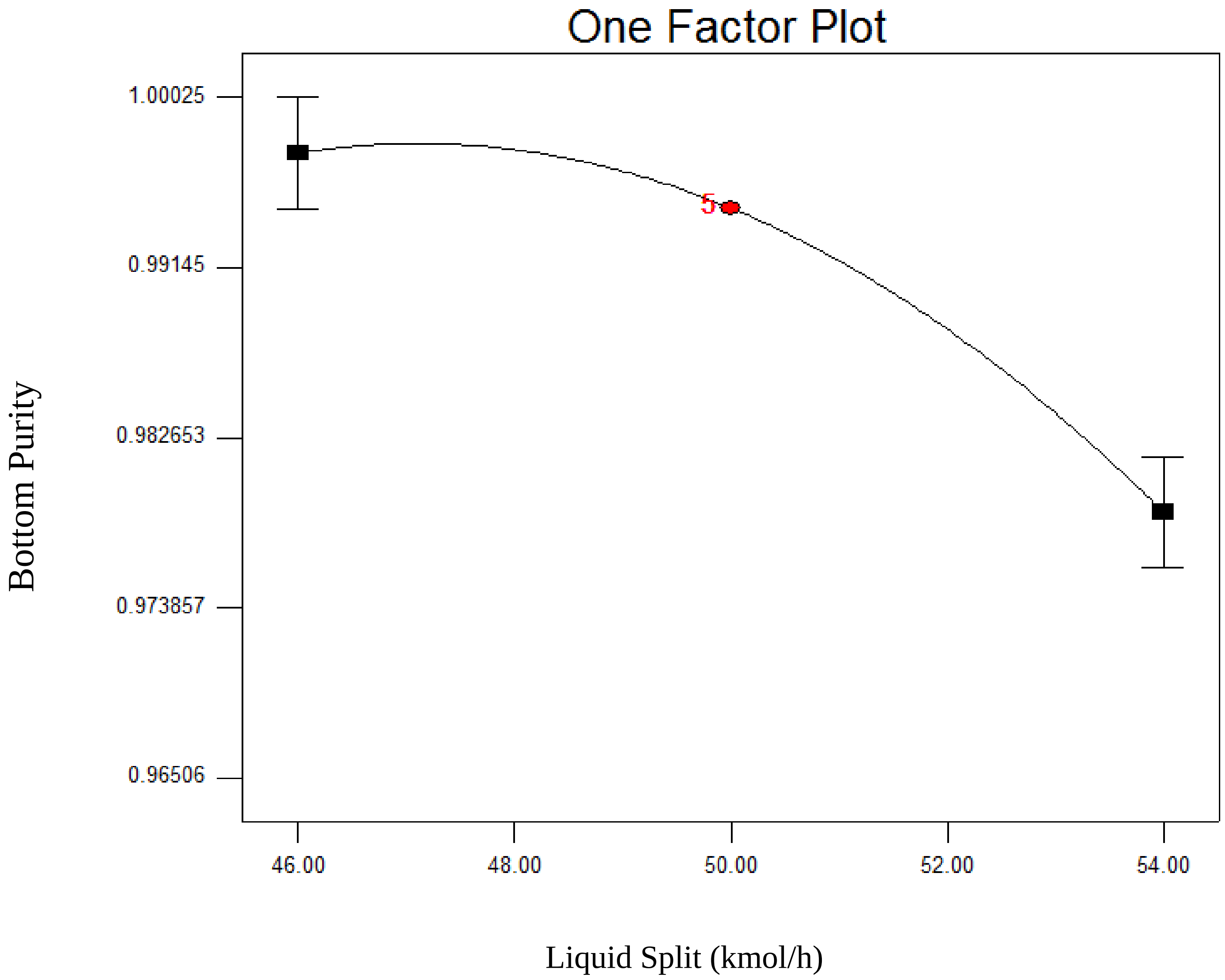

Figure 6.3b: Variation of mole fraction of water in the bottom stream with respect to liquid split

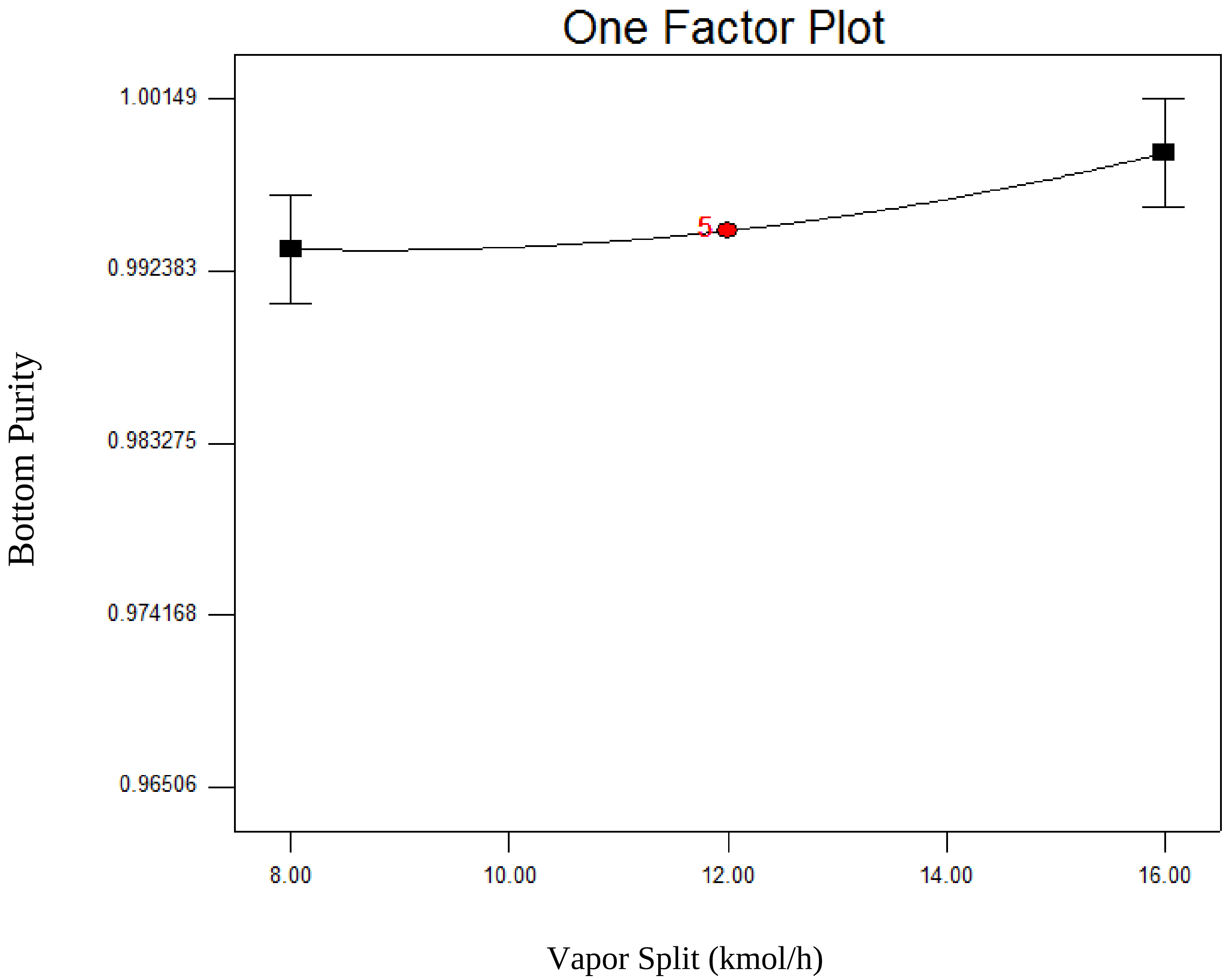

Figure 6.3c: Variation of mole fraction of water in the bottom stream with respect to vapour split

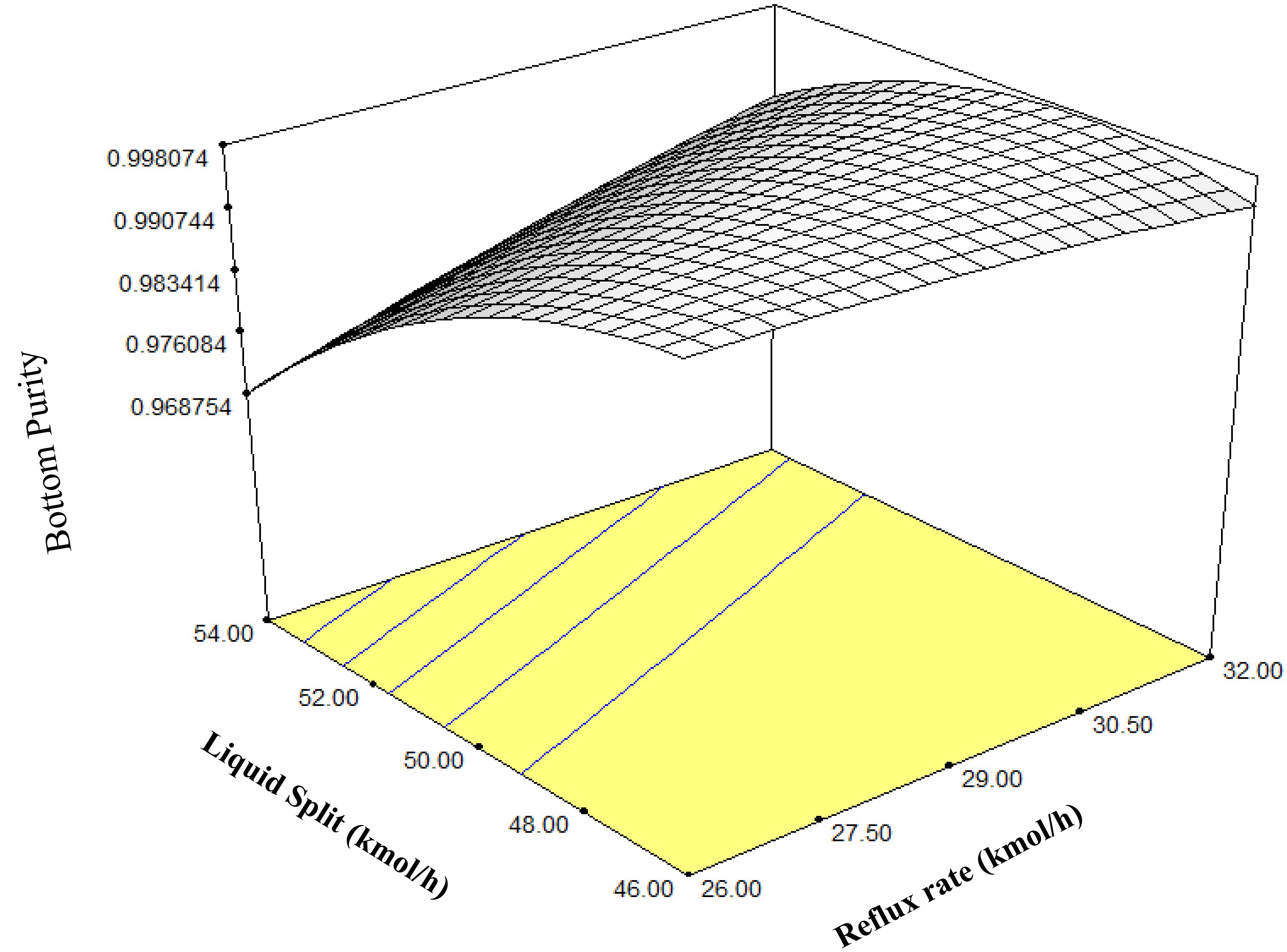

Figure 6.3d: Variation of mole fraction of water in the bottom stream with respect to liquid split and reflux rate

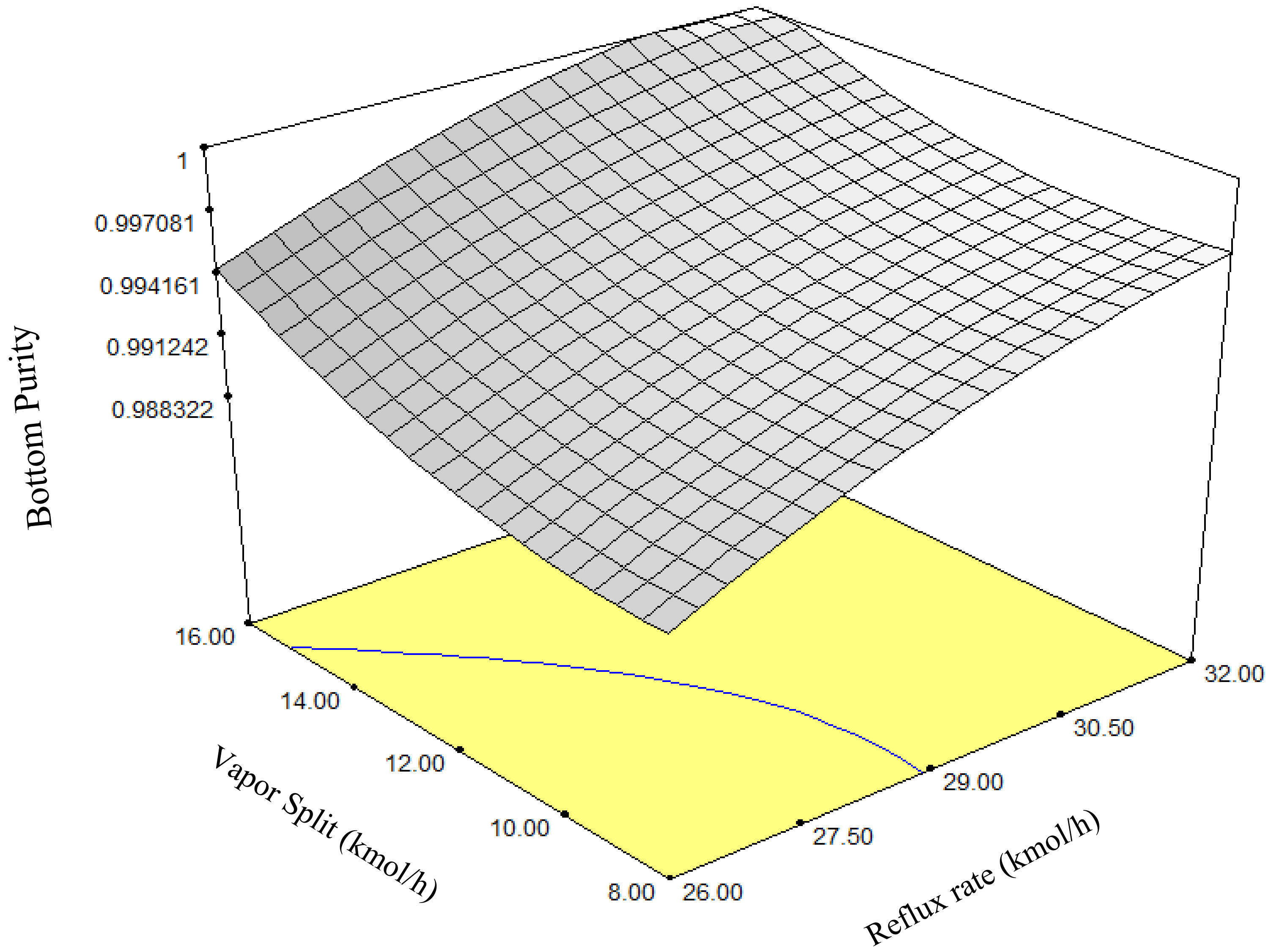

Figure 6.3e: Variation of mole fraction of water in the bottom stream with respect to vapor split and reflux rate

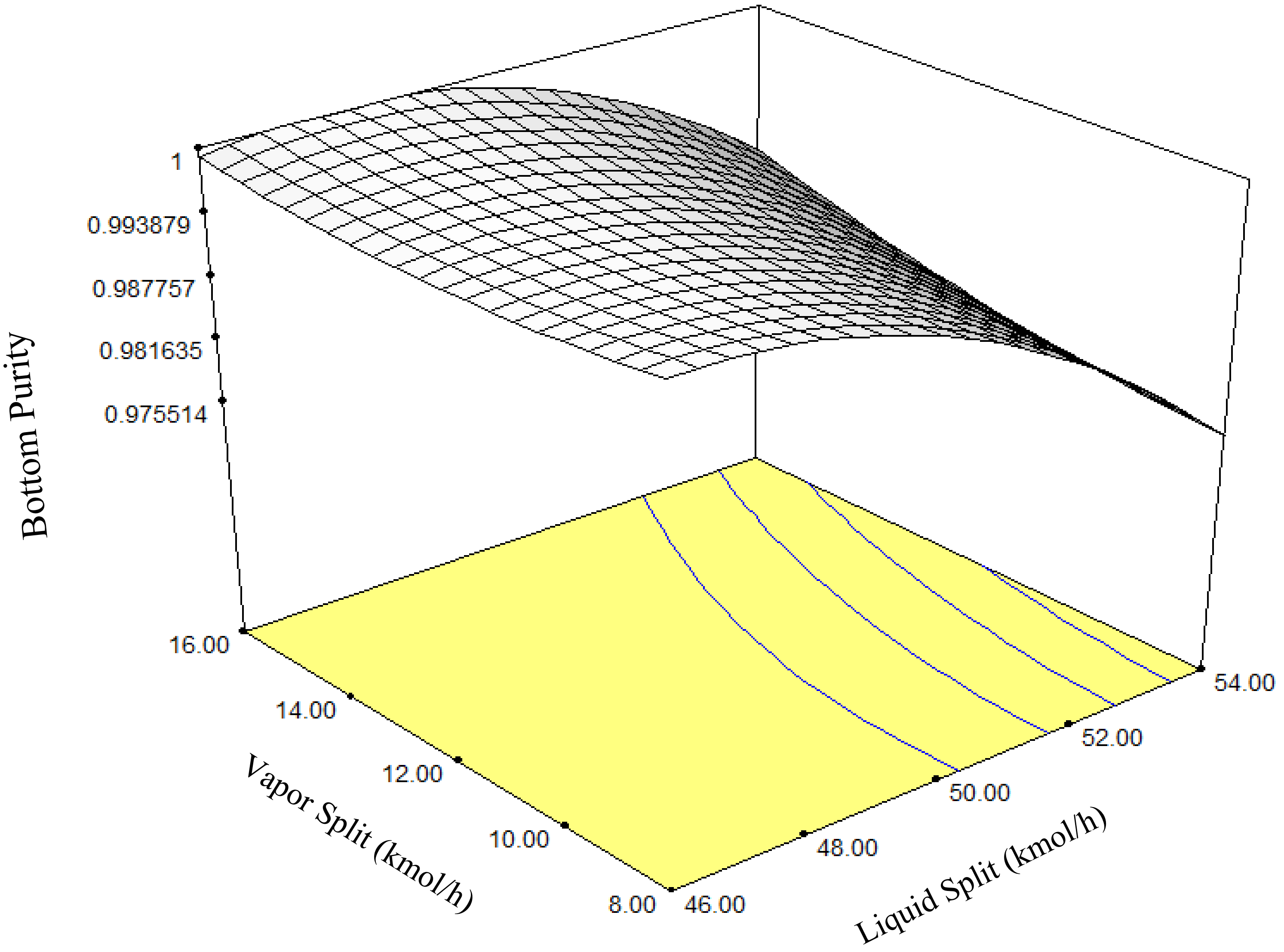

Figure 6.3f: Variation of mole fraction of water in the bottom stream with respect to vapor split and liquid split

6.4: Results for response reboiler duty Qb

Table 6.7a: Sequential Model Sum of Squares for Response: Qb

Source	Sum of Squares	Degree of Freedom	Mean Square	F Value	Prob> F	
Mean	1.44E+12	1	1.44E+12			
Linear	1.26E+09	3	4.21E+08	91.64849	< 0.0001	Suggested
2FI	18151813	3	6050604	1.456087	0.2847	
Quadratic	9191482	3	3063827	0.662708	0.6008	
Cubic	32362371	3	10787457	63660000	< 0.0001	Aliased
Residual	0	4	0			
Total	1.44E+12	17	8.47E+10			

Table 6.7b: Model Summary Statistics for Response: Qb

Source	Std. Dev.	Adjusted		Predicted		
		R-Squared	R-Squared	R-Squared	PRESS	
Linear	2143.069	0.954853	0.944434	0.90596	1.24E+08	Suggested
2FI	2038.476	0.968578	0.949725	0.840494	2.11E+08	
Quadratic	2150.162	0.975529	0.944065	0.608458	5.18E+08	
Cubic	0	1	1		+	Aliased

Table 6.7c: ANOVA for Response Surface Quadratic Model (for reboiler duty Qb)

Analysis of variance table [Partial sum of squares]						
Source	Sum of Squares	Degree of Freedom	Mean Square	F Value	Prob> F	
Model	1.29E+09	9	1.43E+08	31.00542	< 0.0001	significant
r	1.07E+09	1	1.07E+09	231.7656	< 0.0001	
l	1.05E+08	1	1.05E+08	22.77939	0.0020	
v	85942605	1	85942605	18.58944	0.0035	
r^2	1447729	1	1447729	0.313145	0.5932	
l^2	6779.013	1	6779.013	0.001466	0.9705	
v^2	8078195	1	8078195	1.747318	0.2278	
rl	5322249	1	5322249	1.151206	0.3189	
rv	8068440	1	8068440	1.745208	0.2280	
lv	4761124	1	4761124	1.029834	0.3440	
Residual	32362371	7	4623196			
Lack of Fit	32362371	3	10787457			
Pure Error	0	4	0			
Cor Total	1.32E+09	16				

Std. Dev.	2150.162		R-Squared	0.975529	
Mean	290866		Adjusted R-Squared	0.944065	
C.V.	0.739228		Predicted R-Squared	0.608458	
PRESS	5.18E+08		Adequate Precision	19.24938	

Final Equation in Terms of Actual Factors:		
	Qb	=
	135144.6	
	3464.847	* r
	2625.656	* l
	-5583.36	* v
	65.15278	* r2
	2.507812	* l2
	-86.5703	* v2
	-96.125	* r * l
	118.3542	* r * v
	68.1875	* l * v

Model F-value = 31.04 model is significant.

In this case r, l and v are significant model terms.

Adequate Precision = 19.25 indicates an adequate signal.

Figure 6.4(a,b,c,d,e,f) shows the variation of reboiler duty with respect to process parameters with one factor and two factor variations. Figure 6.4a,b shows more or less linear variation of reboiler duty with respect to reflux rate, liquid split respectively and figure 5.4c shows non-linear variation with vapor split. Figure 6.4a show that the reboiler duty increases with increase in reflux rate, figure 6.4b show that as liquid split increases the reboiler duty also increases but not up to considerable amount for a given range of liquid split, figure 6.4c shows the monotonically decreasing attitude of reboiler duty with increase in vapor split in a defined range. Figure 6.4d,e,f shows the three dimensional plot of reboiler duty with respect to combinations of any two parameters form process parameters list. Figure 6.4d shows the variation of reboiler duty with respect to liquid split and reflux rate, plot shows that the reboiler duty decreases with decrease in liquid split and reflux rate. Figure 6.4e shows the variation of reboiler duty with respect to vapor split and reflux rate, plot shows that the reboiler duty doesn’t show any significant variation with vapor split and it decreases with decrease in reflux rate. Figure 6.4f shows the variation of reboiler duty with respect to vapor split and liquid split, plot shows that the reboiler duty decreases with increase in vapor split and decrease in liquid split.

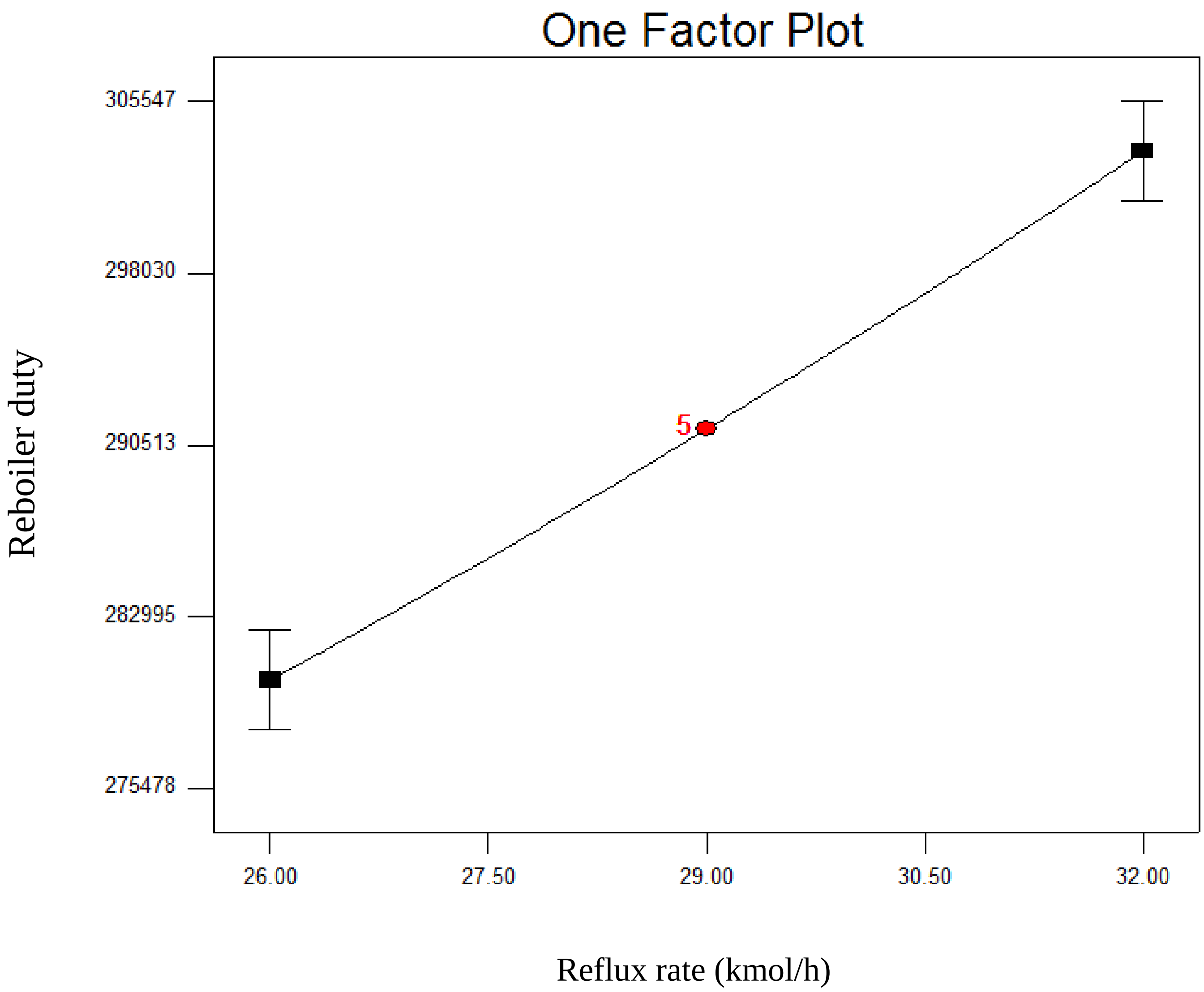

Figure 6.4a: Variation of reboiler duty with respect to reflux rate

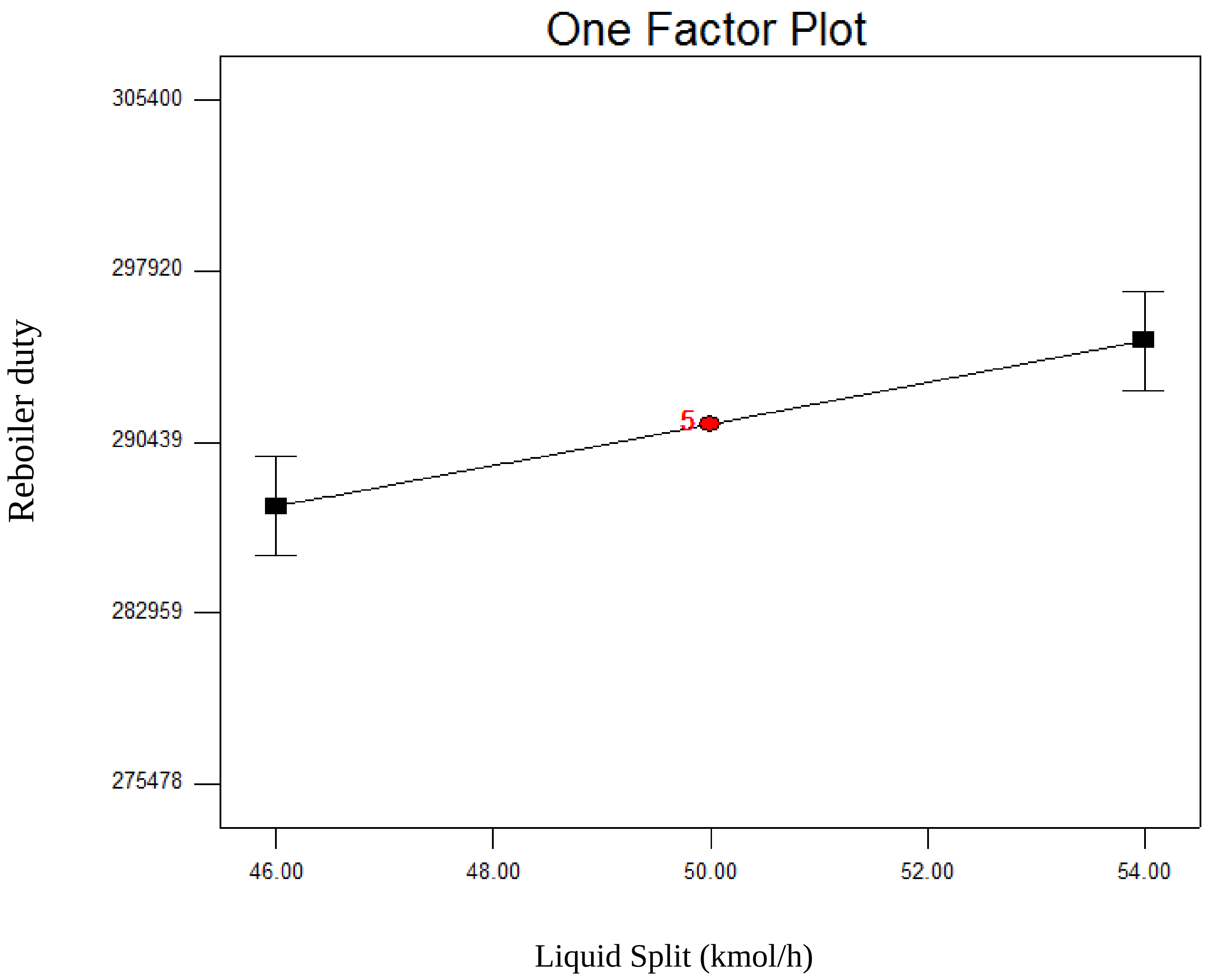

Figure 6.4b: Variation of reboiler duty with respect to liquid split

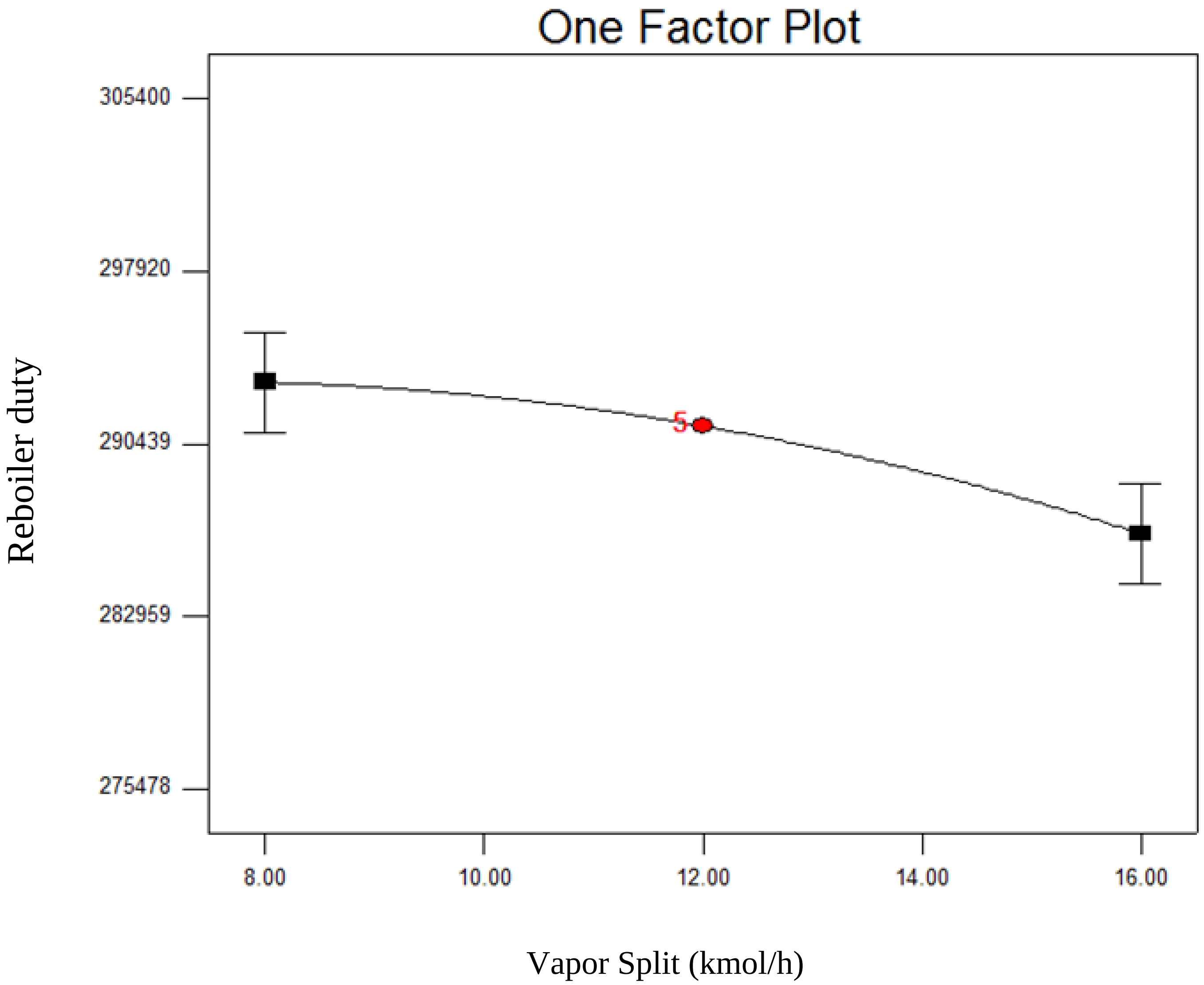

Figure 6.4c: Variation of reboiler duty with respect to vapor split

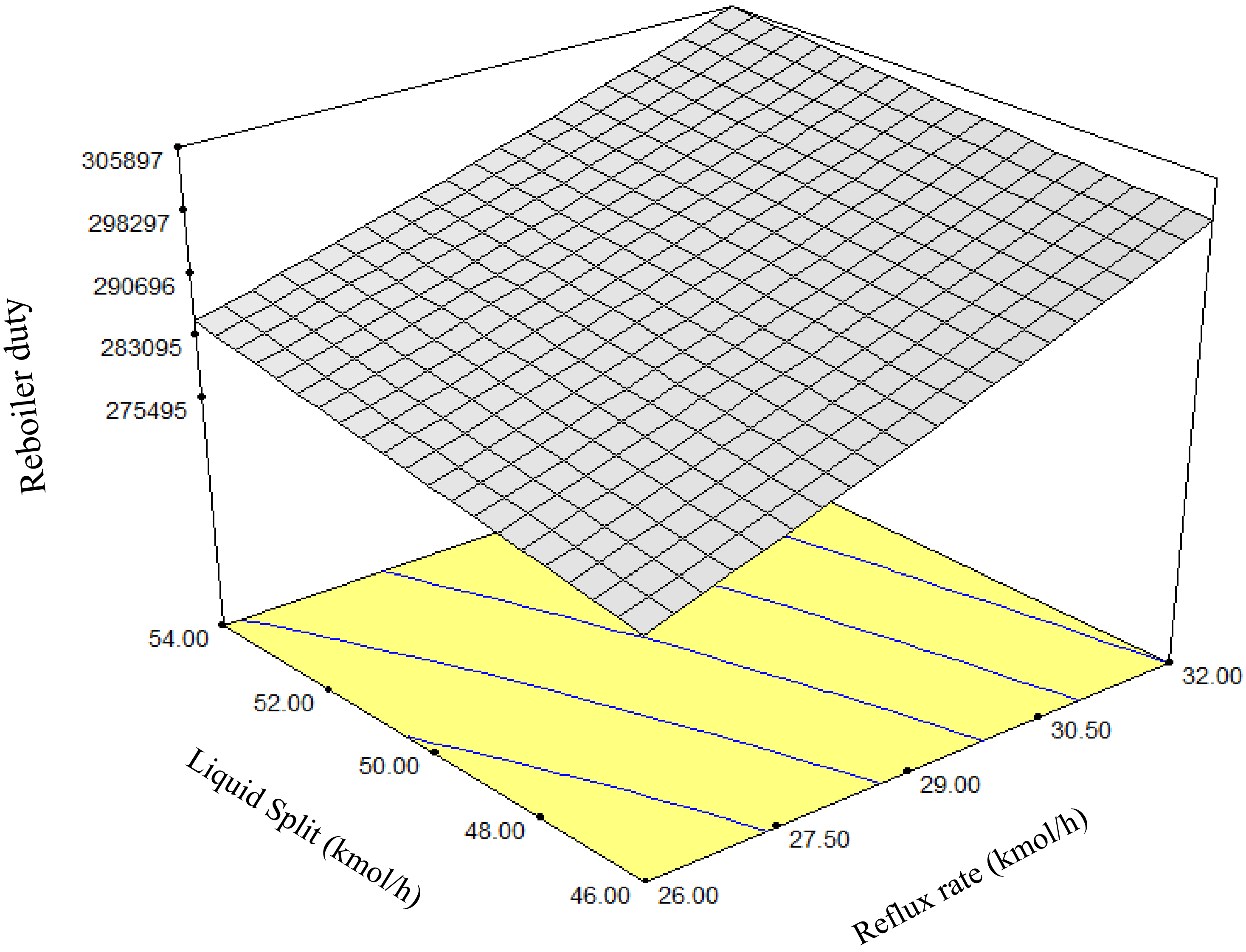

Figure 6.4d: Variation of reboiler duty with respect to liquid split and reflux rate

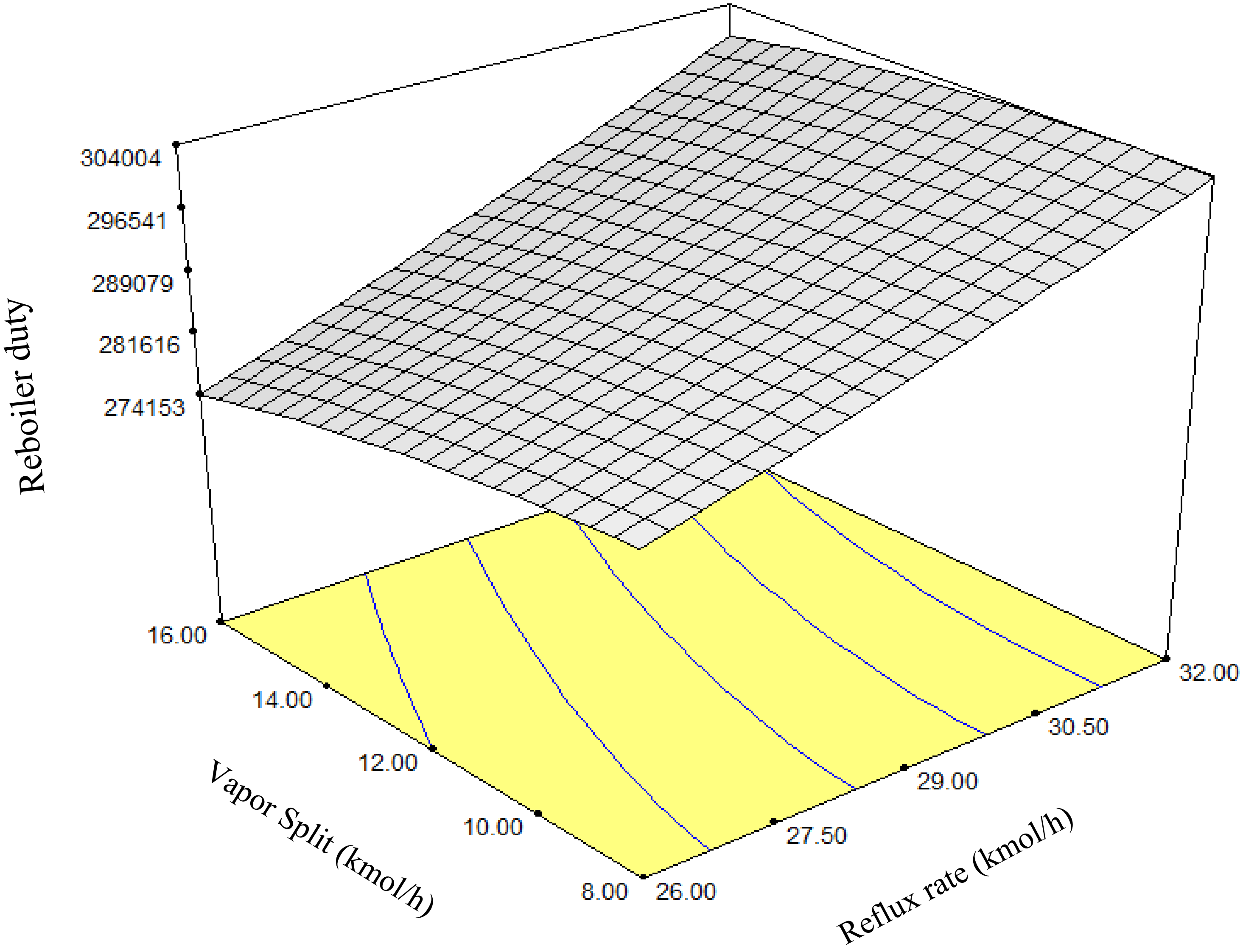

Figure 6.4e: Variation of reboiler duty with respect to vapor split and reflux rate

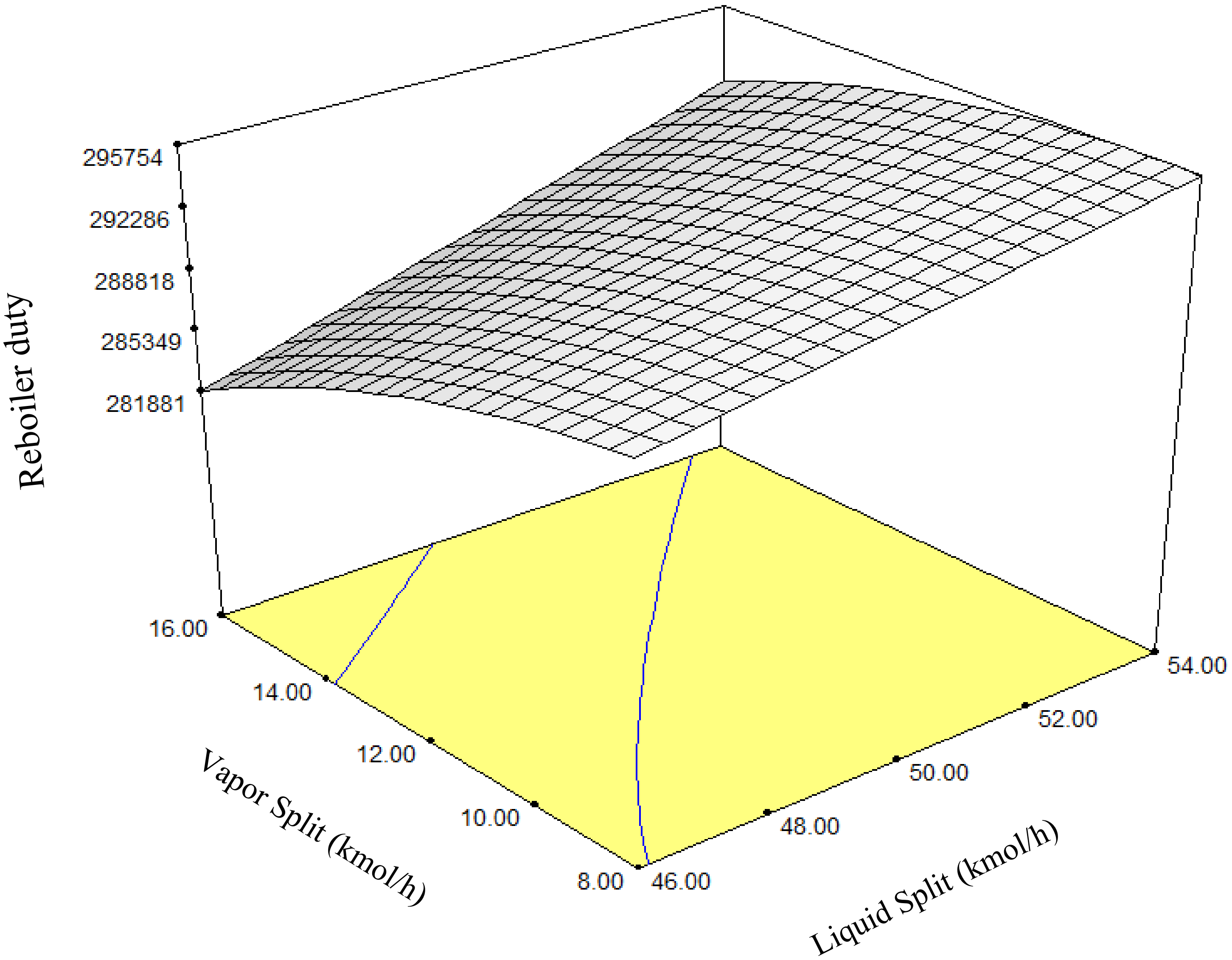

Figure 6.4f: Variation of reboiler duty with respect to vapor split and liquid split

6.5: Results for response condenser duty Qc

Table 6.8a Sequential Model Sum of Squares for Response: Qc

Source	Sum of Squares	Degree of Freedom	Mean Square	F Value	Prob> F	
Mean	6.81E+11	1	6.81E+11			
Linear	1.34E+09	3	4.46E+08	51.04464	< 0.0001	
2FI	70228835	3	23409612	5.404413	0.0181	Suggested
Quadratic	29645654	3	9881885	5.060188	0.0357	Suggested
Cubic	13670083	3	4556694	63660000	< 0.0001	Aliased
Residual	0	4	0			
Total	6.83E+11	17	4.01E+10			

Table 6.8b Model Summary Statistics for Response: Qc

Source	Std. Dev.	Adjusted		Predicted		
		R-Squared	R-Squared	R-Squared	PRESS	
Linear	2955.368	0.92175	0.903692	0.845248	2.25E+08	
2FI	2081.243	0.970149	0.952238	0.884233	1.68E+08	Suggested
Quadratic	1397.451	0.990579	0.978467	0.849266	2.19E+08	Suggested
Cubic	0	1	1		+	Aliased

Model used is quadratic

Table 6.8c: ANOVA for Response Surface Quadratic Model (for condenser duty Qc)

Analysis of variance table [Partial sum of squares]						
Source	Sum of Squares	Degree of Freedom	Mean Square	F Value	Prob> F	
Model	1.44E+09	9	1.6E+08	81.78147	< 0.0001	significant
r	1.23E+09	1	1.23E+09	631.9934	< 0.0001	
l	31157618	1	31157618	15.95479	0.0052	
v	72144072	1	72144072	36.94261	0.0005	
r^2	1234620	1	1234620	0.632208	0.4527	
l^2	978206.3	1	978206.3	0.500907	0.5020	
v^2	25948658	1	25948658	13.28745	0.0082	
rl	4182025	1	4182025	2.141478	0.1868	
rv	32069569	1	32069569	16.42177	0.0049	
lv	33977241	1	33977241	17.39863	0.0042	
Residual	13670083	7	1952869			
Lack of Fit	13670083	3	4556694			
Pure Error	0	4	0			
Cor Total	1.45E+09	16				

Std. Dev.	1397.451		R-Squared	0.990579		
Mean	-200157		Adj R-Squared	0.978467		
C.V.	-0.69818		Pred R-Squared	0.849266		
PRESS	2.19E+08		Adeq Precision	28.78113		

Final Equation in Terms of Actual Factors:		
	Qc	=
	-60302.8	
	-2079.5	* r
	-2137.79	* l
	2209.479	* v
	-60.1667	* r^2
	-30.125	* l^2
	-155.156	* v^2
	85.20833	* r * l
	-235.958	* r * v
	182.1563	* l * v

Model F-value = 81.78 model is significant.

In this case r, l, v, v^2, rv and lv are significant model terms.

Adequate Precision = 28.78 indicates an adequate signal.

Figure 6.5(a,b,c,d,e,f) shows the variation of condenser duty with respect to process parameters with one factor and two factor variations. Figure 6.5a,b shows more or less linear variation of condenser duty with respect to reflux rate, liquid split respectively and figure 6.5c shows non-linear variation with vapor split. Figure 6.5a show that the condenser duty increases with increase in reflux rate, figure 6.5b show that as liquid split increases the condenser duty also increases but not up to considerable amount for a given range of liquid split, figure 6.5c shows the monotonically decreasing attitude of condenser duty with increase in vapor split in a defined range. Figure 6.5d,e,f shows the three dimensional plot of condenser duty with respect to combinations of any two parameters form process parameters list. Figure 6.5d shows the variation of condenser duty with respect to liquid split and reflux rate, plot shows that the condenser duty decreases with decrease in liquid split and reflux rate. Figure 6.5e shows the variation of condenser duty with respect to vapor split and reflux rate, plot shows that the condenser duty doesn’t show any significant variation with vapor split and it decreases with decrease in reflux rate. Figure 6.5f shows the variation of condenser duty with respect to vapor split and liquid split, plot shows that the condenser duty decreases with increase in vapor split and decrease in liquid split.

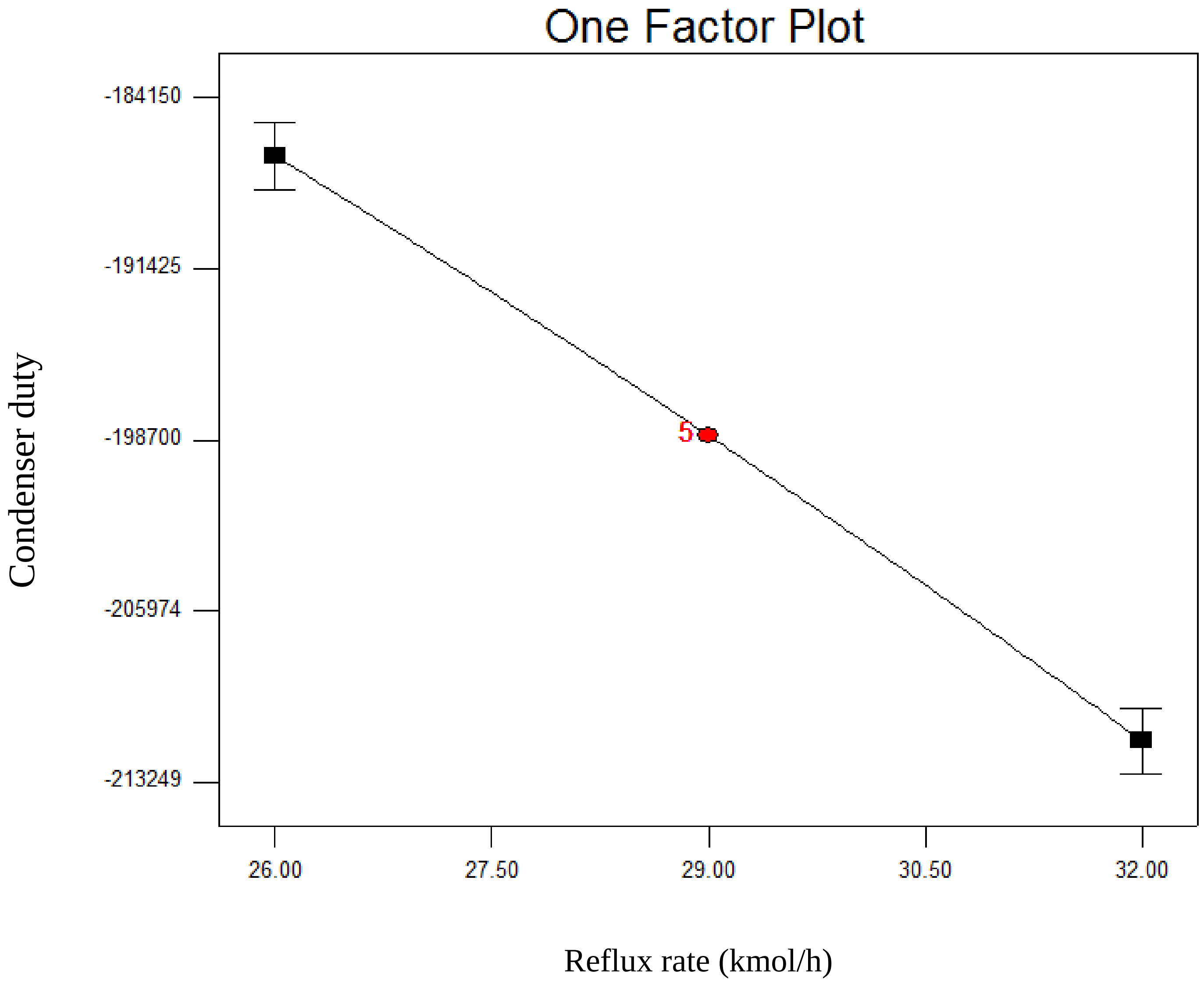

Figure 6.5a: Variation of condenser duty with respect to reflux rate

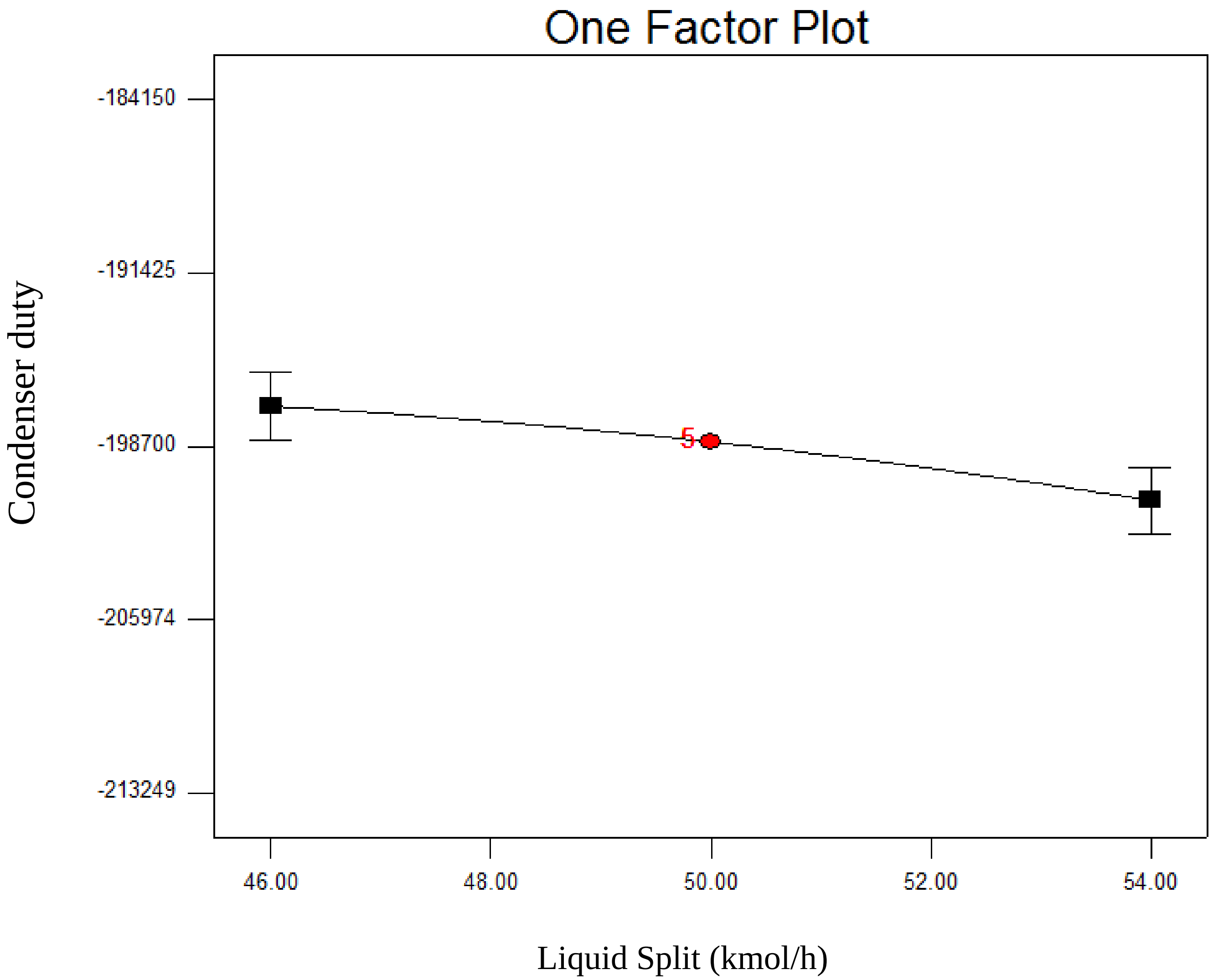

Figure 6.5b: Variation of condenser duty with respect to liquid split

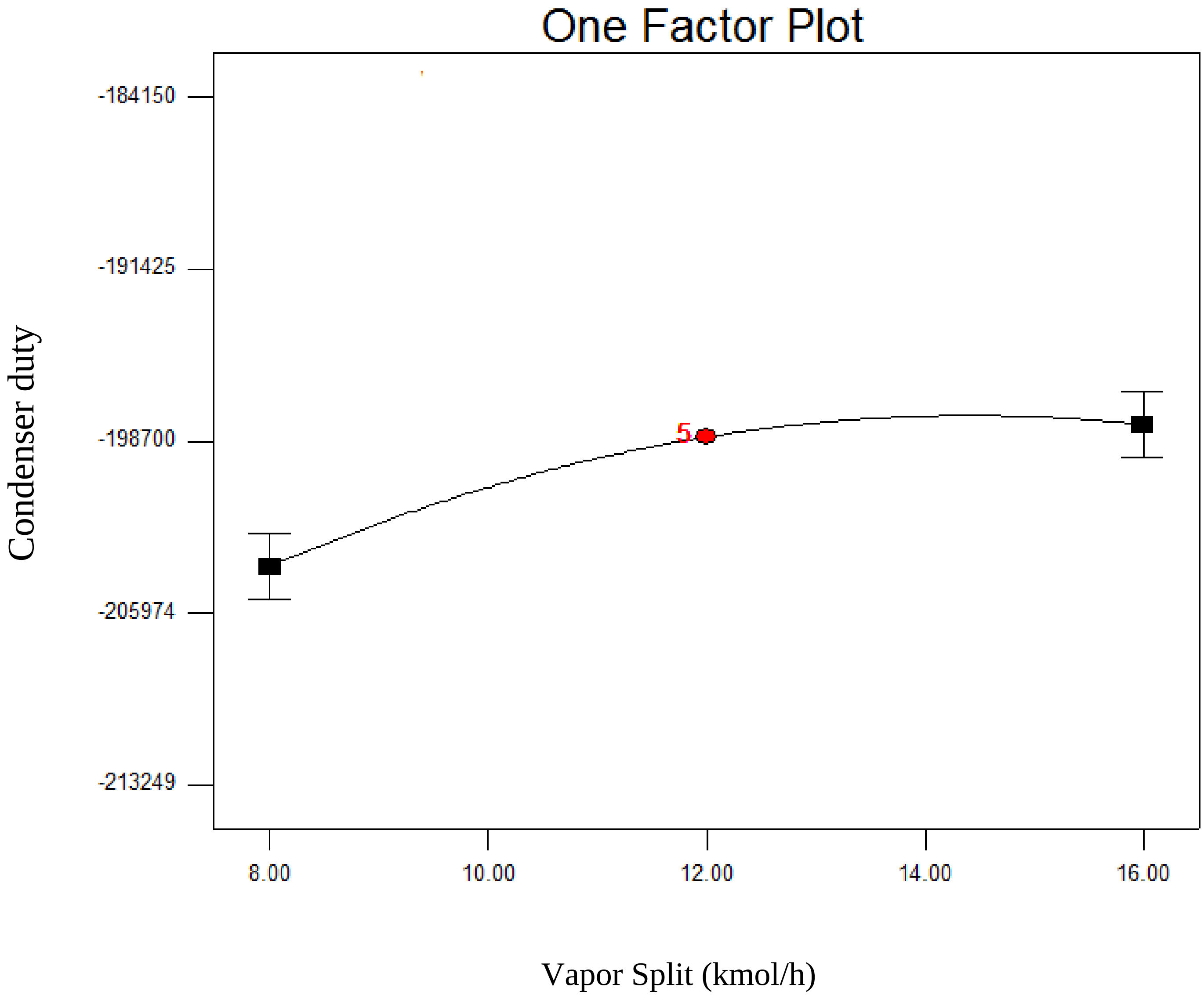

Figure 6.5c: Variation of condenser duty with respect to vapour split

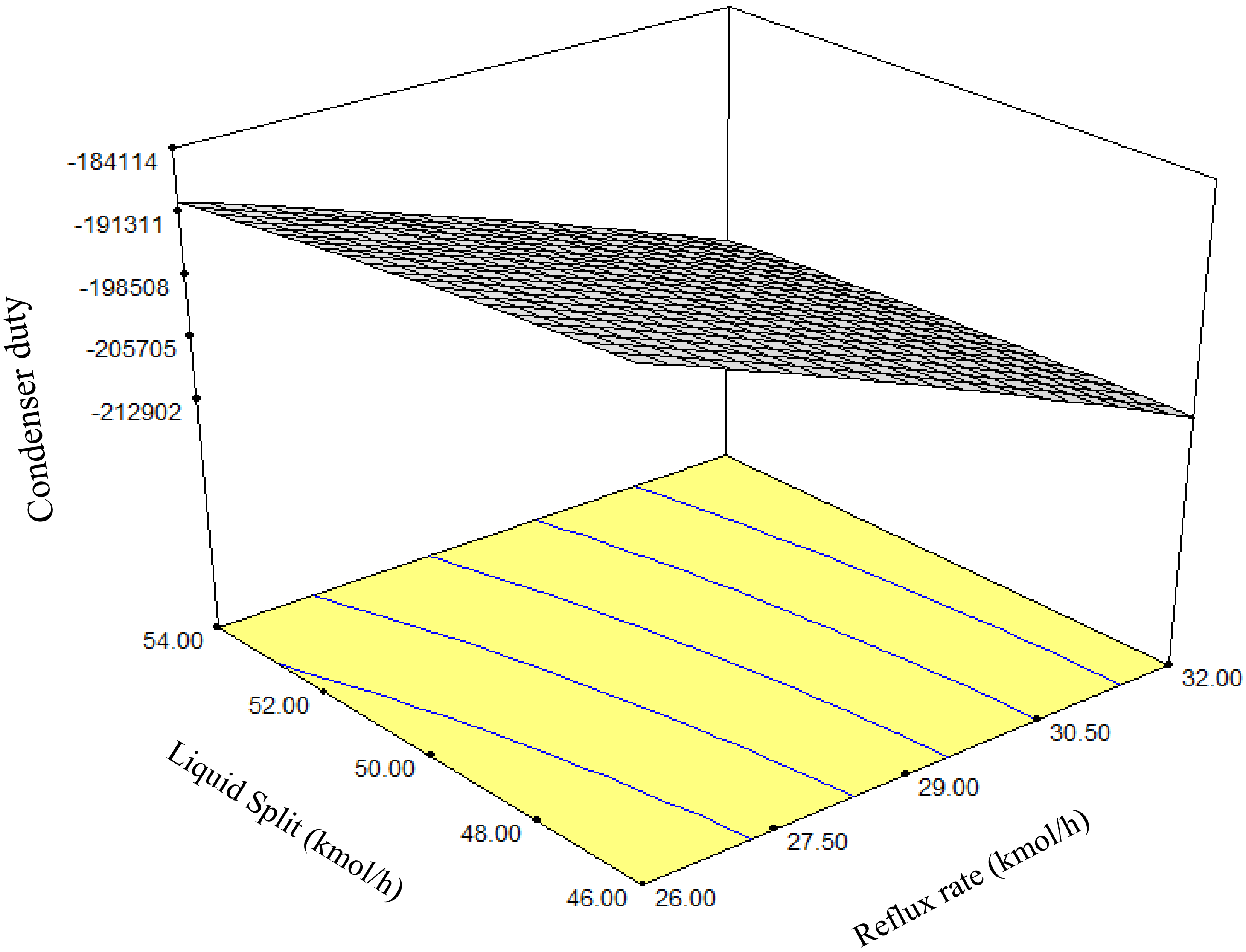

Figure 6.5d: Variation of condenser duty with respect to liquid split and reflux rate

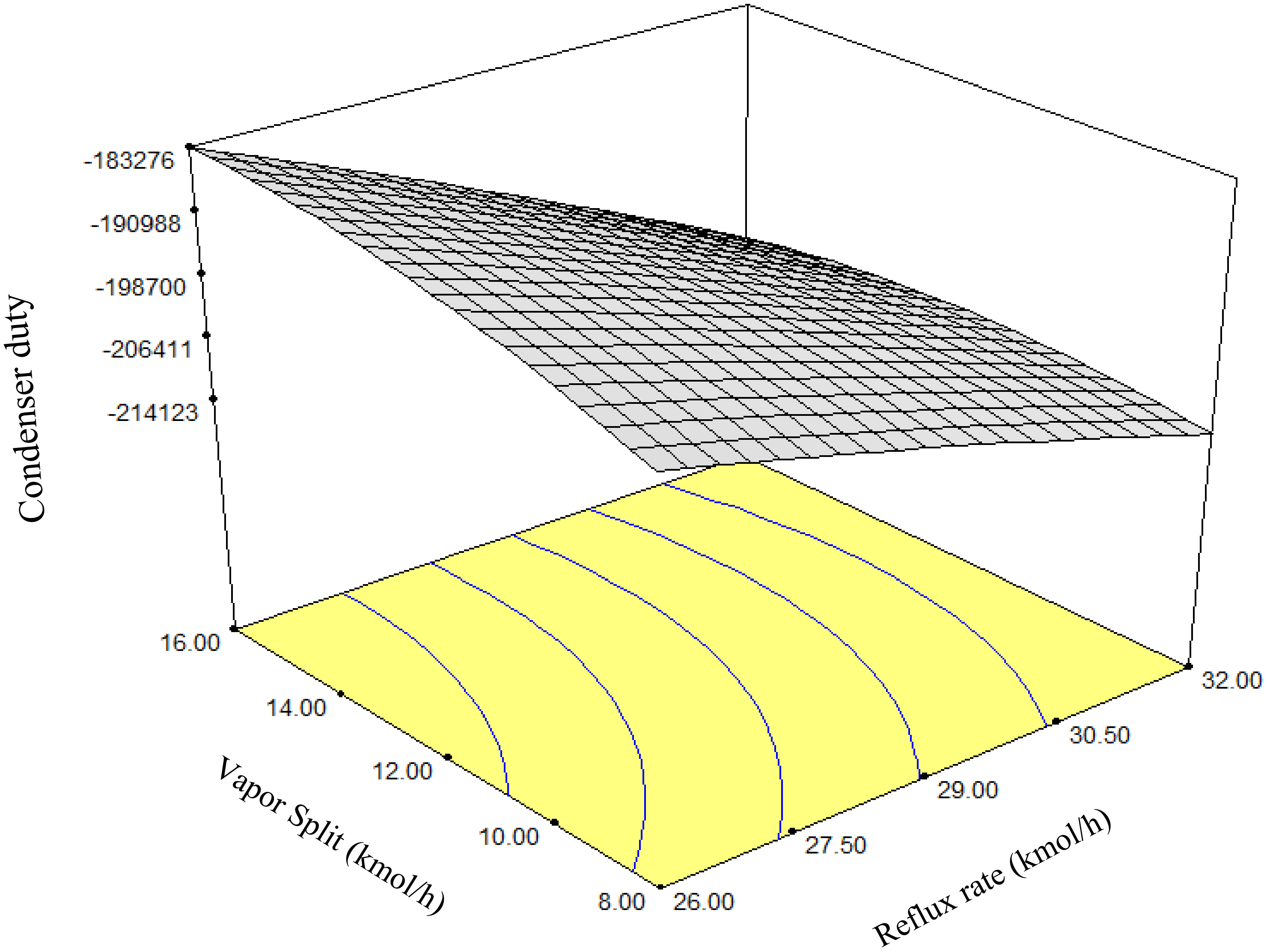

Figure 6.5e: Variation of condenser duty with respect to vapor split and reflux rate

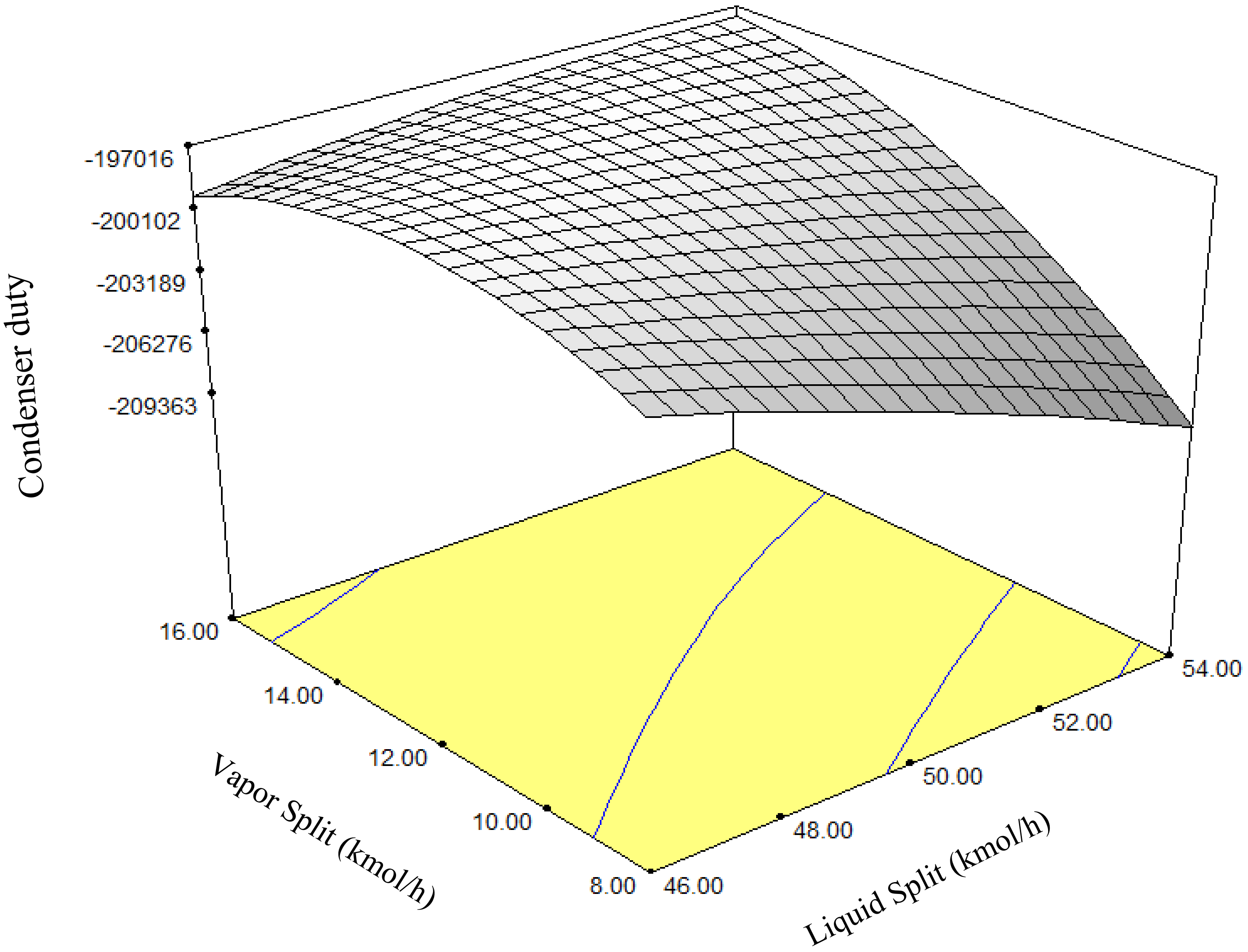

Figure 6.5e: Variation of condenser duty with respect to vapor split and liquid split

6.6: Results for response difference in pressure drop Del P

Table 6.9a: Sequential Model Sum of Squares for Response: Del P

Source	Sum of Squares	Degree of Freedom	Mean Square	F Value	Prob> F	
Mean	0.000307	1	0.000307			
Linear	0.001822	3	0.000607	45.73848	< 0.0001	
2FI	3.11E-05	3	1.04E-05	0.732191	0.5561	
Quadratic	0.000127	3	4.22E-05	19.71446	0.0009	Suggested
Cubic	1.5E-05	3	4.99E-06	63660000	< 0.0001	Aliased
Residual	0	4	0			
Total	0.002302	17	0.000135			

Table 6.9b: Model Summary Statistics for Response: Del P

Source	Std. Dev.	Adjusted		Predicted		
		R-Squared	R-Squared	R-Squared	PRESS	
Linear	0.003644	0.913458	0.893486	0.835278	0.000329	
2FI	0.003762	0.929044	0.88647	0.703758	0.000591	
Quadratic	0.001463	0.992491	0.982836	0.87985	0.00024	Suggested
Cubic	0	1	1		+	Aliased

Model used is quadratic

Table 6.9c: ANOVA for Response Surface Quadratic Model (for Del P)

Analysis of variance table [Partial sum of squares]						
Source	Sum of Squares	Degree of Freedom	Mean Square	F Value	Prob> F	
Model	0.00198	9	0.00022	102.7967	< 0.0001	significant
r	2.14E-06	1	2.14E-06	1.001325	0.3503	
l	1.7E-05	1	1.7E-05	7.961846	0.0257	
v	0.001803	1	0.001803	842.5353	< 0.0001	
r^2	4.74E-08	1	4.74E-08	0.022163	0.8859	
l^2	2.93E-09	1	2.93E-09	0.001369	0.9715	
v^2	0.000126	1	0.000126	58.67937	0.0001	
rl	1.06E-07	1	1.06E-07	0.049518	0.8303	
rv	4.72E-06	1	4.72E-06	2.205891	0.1811	
lv	2.63E-05	1	2.63E-05	12.27347	0.0099	
Residual	1.5E-05	7	2.14E-06			
Lack of Fit	1.5E-05	3	4.99E-06			
Pure Error	0	4	0			
Cor Total	0.001994	16				

Std. Dev.	0.001463		R-Squared	0.992491		
Mean	-0.00425		Adj R-Squared	0.982836		
C.V.	-34.4075		Pred R-Squared	0.87985		
PRESS	0.00024		Adeq Precision	31.65713		

Final Equation in Terms of Actual Factors:		
	Del P	=
	0.049454	
	0.001265	* r
	-0.00212	* l
	-0.00094	* v
	-1.2E-05	* r^2
	1.65E-06	* l^2
	-0.00034	* v^2
	1.36E-05	* r * l
	-9.1E-05	* r * v
	0.00016	* l * v

Model F-value = 102.80 model is significant.

In this case l, v, v^2 and lv are significant model terms.

Adequate Precision = 31.657 indicates an adequate signal.

Figure 6.6(a,b,c,d,e,f) shows the variation of difference in pressure drop at both sides of the wall (Del P) with respect to process parameters with one factor and two factor variations. Figure 6.6a,b shows more or less linear variation of Del P with respect to reflux rate, liquid split respectively and figure 6.6c shows non-linear variation with vapor split. Figure 6.6a,b show that the Del P doesn’t have any significant change with increase in reflux rate and liquid split respectively, figure 6.6c shows the monotonically decreasing attitude of Del P with increase in vapor split in a defined range. Figure 6.6d,e,f shows the three dimensional plot of Del P with respect to combinations of any two parameters form process parameters list. Figure 6.6d shows the variation of Del P with respect to liquid split and reflux rate, plot shows that the Del P decreases with decrease in liquid split and reflux rate. Figure 6.6e shows the variation of Del P with respect to vapor split and reflux rate, plot shows that the Del P doesn't show any significant variation with reflux rate and it decreases with increase in vapor split. Figure 6.6f shows the variation of Del P with respect to vapor split and liquid split, plot shows that the Del P doesn't show any significant variation with liquid split and it decreases with increase in vapor split.

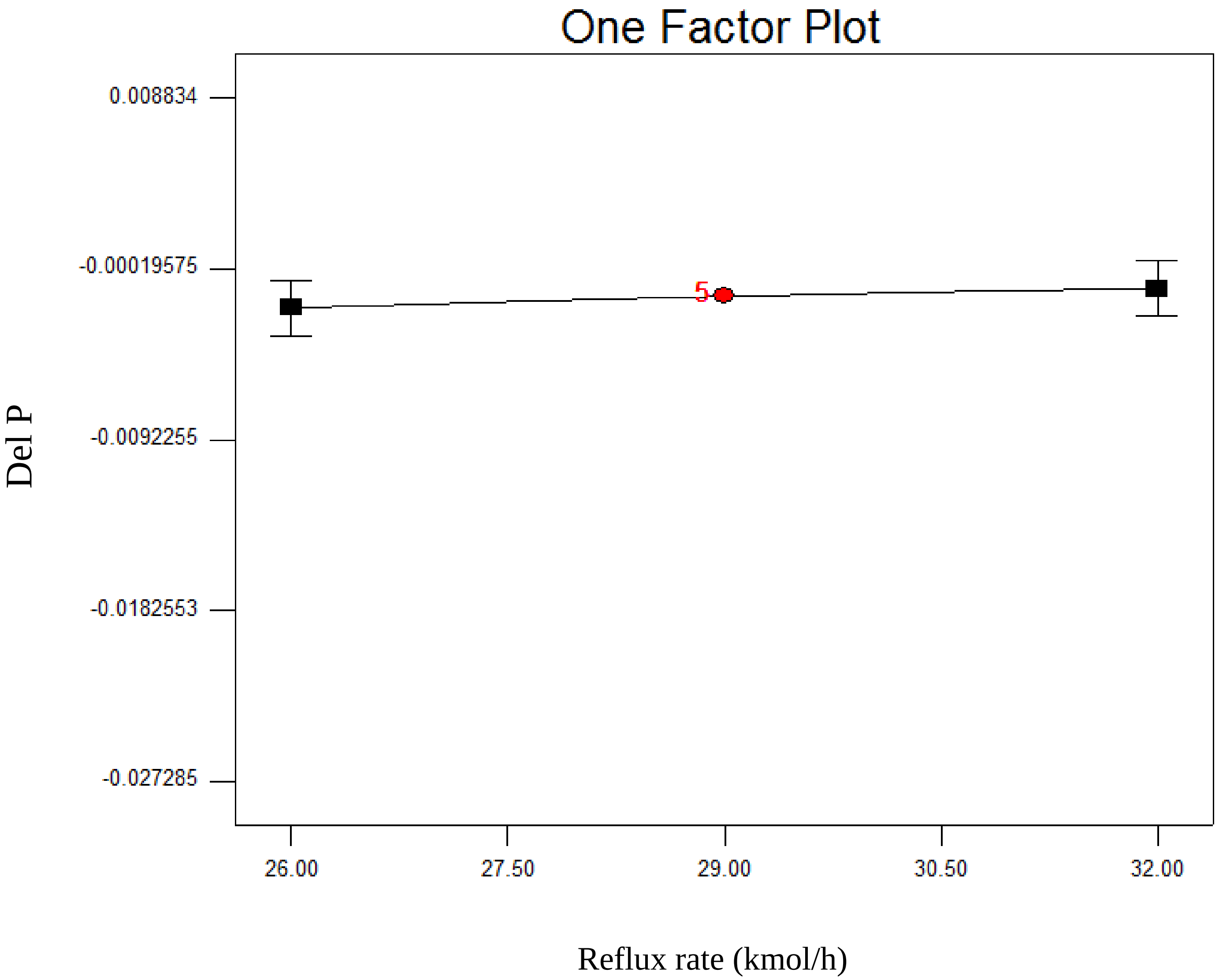

Figure 6.6a: Variation of difference in pressure drop with respect to reflux rate

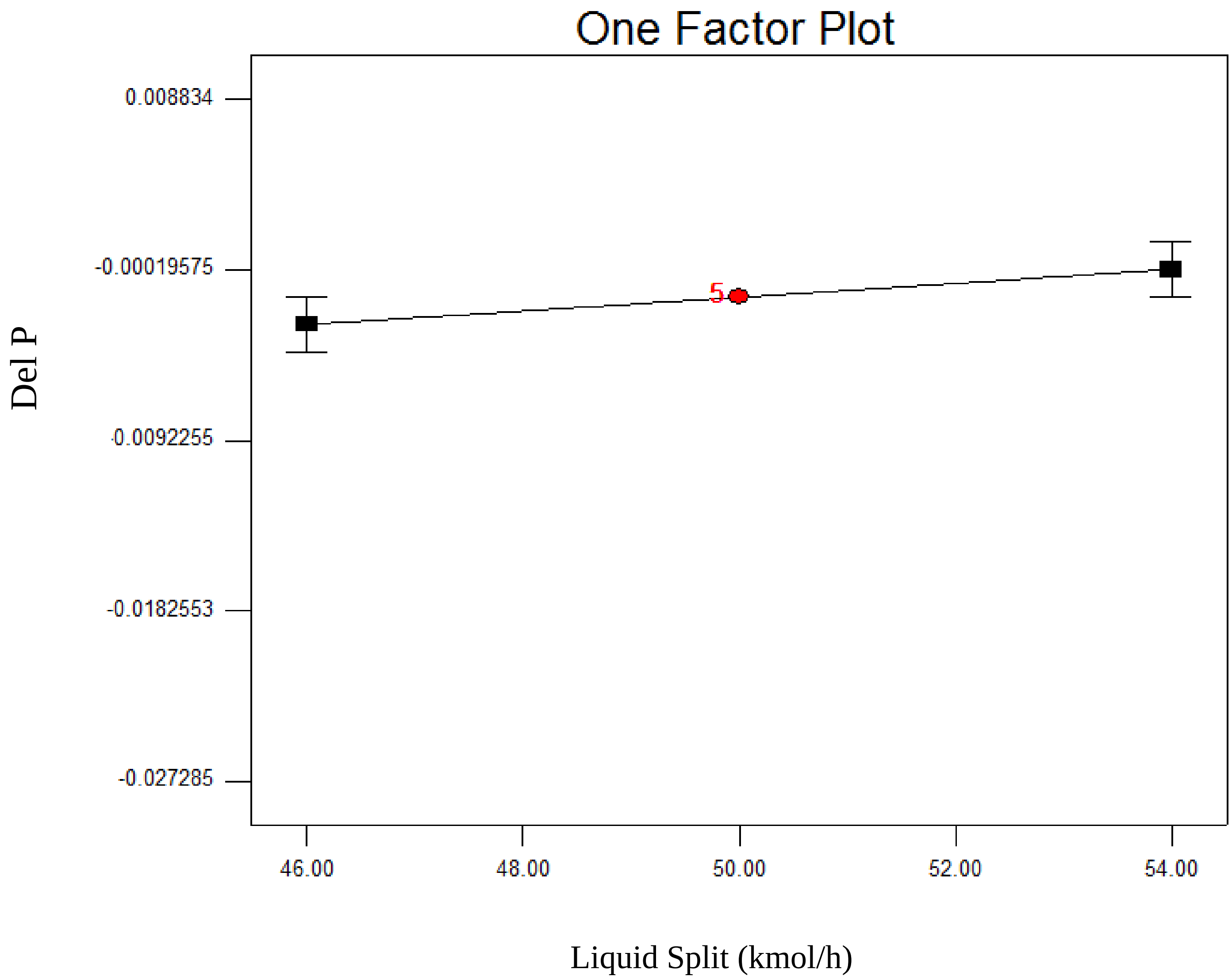

Figure 6.6b: Variation of difference in pressure drop with respect to liquid split

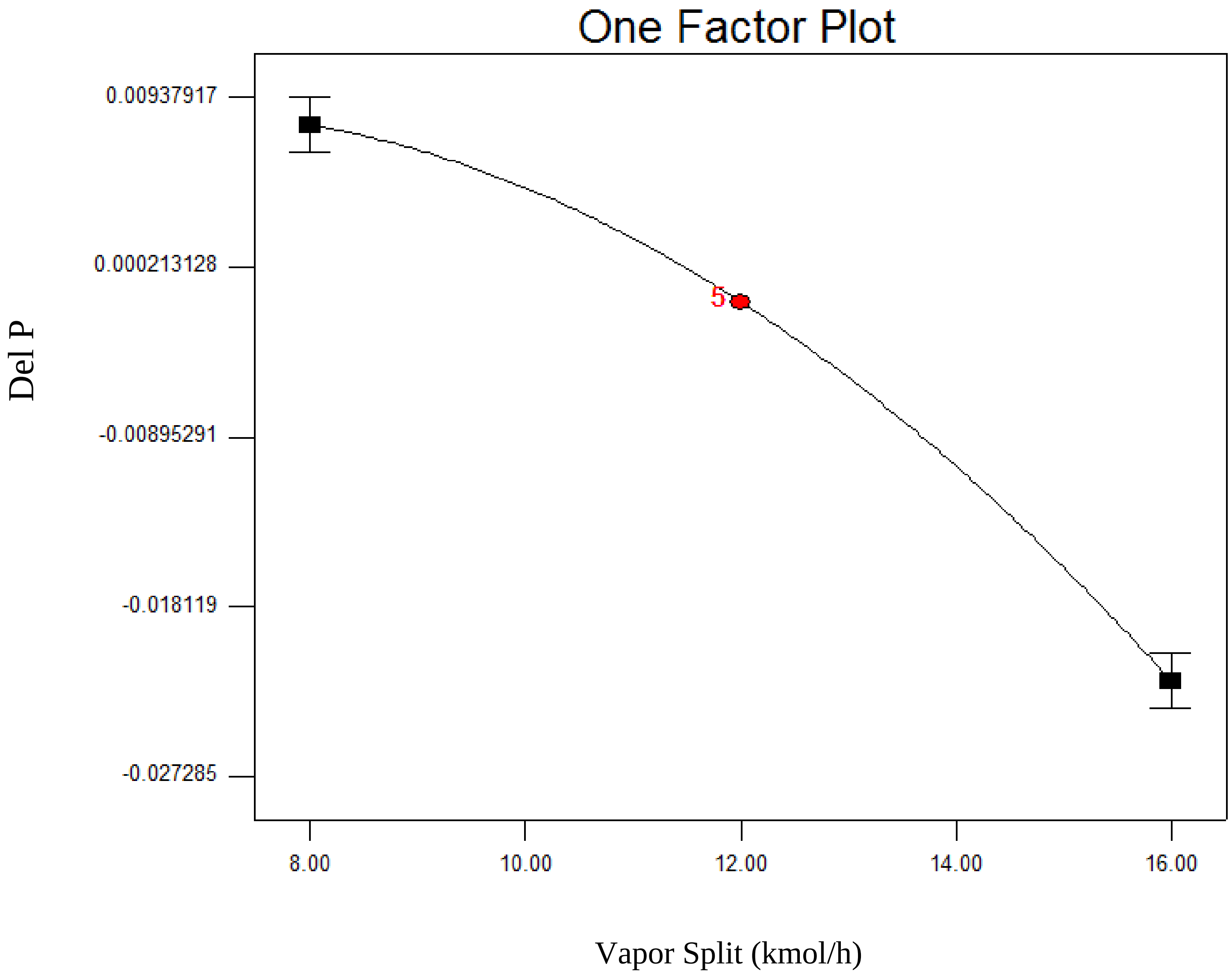

Figure 6.6c: Variation of difference in pressure drop with respect to vapor split

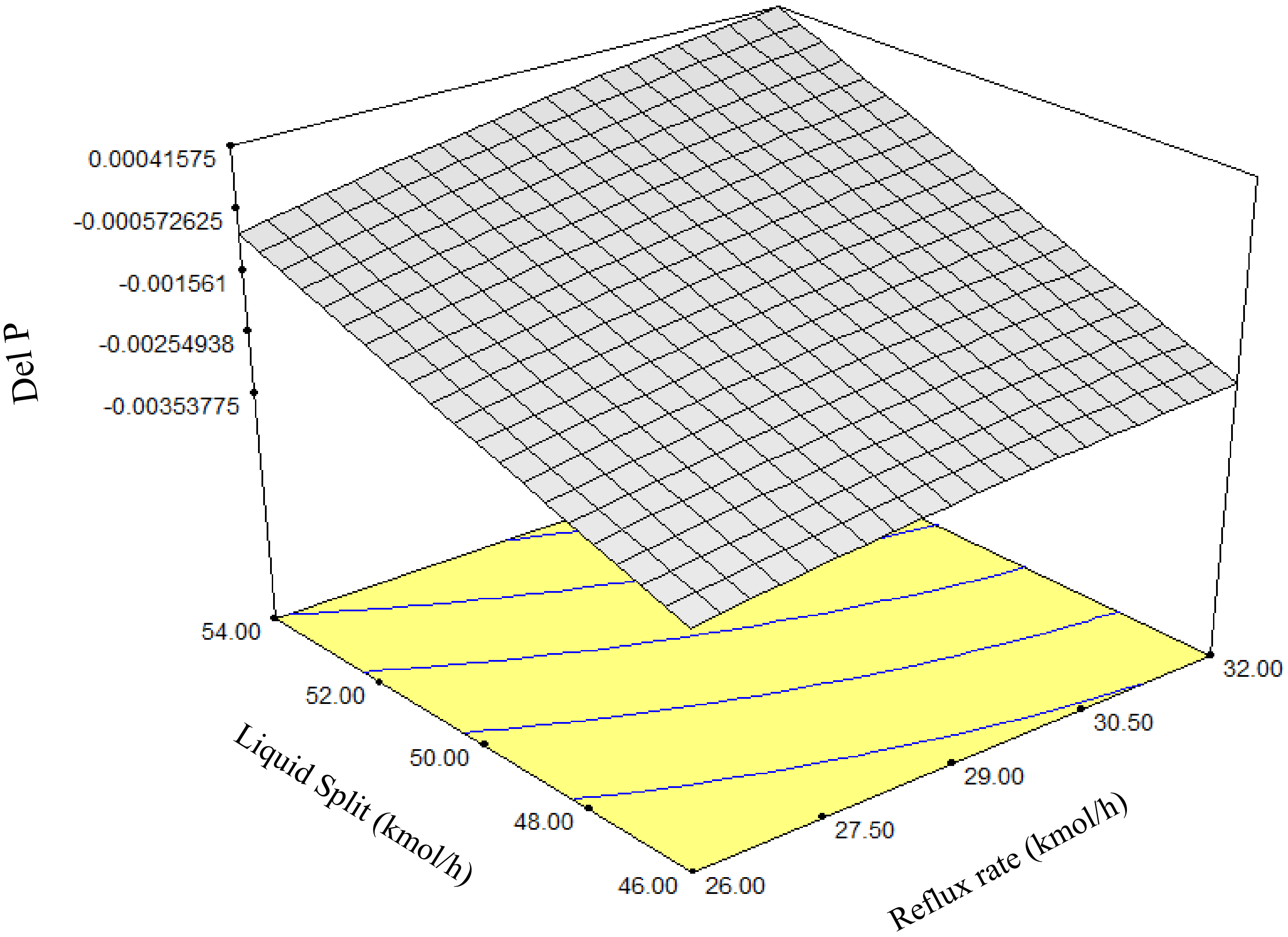

Figure 6.6d: Variation of difference in pressure drop with respect to liquid split and reflux rate

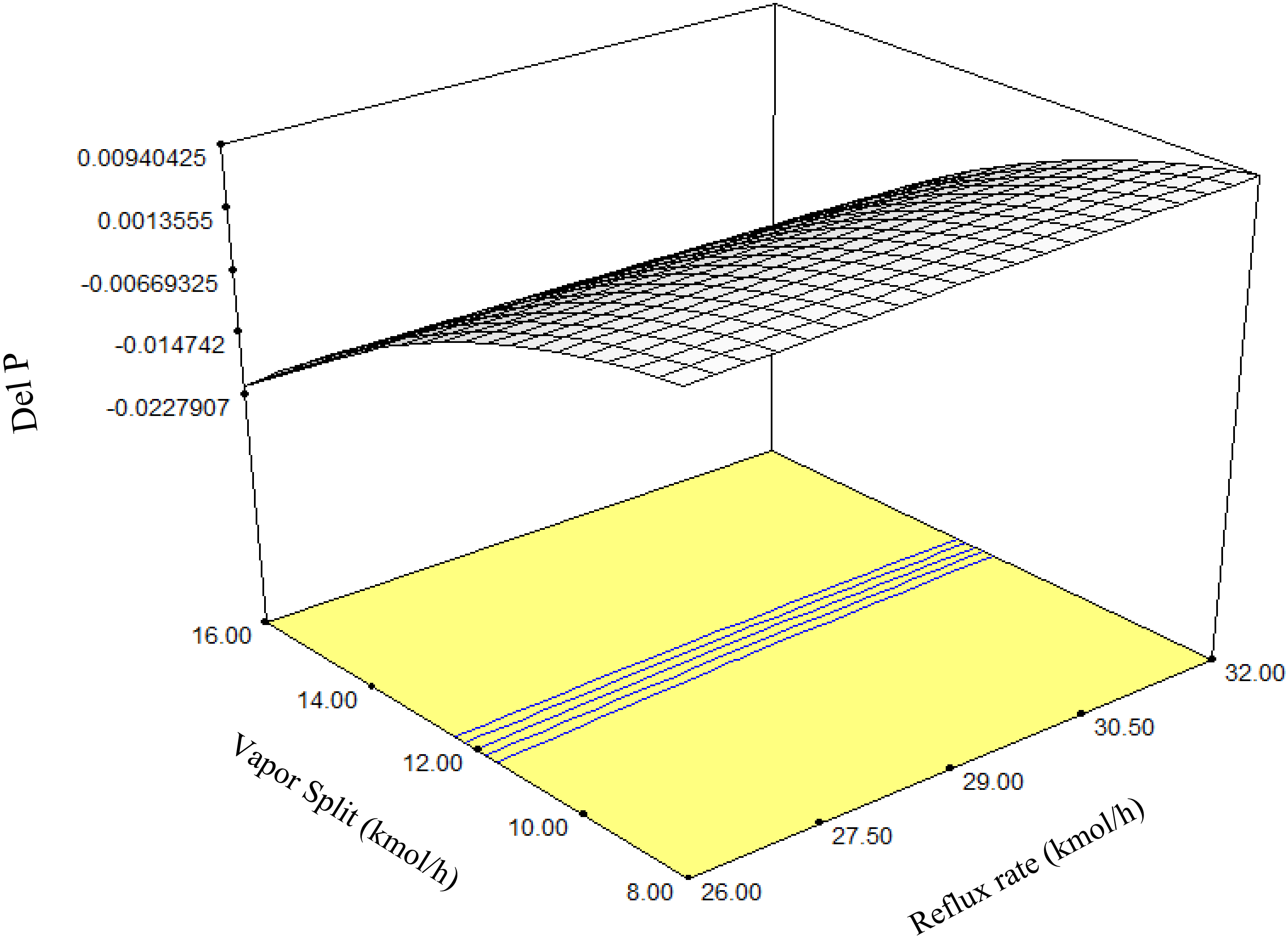

Figure 6.6e: Variation of difference in pressure drop with respect to vapor split and reflux rate

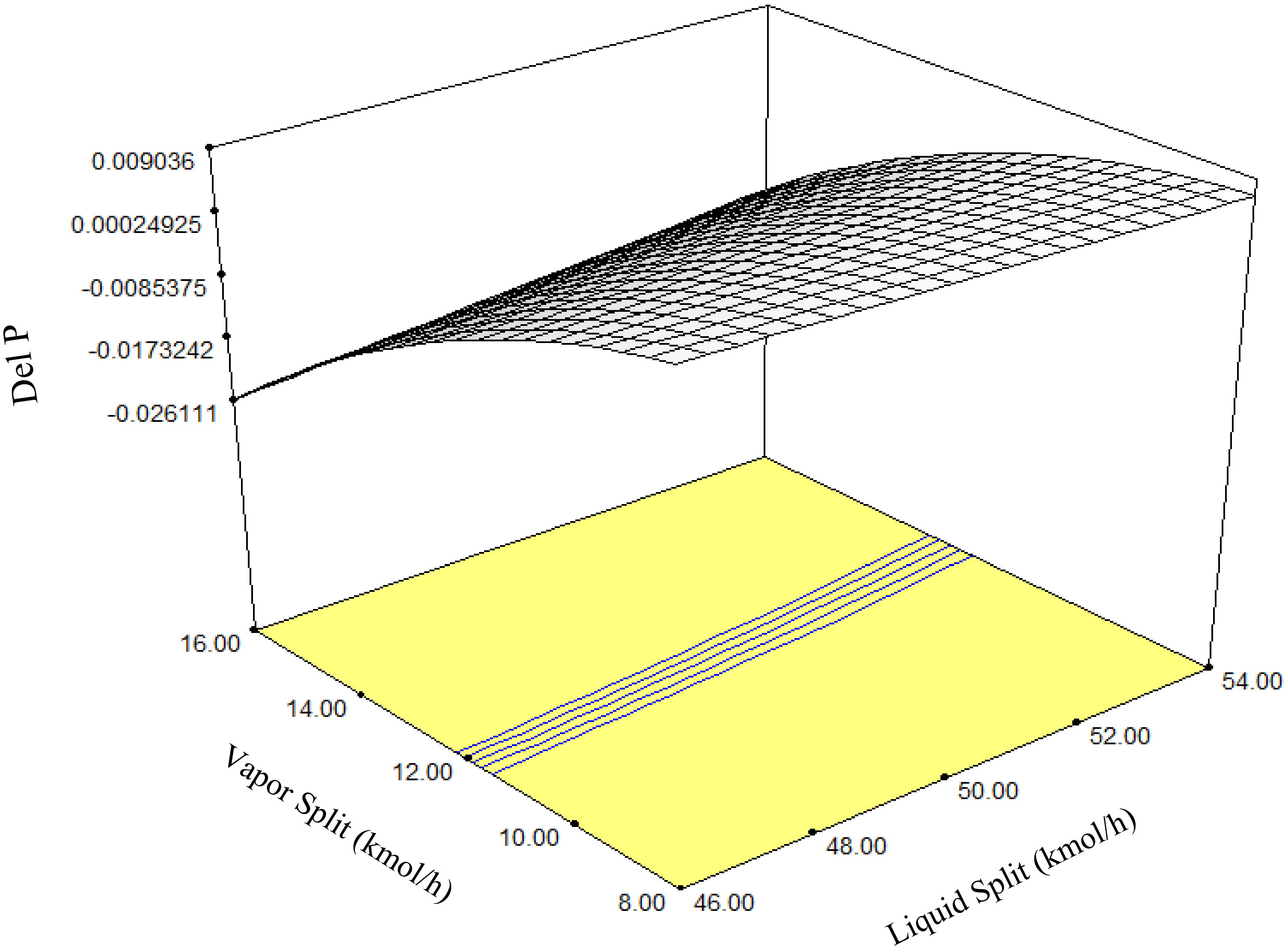

Figure 6.6f: Variation of difference in pressure drop with respect to vapor split and liquid split

On the basis of several simulations performed three optimized results (Table 6.10) are obtained which achieve the desirability of 0.766645, 0.7666 and 0.766599. This is acceptable as desirability greater than 0.7 indicate the adequate optimized result.

Table 6.10: Optimized results: providing three solutions

Solutions									
Number	r	l	v	D	S	B	Qb	Del P	Desirability
1	28.00	48.92	11.39	0.998226	0.932153	0.995422	286934	-5.20618E-008	0.766645
2	28.00	48.84	11.39	0.998336	0.931948	0.995574	286863	-3.04968E-006	0.7666
3	28.00	49.04	11.40	0.998062	0.932464	0.995183	287040	-3.06314E-008	0.766599
3 Solutions found									

6.7: Results obtained from Aspen Plus

Figure 6.7a,b shows the temperature profile for the column C1 and column C2. The temperature profile for column C1 shows that for stage 31 the temperature decreases and then increases which act as a transition from decreasing to increasing of temperature of the stages, The temperature profile for column C2 is constant up to stage 13 and it is monotonically increasing with increase in stage no.

Figure. 6.8a,b shows the concentration profile of DME in the column C1 and column C2. DME existed only in upper section i.e. (rectifying section) and completely absent in stripping section. DME is separated as lightest components because of high volatility. Therefore DME is collected as the top product. This confirms that DME existed only at the top of the column C1and is almost absent in the column C2.

Figure 6.9a,b shows the concentration profile of Methanol in the column C1 and column C2. Methanol existed both in upper section or rectifying section and lower section or stripping. Methanol is separated as middle key component because its volatility lies between dimethyl ether and water. Therefore methanol is collected as the middle key product from the second column C2 product.

Figure 6.10a,b shows the concentration profile of water in the column C1 and column C2. Water existed only in lower section i.e. (stripping section) and completely absent in rectifying section. Water is separated as heaviest components because of low volatility. Therefore Water is collected as the bottom product. This confirms that water existed only at the bottom of the column C1.

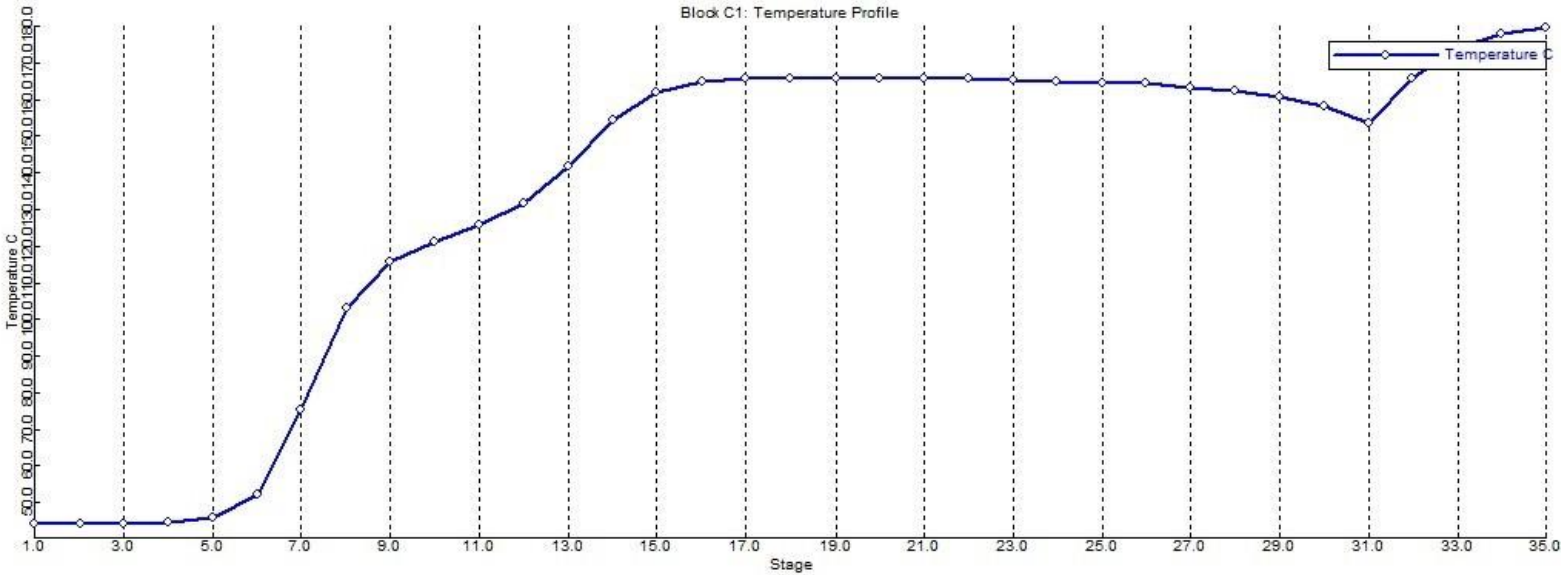

Figure 6.7a: Temperature profile for column C1

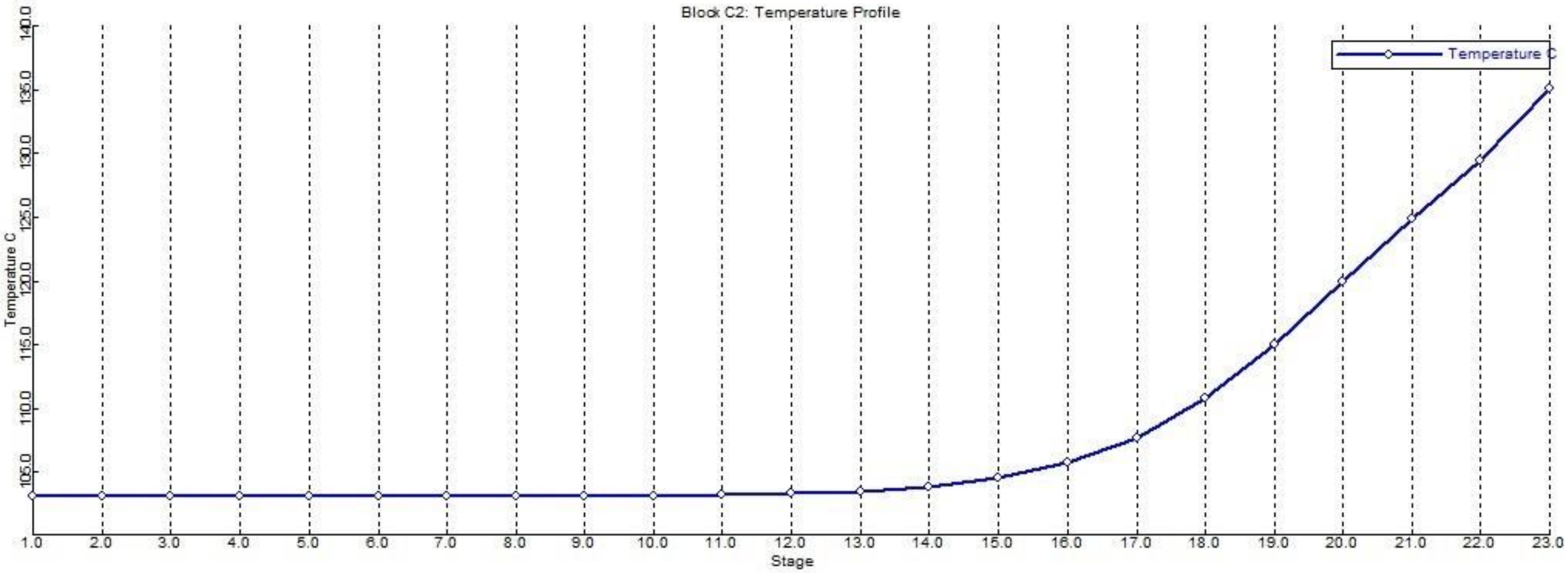

Figure 6.7b: Temperature profile for column C2

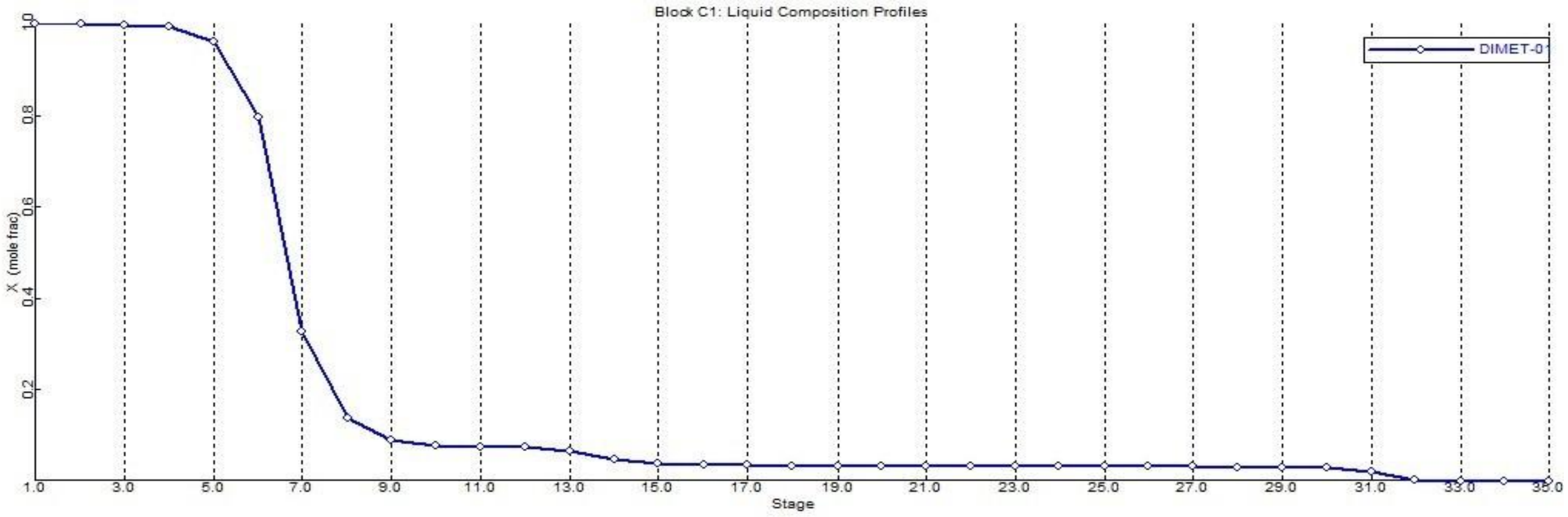

Figure 6.8a: Dimethyl ether composition profile for column C1

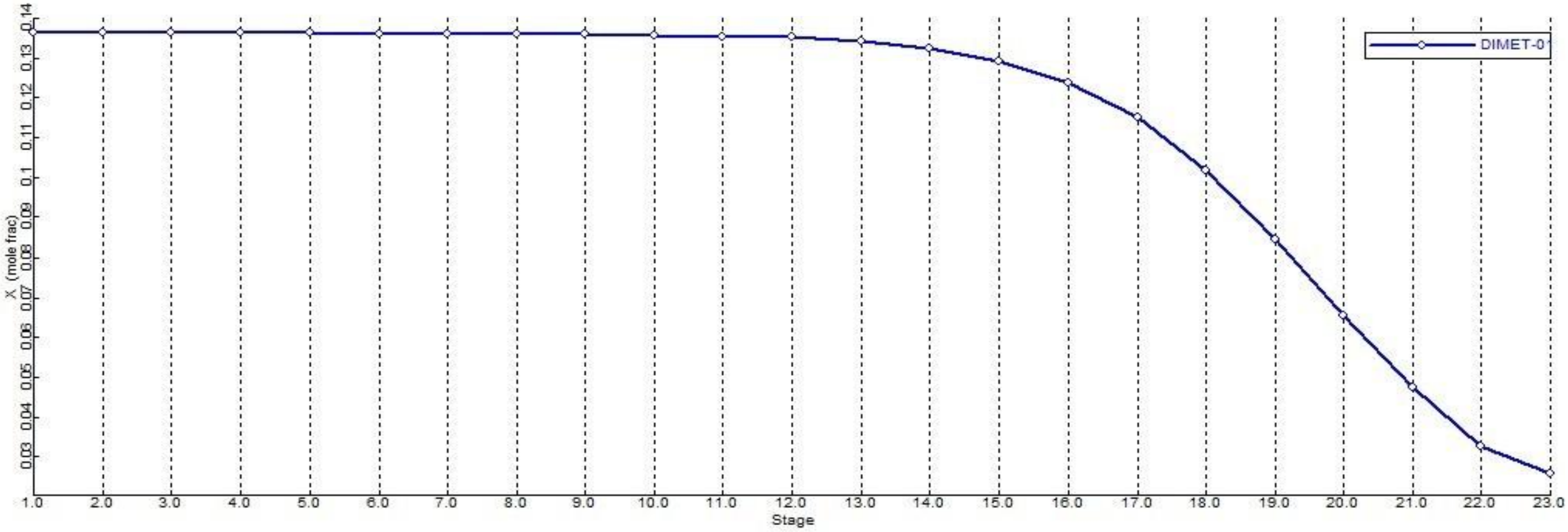

Figure 6.8b: Dimethyl ether composition profile for column C2

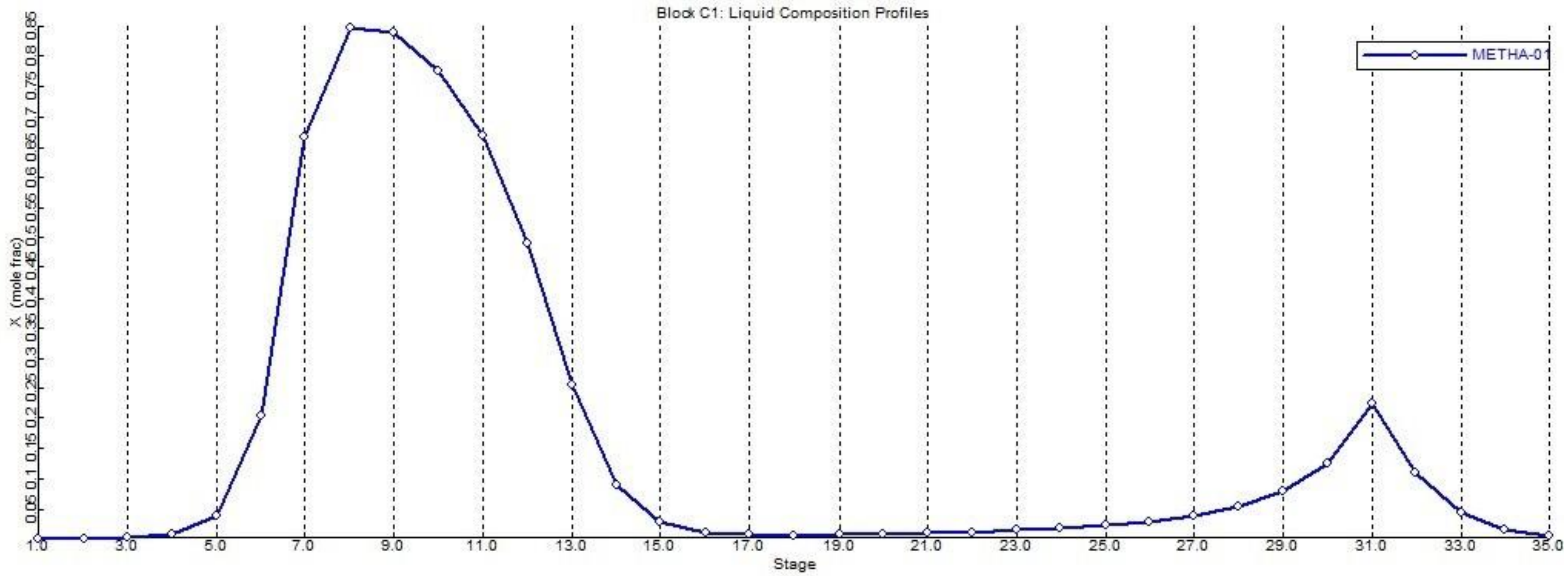

Figure 6.9a: Methanol composition profile for column C1

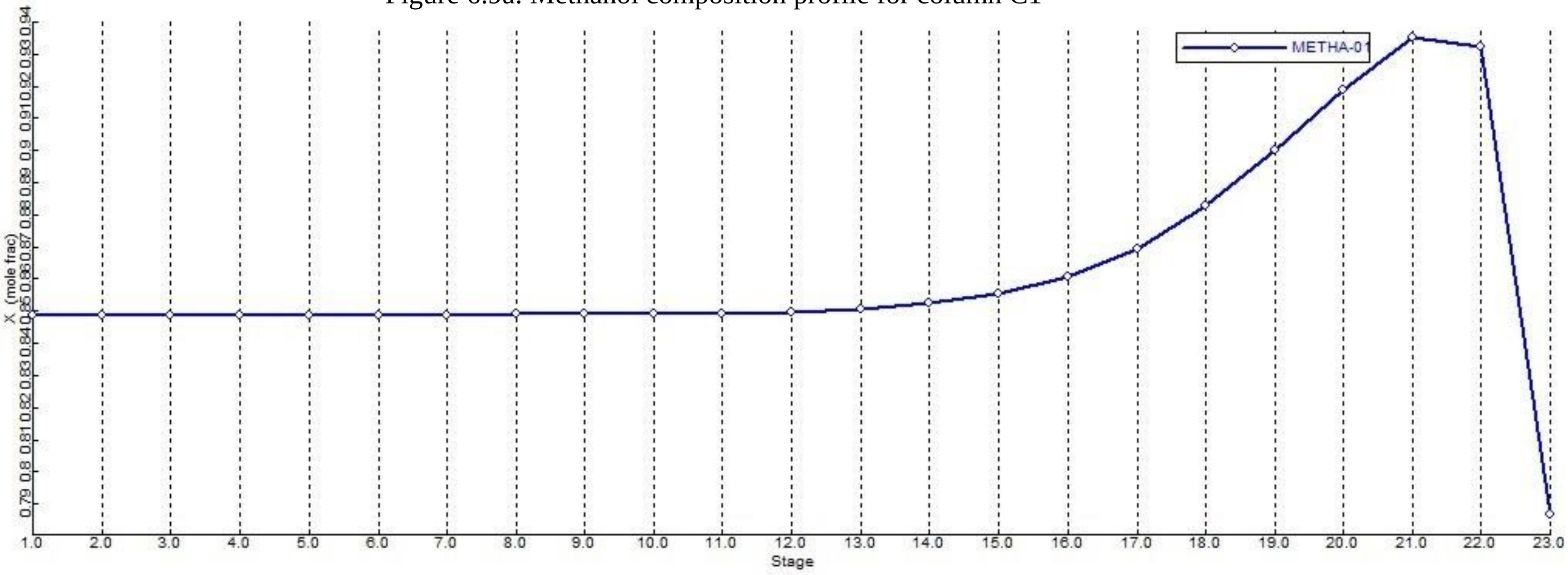

Figure 6.9b: Methanol composition profile for column C2

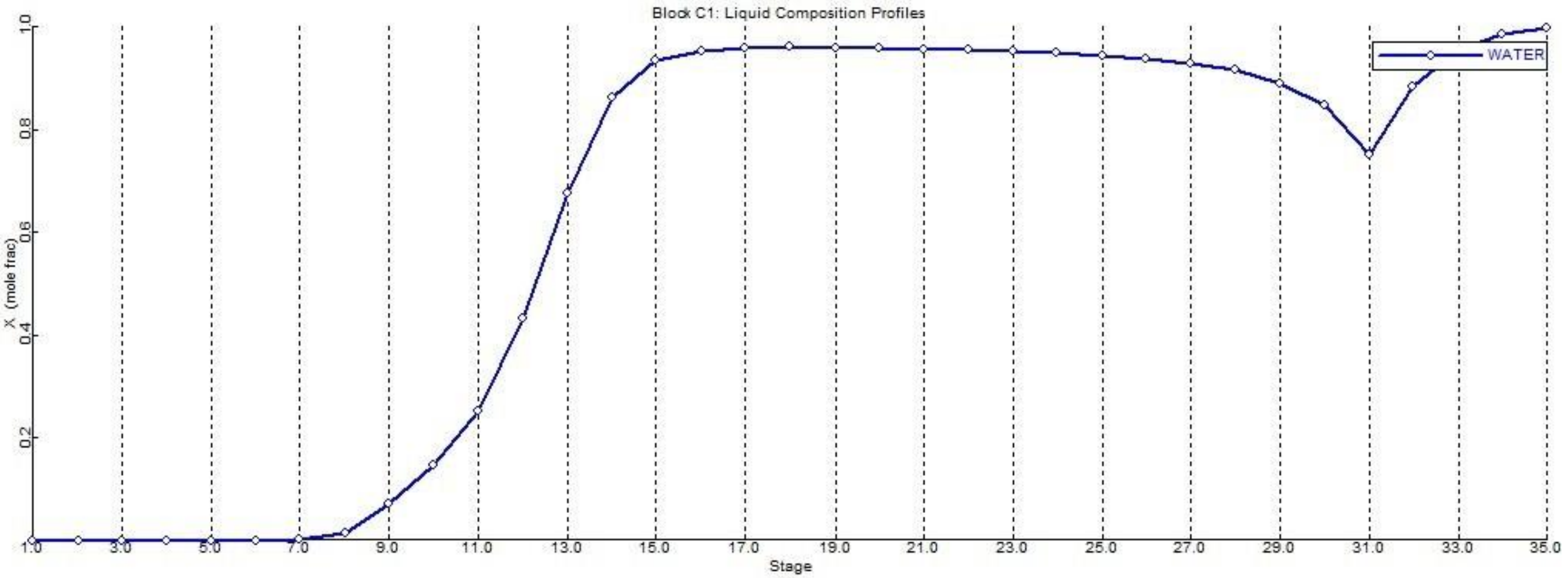

Figure 6.10b: Water composition profile for column C1

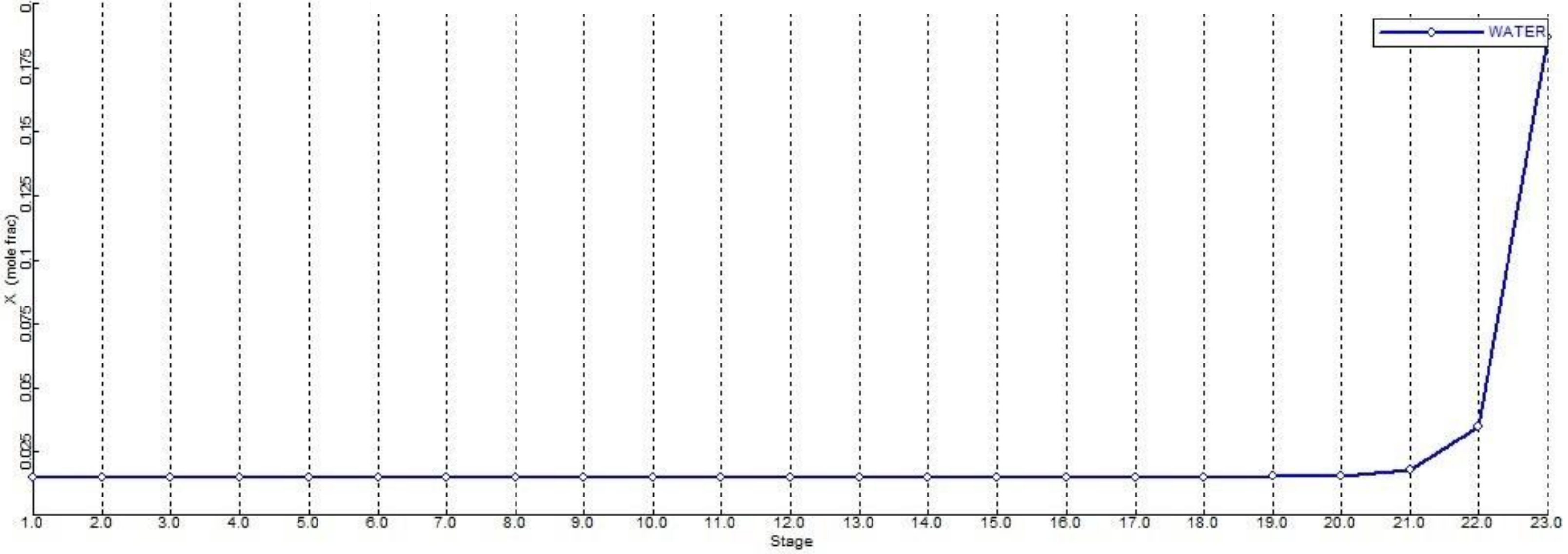

Figure 6.10b: Water composition profile for column C2

Table 6.11: Stream result obtained at an optimized process parameter

	Feed	Distillate	Side draw	Bottom
Substream: MIXED				
Mole Flow kmol/hr				
METHANOL	50	4.66E-04	23.3005	0.0605707
DIMETHYL ETHER	0	12.49953	0.8195492	1.91E-04
WATER	0	4.36E-11	0.879954	12.43919
Total Flow kmol/hr	50	12.5	25	12.49995
Total Flow kg/hr	1602.108	575.8565	800.2067	226.0451
Total Flow cum/hr	2.020515	0.9261666	1.234396	0.2737463
Temperature C	25	44.40108	129.3734	179.269
Vapor Frac	0	0	0	0
Liquid Frac	1	1	1	1
Solid Frac	0	0	0	0
Density kmol/cum	24.74617	13.49649	20.25282	45.66254
Density kg/cum	792.9208	621.7634	648.2576	825.7467
Average MW	32.04216	46.06852	32.00827	18.08368

Table 6.12: Stream composition obtained at an optimized process parameter

	Feed	Distillate	Side draw	Bottom
Methanol	1	3.72914E-05	0.93202	0.004845675
Dimethyl ether	0	0.9999624	0.032781968	1.52946E-05
Water	0	3.4908E-12	0.03519816	0.995139181

6.8: Result Validation: Comparison with the predicted result and actual result

Table 6.13: Result Validation

Responses	Predicted Values		Actual Values		Percentage Error
	Value	Units	Value	Units	
Dimethyl ether composition in distillate	0.9982260		0.9999624		0.171 %
Methanol composition in side draw	0.9321530		0.9320200		0.014 %
Water composition in bottom	0.9954220		0.9951391		0.028 %
Reboiler Duty	286934	Watt	286277	Watt	0.229 %

Difference in pressure drop at both sides of the wall = 0.000199

CHAPTER-7

CONCLUSIONS

The analysis of reactive DWC is being carried out with the consideration of equalization of pressure drop on both sides of the wall, For the complete analysis of the column simulations are performed and beforehand the DOF analysis is much important which provides the no. of independent variables which the analyzer has to provide in order to complete the simulation. The literature presented earlier has not provided the DOF of reactive DWC, in the analysis it was found that the DOF for the column is more than that of DWC due to increase in liquid or vapor holdup parameter, due to which the analysis leads the increment in DOF by no. of reactive stages. It was found that the pressure drop difference plays an important role for the efficient operation of reactive DWC. It acts a deciding factor for reflux rate, liquid split and vapor split which is mainly responsible for the control of reactive DWC. In several literatures the optimized process parameters are calculated without consideration of equal pressure drop on both sides of the wall, but for the feasible operation of reactive DWC the parallel branches should have the equal pressure drops. Although several researchers have reported that the control of reactive DWC is a tedious task, the results obtained clearly explains that the product purities, reboiler duty, condenser duty and the feasible operation of reactive DWC can be obtained by maintaining the process parameters comprising of reflux rate, liquid split and vapor splits.

BIBLIOGRAPHY

1. R.O. Wright, 1949, Fractionation apparatus, US Patent No. 2,471,134
2. Petlyuk, F.B., Platonov, V.M., Slavinskii, D.M., 1965. Thermodynamically optimal method for separating multicomponent mixtures. Int. Chem. Eng. 5, 555
3. Tedder, D.W., Rudd, D.F., 1978. Parametric studies in industrial distillation: Part 1. Design comparison. AIChE J. 24, 303
4. Alatiqi, I.M., Luyben, W.L., 1986. Control of a complex sidestream column/stripper distillation configurations. Ind. Eng. Chem. Process Des. Dev. 25, 1877
5. Fidowski, Z., Krolikowski, L., 1986. Thermally coupled system of distillation columns: optimization procedure. AIChE J. 32, 537
6. Kaibel, G., 1987. Distillation columns with vertical partitions. Chem. Eng. Technol. 10, 92
7. Floudas ,C.A; Anastasiadis, S.H. 1988. Synthesis Of Distillation Sequences With Several Multicomponent Feed And Product Streams. Chemical Engineering Science. Vol 43.No. 9, 2407 2419.
8. Wolff, E.A.; Skogestad,S . 1995. Operation of integrated three product (Petlyuk) distillation columns. Ind.Eng.Chem. Res.34, 2094-2103
9. Finn, A.J. 1996. Rapid assessment of thermally coupled side columns. PII: S0950-4214, 00015-1
10. Agrawal, R; Fidkowski, Z.T. 1998. Are Thermally Coupled Distillation Columns Always Thermodynamically More Efficient for Ternary Distillations? Ind. Eng. Chem. Res. 37, 3444-3454
11. Agrawal, R; Fidkowski, Z.T. 1998. More Operable Arrangements of Fully Thermally Coupled Distillation Columns. AIChE journal vol.44,No. 11, 2565.
12. Agrawal, R; Fidkowski, Z.T. 1999. New Thermally Coupled Schemes for Ternary Distillation. AIChE journal vol.45, No. 3, 485.
13. Halvorsen, I.J., Skogestad, S., 1999. Optimal operation of Petlyuk distillation: understanding the steady-state behaviour. J. Process Control 9, 407–424
14. Agrawal.2001. Processes For Multicomponent Separation, US patent No.6,286,335
15. Agrawal, R. 2001. Multicomponent Distillation Columns with Partitions and Multiple Reboilers and Condensers. Ind. Eng. Chem. Res, 40, 4258-4266

16. Fidkowski, Z.T; Agrawal, R. 2001. Multicomponent Thermally Coupled Systems of Distillation Columns at Minimum Reflux. AIChE journal, Vol.47, No.12, 2713.

17. Tung. 2002. Hydraulically Balanced Fully Thermally Coupled System. US patent No.6,347,533

18. Muralikrishna V,K; Madhavan, K.P; Shah, S.S. 2002. Trans IChemE, Vol 80, Part A

19. Standberg, J; Skogestad, S. 2006. Stabilizing operation of a 4-product integrated kaibel column. IChemE symposium series no. 152,638-647

20. Sotudeh, N; Bahram, H.S. 2007. A Method for the Design of Divided Wall Columns. Chem. Eng. Technol.,30,No. 9, 1284-1291

21. Isopescu, R; Woinaroschy, A; Draghiciu, L. 2008. Rev.Chim. (Bucure ti), 59, Nr.7, 812-815

22. Rangaiah, G. P., Ooi, E. L., & Premkumar, R. 2009. Procedure for quick design of dividing wall columns. Chemical Product and Process Modeling, 4(1). Article 7

23. Premkumar, R., & Rangaiah, G. P. 2009. Retrofitting conventional column sys-tems to dividing wall columns. Chemical Engineering Research and Design, 87, 47–60.

24. Butler. 2010. Processes using dividing wall distillation column, US pub. No. US2010/0168347

25. Shah, V.H.; Agrawal, R. 2010. A Matrix Method for Multicomponent Distillation Sequences. AIChE journal,vol. 56, No. 7,1759-1775

26. Sangal, V.K.; Kumar, V; Mishra, I.M. 2012. Optimization of structural and operational variables for the energy efficiency of a divided wall distillation column. Computers and Chemical Engineering 40, 33-40.

27. Haun, S.; Lien, K.M. 1998. A phenomena based design approach to reactive distillation. Trans IChemE, Vol 76, Part A

28. Huss, R.S.;Chen, F;Malone, M.F.; Doherty, M.F. 1999. Computer- aided tools for the design of reactive distillation systems. PII: S0098-1354/99/00074-5

29. Daniel, G.; Patil P.; Dragomir, R.; Jobson, M. 2006. IChemE Symposium Series No. 152

30. Muller, I.; Kenig, E.Y. 2007. Reactive Distillation in a Dividing Wall Column: Rate-Based Modeling and Simulation. Ind. Eng, Chem. Res.,46, 3709-3719

31. Bumbac, G.; Plesu, A.E.; Plesu, V. 2007. 17th European Symposium on Computer Aided Process Engineering

32. Hernandez, S.; Sandoval- Vergara, R.; Barroso-Munoz, F.M.; Murrieta-Duenas, R.; Hernandez-Escoto, H.; Segovia-Hernandez, J.G.; Rico-Ramirez, V. 2008.Reactive dividing wall distillation columns: Simulation and implementation in a pilot plant. Chemical Engineering and Processing,48, 250-258

33. Miranda-Galindo, E.Y.;Segovia-Hernandez, J.G; Hernandez, S.; Rosa Álvarez, G.; Gutiérrez-Antonio, C.; Briones-Ramírez, A. 2009. Design of Reactive Distillation with Thermal Coupling for the Synthesis of Biodiesel using Genetic Algorithms. 19'th European Symposium on Computer Aided Process Engineering

34. Kiss,A.A; Pragt, J.J; van Strien, J.G. 2009. Chemical Engineering Communications, 196:11, 1366-1374

35. Santander, C.M.G.; Rueda, S.M.G.; Silva, N.D.L.D; Costa, A.C.D.;Filho, R.M.; Maciel, M.R.W.2010. 20'th European Symposium on Computer Aided Process Engineering.

36. Delgado-Delgado,R; Hernández,S; Barroso-Mu˜ noz, F.O. ; Segovia-Hernández,J.G; Castro-Montoya, A.J. 2011. From simulation studies to experimental tests in a reactive dividing wall distillation column. Chemical Engineering Research And Design.

37. Friday, j. R.; Smith, B.D. 1964. An analysis of the equilibrium stage separations problem-formulation and convergence. AIChE JI 10, 698-707.

38. Tomich, J.F. 1970.A new simulation method for equilibrium stage processes. AIChE Jl 16,issue 2, 229-232

39. Naphtali, L.M.; Sandholm, D.P. 1971. Multicomponent separation calculations by linearization. AIChE Jl 17, issue 1, 148-153

40. Hess, F.E.;Holland, C.D. 1977. Solve more distillation problems, Hydrocarbon process. Vol 56, no. 5, 241

41. Hofeling, B.S.; Seader, J.D. 1978. A modified Naphtali-Sandholm method for general systems of interlinked, multistaged separators. AIChE Jl 24, issue 6,1131-1134.

42. Lockett, M.J. 1986. Distillation tray fundamentals, Cambridge. Cambridge university press.

43. Lei, Z; Zou, Z; Dai, C; Li, Q; Chen B. 2011. Synthesis of dimethyl ether (DME) by catalytic distillation. Chemical Engineering Science 66, 3195-3203

44. Sangal V. K., Bichalu L., Kumar V., Mishra I. M. 2012. Importance of pressure drop in divided wall distillation column, Asia Pacific J. of Chemical Engineering, DOI: 10.1002/apj.1633

45. Ferreira, S.L.C.; Santos, W.N.L.; Quintella, C.M.; Neto, B.B.; Bosque-Sendra; Doehlert, J.M. 2004. Doehlert Matrix: a chemometric tool for analytical chemistry-review. Talanta,63,1061-1067

46. Box, G.E.P.; Hunter, J.S. 1957. Multi factor experimental designs for exploring response surfaces. Am.Math.Statist.,28,195-241

47. Derringer, G.; Suich, R. 1980. Simultaneous optimization of several response variables. J. of Quality Technology.,12,214-219

48. Sangal V. K., Kumar V., Mishra I. M. 2012. Divided wall distillation column: rationalization of degree of freedom analysis. Theoretical Foundations of Chemical Engineering, 46 (4), 319-328.

49. Sangal V. K., Kumar V., Mishra I. M. 2012. Optimization of structural and operational variables for the energy efficiency of a divided wall distillation column. Computer & Chemical Engineering, 40 , 33-40.

50. Sangal V. K., Kumar V., Mishra I. M. 2012. Optimization of a divided wall column for the separation of C4-C6 normal paraffin mixture using Box-Behnken design. Chemical Industry & Chemical Engineering Quarterly, DOI: 10.2298/CICEQ121019047S.